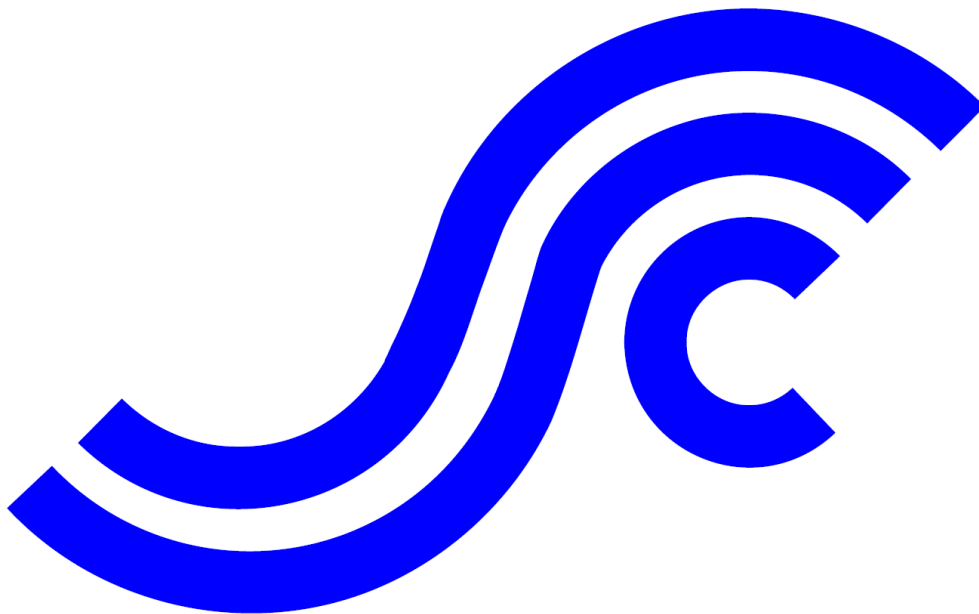


SSC-474

**STRUCTURAL ASSESSMENT OF AGED
SHIPS**

By G. Walker, B. Connell, and S. Kery

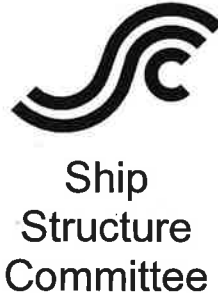


This document has been approved
for public release and sale; its
distribution is unlimited.

SHIP STRUCTURE COMMITTEE
2018

Member Agencies:

American Bureau of Shipping
Defence Research & Development Canada
Maritime Administration
Military Sealift Command
Naval Sea Systems Command
Office of Naval Research
Society of Naval Architects & Marine Engineers
Transport Canada
United States Coast Guard



Address Correspondence to:

Commandant (CG-ENG-2/SSC)
ATTN: Executive Director, SSC
US Coast Guard
2703 Martin Luther King Jr. Ave SE
Washington, DC 20593-7509
Website: <http://www.shipstructure.org>

SSC – 474
SR – 1478

7 June 2018

STRUCTURAL ASSESSMENT OF AGED SHIPS

The drive to improve efficiency and load carrying capability has led to highly optimized ship structures often utilizing thinner and higher strength materials to minimize ship weight. This has resulted in increased inspection and maintenance requirements to ensure structural integrity throughout the life of the vessel. At the same time, there is increased pressure to reduce vessel downtime and maintenance costs, all contributing to increasing the risk of structural failure.

This report describes the development of an assessment process to predict the survivability of a corrosion-degraded ship in specific wave conditions. The method developed utilizes a ship specific 3-D hydrodynamic model to simulate the ship's rigid body dynamic response to wave conditions, measuring the resulting ship motions and pressure distribution on the hull. Pressure and acceleration data from the hydrodynamic model is then input into a 3-D finite element model of the degraded ship structure where the resulting stresses in stiffeners and plating are assessed against various failure modes, including buckling modes, which are calculated according to IACS Common Structural Rules. The results form the basis of a degraded ship strength assessment, which can be provided to a ship owner and operator to make operational and repair decisions.

We thank the authors and Project Technical Committee for their dedication and research toward completing the objectives and tasks detailed throughout this paper and continuing the Ship Structure Committee's mission to enhance the safety of life at sea.



J. P. NADEAU
Rear Admiral, U.S. Coast Guard
Co-Chairman, Ship Structure Committee



L. C. SELBY
Rear Admiral, U.S. Navy
Co-Chairman, Ship Structure Committee

SHIP STRUCTURE COMMITTEE

RDML John Nadeau
U. S. Coast Guard Assistant Commandant
for Prevention Policy (CG-5P)
Co-Chair, Ship Structure Committee

RDML Lorin Selby
Chief Engineer and Deputy Commander
For Naval Systems Engineering (SEA05)
Co-Chair, Ship Structure Committee

Mr. Jeffrey Lantz
Director, Commercial Regulations and Standards (CG-5PS)
U.S. Coast Guard

Mr. Derek Novak
Senior Vice President, Engineering & Technology
American Bureau of Shipping

Mr. H. Paul Cojeen
Society of Naval Architects and Marine Engineers

Dr. John MacKay
Head, Warship Performance, DGSTCO
Defence Research & Development Canada - Atlantic

Mr. Kevin Kohlmann
Director, Office of Safety
Maritime Administration

Mr. Luc Tremblay
Executive Director, Domestic Vessel Regulatory Oversight
and Boating Safety, Transport Canada

Mr. Albert Curry
Deputy Assistant Commandant for Engineering and
Logistics (CG-4D)
U.S. Coast Guard

Mr. Eric Duncan
Group Director, Ship Integrity and Performance Engineering
(SEA 05P)
Naval Sea Systems Command

Mr. Neil Lichtenstein
Deputy Director N7x, Engineering Directorate
Military Sealift Command

Dr. Thomas Fu
Director, Ship Systems and Engineering Research Division
Office of Naval Research

SHIP STRUCTURE SUB-COMMITTEE

UNITED STATES COAST GUARD (CVE)

CAPT Benjamin Hawkins
Mr. Charles Rawson
Mr. Jaideep Sirkar

AMERICAN BUREAU OF SHIPPING

Mr. Craig Bone
Dr. Gu Hai
Mr. Daniel LaMere
Ms. Christina Wang

SOCIETY OF NAVAL ARCHITECTS AND MARINE ENGINEERS

Mr. Frederick Ashcroft
Dr. Roger Basu
Dr. Robert Sielski
Dr. Paul Miller

DEFENCE RESEARCH & DEVELOPMENT CANADA ATLANTIC

Dr. Malcolm Smith
Mr. Cameron Munro

MARITIME ADMINISTRATION

Mr. Chao Lin
Mr. Todd Hiller
Mr. Todd Ripley
Mr. Richard Sonnenschein

TRANSPORT CANADA

Ms. Abigail Fyfe
Mr. Bashir Ahmed Golam

UNITED STATES COAST GUARD (FLEET)

CAPT George Leshner
Mr. Frank DeBord
Mr. Martin Hecker
Mr. Timothy McAllister

NAVSEA/NSWCCD

Mr. David Qualley
Mr. Daniel Bruchman
Mr. Dean Schleicher
Dr. Pradeep Sensharma

MILITARY SEALIFT COMMAND

Ms. Jeannette Viernes

OFFICE OF NAVAL RESEARCH

Dr. Paul Hess

PROJECT TECHNICAL COMMITTEE

The Ship Structure Committee greatly appreciates the contributions of the individuals that volunteered their time to participate on the Project Technical Committee, listed below, and thanks them heartily. They were the subject matter expert representatives of the Ship Structure Committee to the contractor, performing technical oversight during contracting, advising the contractor in cognizant matters pertaining to the contract of which the agencies were aware, and performing technical peer review of the work in progress and upon completion.

Chair:

Mr. Jason Cordell, US Coast Guard

Members:

Dr. James Huang, Department of National Defence Headquarters, Canada

Dr. Miguel Nunez, European Maritime Safety Agency (Lisbon)

Mr. Jose Rosas, ClassNK Panama Office

Dr. Pradeep Sensharma, US Naval Sea Systems Command

Mr. Alan Spackman, International Association of Drilling Contractors

Ship Structure Committee Executive Director:

LT Jonathan Duffett, US Coast Guard

1. Report No. SSC - 474		2. Government Accession No.		3. Recipient's Catalog No.	
4. Title and Subtitle STRUCTURAL ASSESSMENT OF AGED SHIPS				5. Report Date 2/22/2018	
				6. Performing Organization Code	
7. Author(s) Gregory Walker, Brendan Connell, Sean Kery.				8. Performing Organization Report No. SR-1478	
9. Performing Organization Name and Address CSRA 1201 M Street, SE Washington, DC 20003				10. Work Unit No. (TRAIS)	
				11. Contract or Grant No.	
12. Sponsoring Agency Name and Address Ship Structure Committee COMMANDANT (CG-5212/SSC) ATTN (ADMIN ASST/SHIP STRUCTURE COMMITTEE) US COAST GUARD 2100 2ND ST SW STOP 7126 Washington, DC 20593-7126				13. Type of Report and Period Covered Final Report xx/xx/2018-xx/xx/2018	
				14. Sponsoring Agency Code CG-5P	
15. Supplementary Notes Sponsored by the Ship Structure Committee. Jointly funded by its member agencies. The research completed by the above author for the Ship Structure Committee was reviewed by the Project Technical Committee for satisfactory completion of the objectives outlined in the Statement of Work developed and approved for funding by the Principal Members of the Ship Structure Committee.					
16. Abstract This report describes the development of an assessment process to accurately predict the survivability of a corrosion-degraded ship in specific wave conditions. The method developed utilizes a ship specific 3-D hydrodynamic model to simulate the ship's rigid body dynamic response to wave conditions, measuring the resulting ship motions and pressure distribution on the hull. Pressure and acceleration data from the hydrodynamic model is then input into a 3-D finite element model of the degraded ship structure where the resulting stresses in stiffeners and plating are assessed against various failure modes, including buckling modes, which are calculated according to IACS Common Structural Rules. The results form the basis of a degraded ship strength assessment which can be provided to a ship owner and operator to make operational and repair decisions.					
17. Key Words corrosion, wastage, hull girder failure, buckling, hydrodynamic pressure, WASIM, FEMAP			18. Distribution Statement Distribution is available to the public through: National Technical Information Service U.S. Department of Commerce Springfield, VA 22151 Ph. (703) 487-4650		
19. Security Classif. (of this report) Unclassified		20. Security Classif. (of this page) Unclassified		21. No. of Pages 69	22. Price

Conversion Factors

(Approximate conversions to metric measures)

To convert from	to	Function	Value
LENGTH			
inches	meters	divide	39.3701
inches	millimeters	multiply by	25.4000
feet	meters	divide by	3.2808
VOLUME			
cubic feet	cubic meters	divide by	35.3149
cubic inches	cubic meters	divide by	61,024
SECTION MODULUS			
inches ² feet ²	centimeters ² meters ²	multiply by	1.9665
inches ² feet ²	centimeters ³	multiply by	196.6448
inches ⁴	centimeters ³	multiply by	16.3871
MOMENT OF INERTIA			
inches ² feet ²	centimeters ² meters	divide by	1.6684
inches ² feet ²	centimeters ⁴	multiply by	5993.73
inches ⁴	centimeters ⁴	multiply by	41.623
FORCE OR MASS			
long tons	tonne	multiply by	1.0160
long tons	kilograms	multiply by	1016.047
pounds	tonnes	divide by	2204.62
pounds	kilograms	divide by	2.2046
pounds	Newtons	multiply by	4.4482
PRESSURE OR STRESS			
pounds/inch ²	Newtons/meter ² (Pascals)	multiply by	6894.757
kilo pounds/inch ²	mega Newtons/meter ² (mega Pascals)	multiply by	6.8947
BENDING OR TORQUE			
foot tons	meter tons	divide by	3.2291
foot pounds	kilogram meters	divide by	7.23285
foot pounds	Newton meters	multiply by	1.35582
ENERGY			
foot pounds	Joules	multiply by	1.355826
STRESS INTENSITY			
kilo pound/inch ² inch ^{1/2} (ksi√in)	mega Newton MNm ^{3/2}	multiply by	1.0998
J-INTEGRAL			
kilo pound/inch	Joules/mm ²	multiply by	0.1753
kilo pound/inch	kilo Joules/m ²	multiply by	175.3

Table of Contents

1	INTRODUCTION	1
1.1	Purpose	1
1.2	Background	1
1.3	Scope	1
2	SHIP SELECTION	3
3	MODELS	3
3.1	Hydrodynamic Model	3
3.1.1	Hydrodynamic Pressure Distribution	4
3.1.2	Hydrodynamic Simulation Cases	5
3.1.3	Hydrodynamic Data Output	7
3.2	Structural Model	8
3.2.1	FEMAP Model Grouping	8
3.2.2	Units	10
3.2.3	Material Properties	10
3.2.4	Mass Modeling	11
3.2.5	Corrosion Modeling	12
3.2.6	Load Application	13
3.2.7	Load Cases	14
3.3	Yielding Criteria	15
3.4	Buckling Criteria	16
3.4.1	Plate Buckling	16
3.4.2	Stiffener Buckling	16
4	STRUCTURAL ANALYSIS	17
4.1	Model Plots and Stress Results	18
4.2	Determining Buckling Capacities	24
4.2.1	Buckling Strength – Hull Bottom Longitudinal Stiffeners	25
4.2.2	Buckling Strength – Hull Bottom Plating	28
5	STRENGTH ASSESSMENT	31
6	CONCLUSIONS	33

List of Tables

Table 2-1:	General particulars for ESB Vessel	3
Table 3-1:	Hydrodynamic Analysis Run Matrix	6
Table 3-2:	Comparison of Wavelength to Ship Length	6
Table 3-3:	System of Units used for the Structural Analysis of the ESB	10
Table 3-4:	Structural Material Specifications	11
Table 3-5:	ESB Longitudinal Weight Distribution Numbers	12
Table 3-6:	Acceleration Data	14
Table 3-7:	Final Load Cases (All Hogging)	15
Table 4-1:	Maximum Yielding Assessment Results	19
Table 4-2:	ESB Hull Bottom Longitudinal Stiffener Buckling Response for 0%, 25% & 40% Corrosion	25
Table 4-3:	Hull Bottom Plating Buckling Response	28

List of Illustrations

Figure 3-1: WASIM-Generated Bending Moment.....	4
Figure 3-2: Mid-Hull 100 Panels (in Red) Where Pressure is Measured (WASIM Screengrab)	5
Figure 3-3: Aft-Hull and Fore-Hull 100 Panels (in Red) Where Pressure is Measured	5
Figure 3-4: ESB Finite Element Model	8
Figure 3-5: Main Transverse Bulkhead Locations	9
Figure 3-6: ESB Midbody Sections	9
Figure 3-7: ESB Midbody Section Cutaway	10
Figure 3-8: ESB Material Specification Key	11
Figure 3-9: ESB Longitudinal Weight Distribution Graph.....	12
Figure 3-10: Pressure Point Locations and 14m Hog Wave Pressure Distribution	13
Figure 4-1: 0% Corroded (14m) Maximum Sag - Von Mises Stress Plot.....	17
Figure 4-2: 0% Corroded (14m) Maximum Hog - Von Mises Stress Plot	18
Figure 4-3: 0% Corroded (14m) Maximum Hog – Normal X Stress Plot.....	18
Figure 4-4: Hull Bottom Plating - 0% Corrosion – 14m Hog – Von Mises Stress	20
Figure 4-5: Main Deck Plating – 0% Corrosion – 14m Hog – Von Mises Stress.....	20
Figure 4-6: Main Deck Inner Top Plating - 0% Corrosion – 14m Hog – Von Mises Stress	21
Figure 4-7: Main Deck Framing - 0% Corrosion – 14m Hog – Von Mises Stress	21
Figure 4-8: Inner Bottom Plating – 0% Corrosion – 14m Hog – Von Mises Stress	22
Figure 4-9: Inner Bottom Framing – 0% Corrosion – 14m Hog – Von Mises Stress	22
Figure 4-10: Long’l Blkhd – 0% Corrosion – 14m Hog – Von Mises Stress	23
Figure 4-11: Transverse Frames and Bulkheads – 0% Corrosion – 14m Hog – Von Mises Stress	23
Figure 4-12: Section 2 – 0% Corrosion – 14m Hog – Von Mises Stress	24
Figure 4-13: Hull Bottom Stiffener Buckling Response – 14m – 0% Corrosion.....	26
Figure 4-14: Hull Bottom Stiffener Buckling Response – 14m – 0% Corrosion.....	26
Figure 4-15: Hull Bottom Stiffener Buckling Response – 14m – 0% Corrosion.....	27
Figure 4-16: Hull Bottom Plating Buckling Response vs Transverse Location – 0% Corrosion	29
Figure 4-17: Hull Bottom Plating Buckling Response vs Transverse Location – 25% Corrosion	29
Figure 4-18: Hull Bottom Plating Buckling Response vs Transverse Location – 40% Corrosion	30
Figure 4-19: Hull Bottom Plating Buckling Response vs Longitudinal Location – 0% Corrosion	30
Figure 4-20: Hull Bottom Plating Buckling Response – 14m Hog	31
Figure 5-1: Unreinforced Opening in Longitudinal Deck Framing - 25% Corrosion - 14m Hog.....	32
Figure 5-2: Unreinforced Opening in Longitudinal Deck Framing - 25% Corrosion - 11.5m Hog.....	32

List of Appendices

Appendix A	Range of Seakeeping Analysis Conditions Recommended for a Full Analysis .	A-1
Appendix B	Hydrodynamic Pressure Distributions	B-1
Appendix C	Structural Model Preparation Procedures	C-1
Appendix D	Buckling Calculations	D-1
Appendix E	ESB Buckling Response.....	E-1

List of Appendix Illustrations

Figure A-1:	Wave Energy Vs Sea State and 1m Significant Wave Height Bins	A-2
Figure B-1:	14m Sag Wave.....	B-1
Figure B-2:	11.5m Hog Wave	B-1
Figure B-3:	11.5m Sag Wave	B-2
Figure B-4:	9m Hog Wave.....	B-2
Figure B-5:	9m Sag Wave.....	B-2
Figure B-6:	6m Hog Wave.....	B-3
Figure B-7:	6m Sag Wave.....	B-3
Figure B-8:	4m Hog Wave.....	B-3
Figure B-9:	4m Sag Wave.....	B-4
Figure C-1:	FEMAP’s “Data Surface Editor” Menu.....	C-2
Figure C-2:	FEMAP’s “Define Options for Variation” Menu	C-2
Figure C-3:	FEMAP’s Entity Selection Menu	C-3
Figure C-4:	FEMAP’s Load Generation Menu.....	C-4
Figure C-5:	FEMAP’s Face Selection Menu	C-4
Figure C-6:	FEMAP’s “Select Type of Load” Menu	C-6
Figure C-7:	Typical FEMAP Beam Property Card	C-8
Figure C-8:	FEMAPs “Cross Section Definition” Menu.....	C-8
Figure C-9:	FEMAP’s “Send Results to Data Table” menu	C-10
Figure C-10:	FEMAP’s “Results to Add to Data Table” menu	C-11
Figure C-11:	FEMAP’s “Entity Selection...” menu	C-11
Figure C-12:	FEMAP’s “Data Table” Stress Output Listing Example.....	C-12
Figure D-1:	Plate Buckling Factor (K_X).....	D-1
Figure D-2:	Plate Buckling Correction Factor (F_{Long})	D-1
Figure D-3:	Plate Buckling Factor (K_Y).....	D-2
Figure E-1:	Hull Stiffener Buckling Response – Hog Wave - 0% Corrosion	E-1
Figure E-2:	Hull Stiffener Buckling Response – Sag Wave - 0% Corrosion	E-1
Figure E-3:	Hull Stiffener Buckling Response for Various Corrosion Levels – 14m Hog Wave.....	E-2
Figure E-4:	Hull Plating Buckling Response - Hog Wave - 0% Corrosion	E-2
Figure E-5:	Hull Plating Buckling Response – Sag Wave - 0% Corrosion.....	E-3
Figure E-6:	Hull Plating Buckling Response – Sag Wave - 25% Corrosion.....	E-3

List of Appendix Tables

Table C-1: Raw WASIM Position and Pressure Data C-1
Table C-2: Accelerations at time of MAX HOG Wave..... C-5
Table C-3: PID10008, 0% Corroded..... C-9
Table C-4: PID10008 - 25% Corrosion – Zero’d Shape..... C-9
Table C-5: PID 10008 – 25% Corrosion – Updated Shape..... C-9
Table C-6: EXCEL File “NODE_LISTING.XLSX” – Node Positions..... C-14
Table C-7: EXCEL File: “BREAKOUT.XLSX” – Element Data C-14
Table C-8: EXCEL File “LC04H25.XLSX” – Stress Output C-15
Table C-9: EXCEL File “ESB_PRESSURE.XLSX” – Hull Pressure..... C-16
Table C-10: EXCEL File: “PID_PROPS.XLSX” – Stiffener Properties - Corrosion= 0% C-17
Table C-11: EXCEL File: “PID_PROPS.XLSX” – Shell Properties – Corrosion=0% C-17

List of References

1. Ochi, Michael K., "Wave Statistics for the design of Ships and Ocean Structures"; SNAME Transactions, Vol86, 1978, pp 47-76
2. NASSCO, "Longitudinal Strength Assessment (ESB)"; NAVSEA Dwg #835-8468392 Rev B (NASSCO Dwg # 543-341-7066 Rev B), 25-May-2017
3. American Bureau of Shipping (ABS), "Rules for Building and Classing Steel Vessels", 2016, Part 5A & 5B (Specific Vessel Types)
4. International Association of Classification Societies (IACS), "Common Structural Rules for Bulk Carriers and Oil Tankers", 1-Jul-2015; Part 1, Chapter 8, Section 5 (Buckling Capacity)

1 INTRODUCTION

1.1 Purpose

The purpose of this project is to develop an assessment process to accurately predict the survivability of a corrosion-degraded ship in specific wave conditions. The process could then be employed to assess degraded ship structures against specific sea conditions, thereby providing the ship owner and crew with more detailed information on which to make operational and repair decisions. This ultimately allows them to understand the risk of, and help minimize the probability of structural failure when operational requirements, budgets or schedule do not permit the full remediation of the degradation. It may also be useful when assessing when a specific hull needs to be removed from service and scrapped.

1.2 Background

The drive to improve efficiency and load carrying capability has led to highly optimized ship structures often utilizing thinner and higher strength materials to minimize light ship weight. This has resulted in increased inspection and maintenance requirements to ensure structural integrity throughout the life of the vessel. At the same time there is increased pressure to reduce vessel downtime and maintenance costs, all contributing to increasing the risk of structural failure.

Previous attempts to model strength-degraded ship structures have used dimensional and form factors to model the ship, which is subjected to various headings and sea states to estimate vertical, lateral, and torsional moments. The output is derived using numerical techniques and empirical data. These outputs are then input into various reliability models of the component failure modes which are analyzed in series to predict the probability of failure occurring. Ship management can then use this probability to decide whether to subject the vessel to a specific wave condition.

In contrast, the method developed and applied herein utilizes detailed 3-D models that are specific to one ship, thus allowing a more refined engineering analysis to support decisions on whether to limit the wave environments that the ship is allowed to encounter. The developed process utilizes a ship-specific 3-D hydrodynamic model to simulate the ship's rigid-body dynamic response to an array of wave conditions, and measures the resulting ship motions and hydrodynamic pressure distribution on the hull, in the time domain. Pressure and acceleration data from the hydrodynamic model are then input into a detailed 3-D finite element model (FEM) of the degraded ship structure. The resulting stresses in hull beams and plating are assessed against various failure modes, including buckling modes, which are calculated according to the IACS Common Structural Rules (Ref. 4).

1.3 Scope

The overall objective of the project is to develop a process for evaluating degraded ship structure under various seaway conditions. To meet this objective within the available time and funding constraints, simplifying approaches and assumptions were used. The key ones are listed below.

- 1) While the entire hull and deckhouse structure was included in the structural finite element model, only the ship's mid-body region was evaluated for structural failure. This was considered acceptable because this is the region where maximum wave-induced hull girder bending occurs.
- 2) Green sea loads and bottom slamming were not addressed, because these are hard to quantify and model, and tend to occur far from the midships region where longitudinal hull girder stresses are highest.
- 3) Hydrostatic and sloshing pressures from liquids inside tanks were not modeled. The internal liquid pressure acting on the tank walls that also form the hull surface tend to cancel the external hydrostatic and hydrodynamic (wave) loading. Thus it is generally conservative to assume no internal pressure here. And since the interior tank bulkheads are often loaded by internal fluids on both sides, in which case the pressures largely cancel each other, fluid loads on interior bulkheads were neglected. This is also justified because the focus of this analysis is hull girder integrity, so bulkhead integrity was a secondary consideration.
- 4) To minimize the number of load cases, only seaway loads associated with bow/head seas in long crested waves were modeled. Luckily, ships tend to take this heading to the waves in a storm. Similarly, only one wave modal period was analyzed for each significant wave height. Modal periods that produce wavelengths close to the ship's length tend to be more critical.
- 5) This analysis utilized measured pressures and accelerations resulting from only 20-minute hydrodynamic runs, whereas longer and/or more runs are required to produce statistically significant maxima, and generate meaningful statistics on probability of exceedance for a given exposure time.
- 6) Corrosion is applied as a uniform percent reduction in plating and stiffener (web and flange) thicknesses throughout the entire ship. This doesn't reflect reality in terms of corrosion distribution but is conservative and vastly simplifies the analysis.
- 7) Service life (fatigue life) is not addressed in this project. Several years ago, there was an extensive structural evaluation performed on a variety of in-service U.S. Navy ships, as part of a joint NAVSEA-ABS project which included remaining fatigue life estimation. While fatigue life is affected by widespread corrosion, it was not shown to be as predominant an issue as loss of local hull strength which has an immediate impact on seaworthiness.

2 SHIP SELECTION

Several different hull forms were considered based upon the availability of seakeeping and structural model data.

The US Coast Guard's 378 Hamilton Class Cutter was initially proposed because it has documented in-service hull and corrosion evaluations available. However, no usable FEM or useful seakeeping model files were located. The Expeditionary Sea Base (ESB), a U.S. Navy Auxiliary ship, was chosen because of the availability of both FEA and seakeeping models along with several other advantages listed below:

- Commercial/Navy Hybrid
- Structure Designed to ABS SVR
- ABS Classed

General particulars of the ESB are shown in Table 2-1.

Table 2-1: General Particulars for ESB Vessel

Length Overall	785.2	feet	239.3	meters
Length between Perpendiculars	765.1	feet	233.2	meters
Max Beam	164.0	feet	50.0	meters
Depth to Main Deck	50.7	feet	15.5	meters
Minimum Draft	31.2	feet	9.5	meters
Voyage Draft	34.3	feet	10.5	meters
Maximum Draft	39.4	feet	12.0	meters

3 MODELS

3.1 Hydrodynamic Model

The numerical hydrodynamic modeling and analysis tool chosen for the project is the non-linear Rankine panel code initially developed at MIT by Dr. David Kring, and currently licensed to DNV-GL as the solver in their WASIM software. The particular versions of WASIM and its user interface (Hydro-D) used for this analysis were V5.1-03 and V4.5-08 respectively. As with the creation of any hydrodynamics model the process starts with input of the "offsets", i.e. X/Y coordinates, of points on a series of section cuts spanning the length of the hull form. Other similar codes such as Fredyn, Aegir or LAMPS could have been used but each different program and in many cases each version, uses a somewhat different custom input format. In the case of this study, the WASIM-compatible input files for the ESB hull form had already been developed. This was in the form of a text file that was loaded into WASIM and Hydro-D.

The WASIM software simulates three dimensional wave loading on the ship, computing both global responses and local loading on any displacement hull moving at forward speed. Data output includes:

- Ship Motions Summary
- Ship Accelerations Summary
- Shear Force and Bending Moment Statistics
- Hydrodynamic pressure distribution on the hull
- Plottable maximum and minimum shear forces and bending moments
- Extreme hogging and sagging values in the time series and 6 DOF accelerations at those time steps

The pressure distribution across the hull and acceleration at the ship's center of gravity from each wave selected are used as inputs to the FEA model of the degraded ship. The time step selected for each wave is that which maximizes the bending moment near midships. While midships is about 120m forward of the Aft Perpendicular (AP), as shown in Figure 3-1, the maximum occurred a little further forward of this, and this is the maximum that was used. Note that the absolute values of the bending moments are shown in this figure.

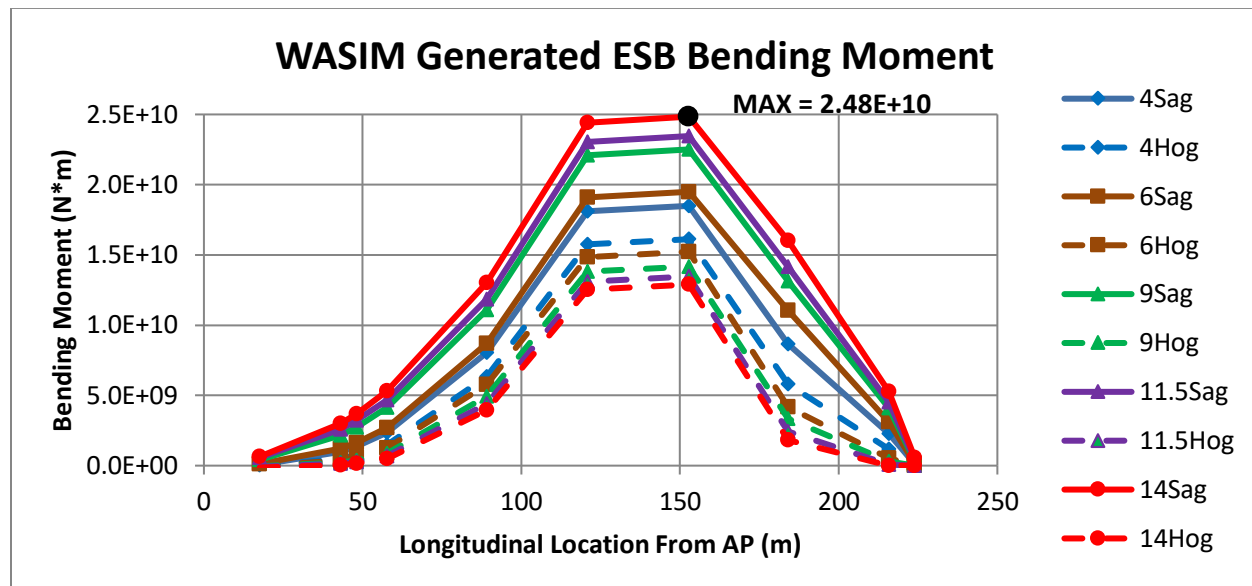


Figure 3-1: WASIM-Generated Bending Moment

The legend on the right hand side of the chart contains the significant wave height in meters followed by the type of bending moment on the hull (hogging or sagging). Thus: 4SAG is a 4 meter significant wave height that puts the ship in the sagging condition.

3.1.1 Hydrodynamic Pressure Distribution

The WASIM software allows the output of pressure distribution from the sea on the hull exterior but has restrictions on the number of panels that can be selected for pressure reporting. Either all panels must be selected, or the user may select up to 100 panels, with the latter decreasing output

file size and computing time. Instead of running the simulations with all panels selected, three different groups of 100 panels each, corresponding to the fore-hull, mid-hull, and aft-hull of the ship were chosen and the remaining panel pressures were interpolated after importing into the FEA model. Each simulation configuration is run three times where the only difference is which panel set was turned on. To ensure identical ship motions and pressure distributions were produced between the runs, the same wave component phase seed (start time) was used for each set of three runs. Statistical properties of the ship motions, i.e. displacements, velocities, and accelerations, and of the waves themselves, for one set of three runs were compared. The differences between them were zero out to at least 4 decimal places, therefore the waves and motions were considered statistically identical for all three runs in the set.

Figure 3-2 and Figure 3-3 below show the panels selected for pressure reporting (highlighted in red). Some are above the still waterline, but most are below, where the highest pressures occur.

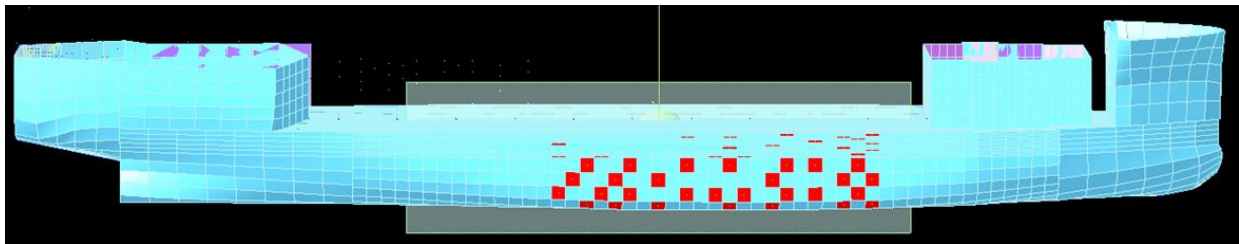


Figure 3-2: Mid-Hull 100 Panels (in Red) Where Pressure is Measured (WASIM Screenshot)

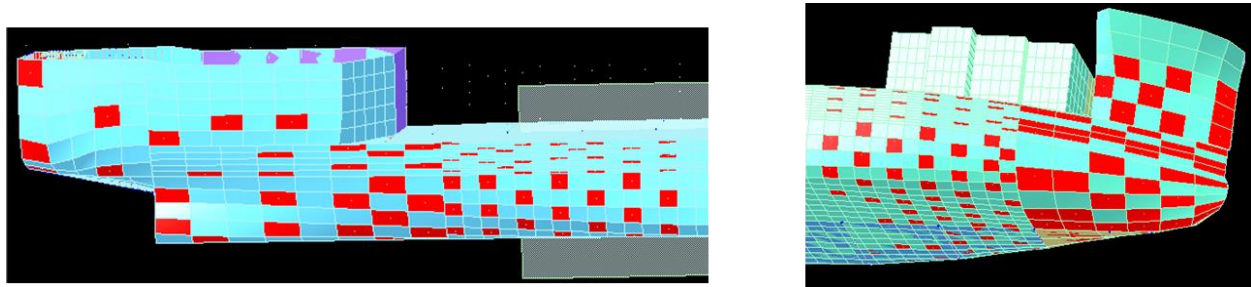


Figure 3-3: Aft-Hull and Fore-Hull 100 Panels (in Red) Where Pressure is Measured

3.1.2 Hydrodynamic Simulation Cases

Five different hydrodynamic simulation cases were analyzed, where the significant wave height and an associated wave modal period were varied between all cases, and the ship speed differs for some of these cases. The simulation cases were limited to head seas in long-crested waves to keep the number of inputs to the FEA model manageable.

The hydrodynamic simulations were also limited to a single draft condition. The AMCM Mission Loaded Departure condition was selected because it includes minimal sea water ballast in the tanks near midships, maximizing the hogging stresses, which are the most critical for the ESB, because the structural, machinery and outfitting weights are concentrated near the ends of the ship.

The run matrix of the modeled simulation cases is shown in Table 3-1.

Table 3–1: Hydrodynamic Analysis Run Matrix

Ship Speed		H1/3	Tm	Wave Heading		Crested	Draft	Trim	Duration	Run	Run	Run
knots	m/s	m	seconds	Degrees	words		m		seconds	Bow	mid	aft
										100 pts	100 pts	100 pts
16	8.23	4	9.7	180	Head Seas	Long	9.5	Level	1200			
9	4.63	6	12.4	180	Head Seas	Long	9.5	Level	1200			
5	2.57	9	15	180	Head Seas	Long	9.5	Level	1200			
5	2.57	11.5	15.7	180	Head Seas	Long	9.5	Level	1200			
5	2.57	14	16.4	180	Head Seas	Long	9.5	Level	1200			

The significant wave heights used in the investigation range from the top of sea state 5 to the top of sea state 8. The Bretschneider wave spectrum was used with the modal period for each significant wave height corresponding to the most probable. The duration of each run was kept low (20 minutes) to save analysis time because hydrodynamic simulation accuracy and statistical significance was not the goal but rather the modeling method development.

For a full analysis the run durations would be longer and/or more numerous to make sure the outputs are statistically significant. Also, the output values would be adjusted using, for example, Ochi's Method described in Reference 1, based on the projected duration in the given sea condition, and the acceptable probability of exceedance.

Table 3–2 shows that the 6m wave case (in green) with a 12.4 second modal period has almost the same wavelength as the ship length, which is the classical design case used to check the longitudinal strength of a ship balanced atop a wave crest at midships, maximizing hogging, or supported near its ends by two wave crests, maximizing sagging. Shorter and longer period waves tend to be less critical for longitudinal strength. This becomes relevant when trying to understand why 'smaller' waves sometimes produce higher stresses in the structural analyses covered later in this report.

Table 3–2: Comparison of Wavelength to Ship Length

Ship LOA	239.3	meters
Ship LBP	233.2	meters
H1/3	Tm	Lambda
meters	seconds	meters
4	9.7	146.9
6	12.4	240.0
9	15	351.2
11.5	15.7	384.7
14	16.4	419.8

A discussion of the range of conditions to model for a more complete analysis is included as Appendix A.

3.1.3 Hydrodynamic Data Output

The WASIM software allows for user-defined cut planes at which the program then calculates the 3-axis shear force and 3-axis bending moment time series. A cut plane was included near midships.

The maximum bending moments at the midship section over the course of the evaluated time series, for both hog and sag conditions, were identified. The pressure distribution at the associated time step was extracted for import to the FEA model. The 6DOF accelerations at the CG at this time step were also extracted for application to the FEA model. It is notable that the accelerations at the time of maximum hogging or sagging are not the maximum accelerations that occur throughout the whole time series.

3.2 Structural Model

3.2.1 FEMAP Model Grouping

The structural FEM used for the project began with a FEMAP v11.0.0 model of the ESB ship structure developed by NASSCO as a Detailed Design and Construction phase deliverable to the Navy. This model required substantial re-formatting to enable the analysis defined herein. For instance, the material and property cards required consolidation, and the element directionality and orientation were made common as required.

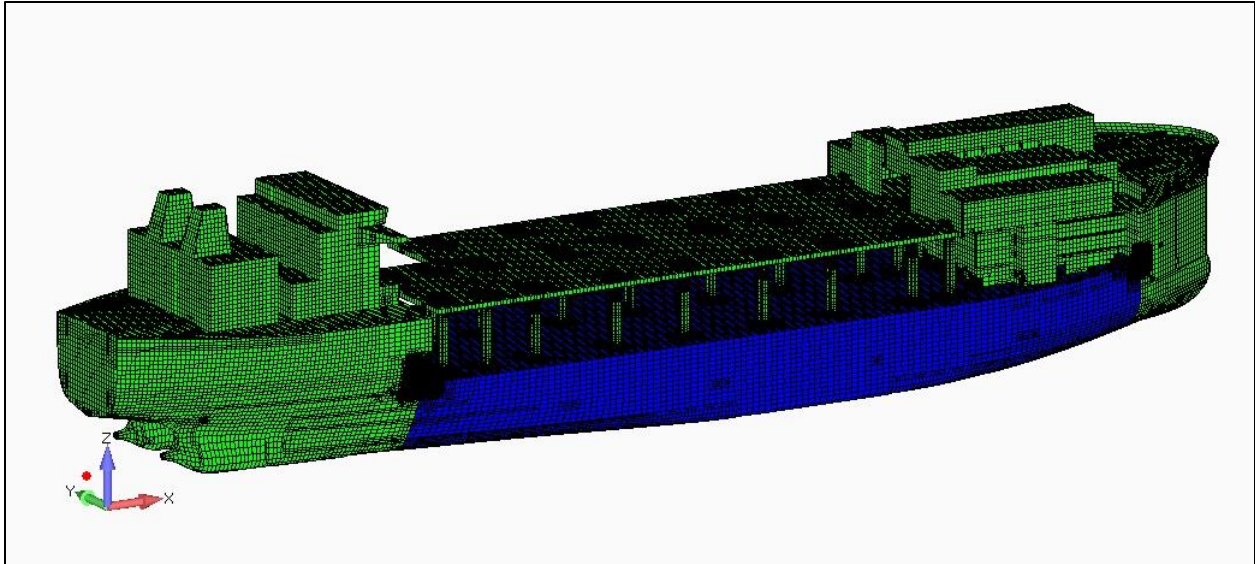


Figure 3-4: ESB Finite Element Model
(Midbody analysis region in **BLUE**)

The final model consists of 335,159 plate and 170,857 beam elements. The main structural components such as the shell, main deck, inner-bottom, longitudinal and transverse bulkheads, and the deck framing were all formed into separate groups within FEMAP.

These groups were further divided into the five (5) major sections of the midbody of the ESB vessel with each section break at a main transverse bulkhead. (See Figure 3-5 and Figure 3-6) These sections are numbered from aft (1) to forward (5).

The node spacing is approximately 1.3m, which provides a good balance between results fidelity and analysis manageability. At least one plate element exists between longitudinal stiffeners, with a minimum of three (3) elements between primary supporting members.

The ship is not constrained to ground with any pinned or fixed connections. Rather, inertial relief is employed which acts equal and opposite to the net pressure load which otherwise would lift the ship vertically.

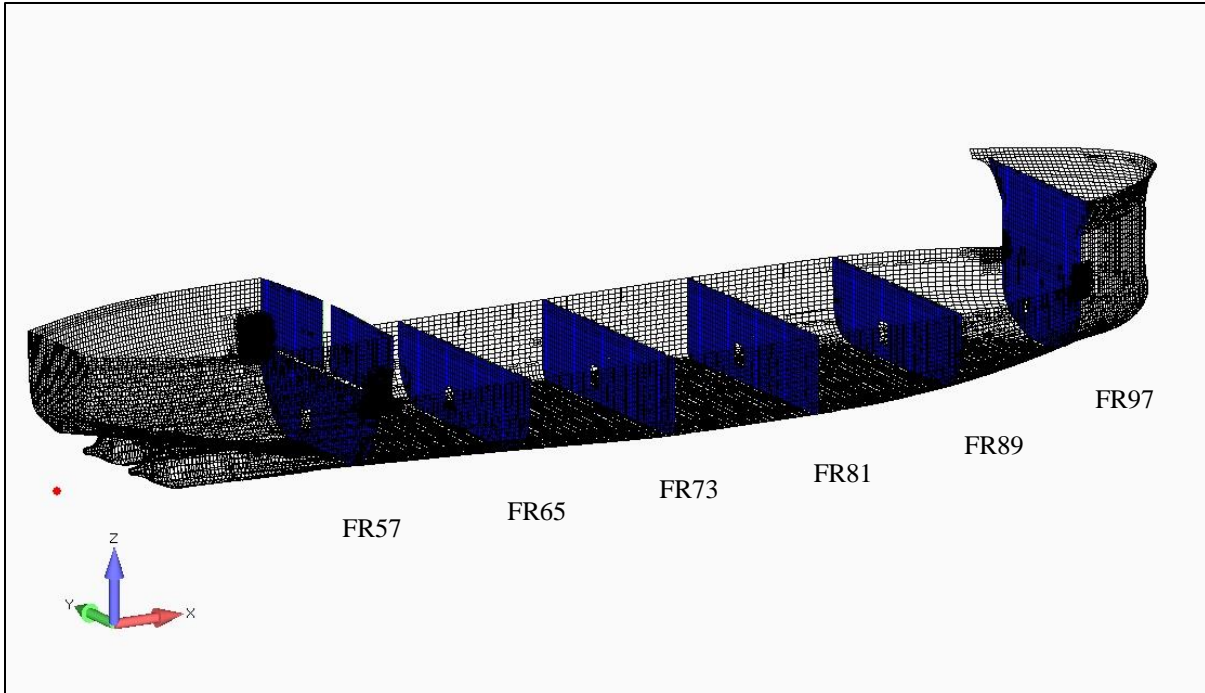


Figure 3-5: Main Transverse Bulkhead Locations

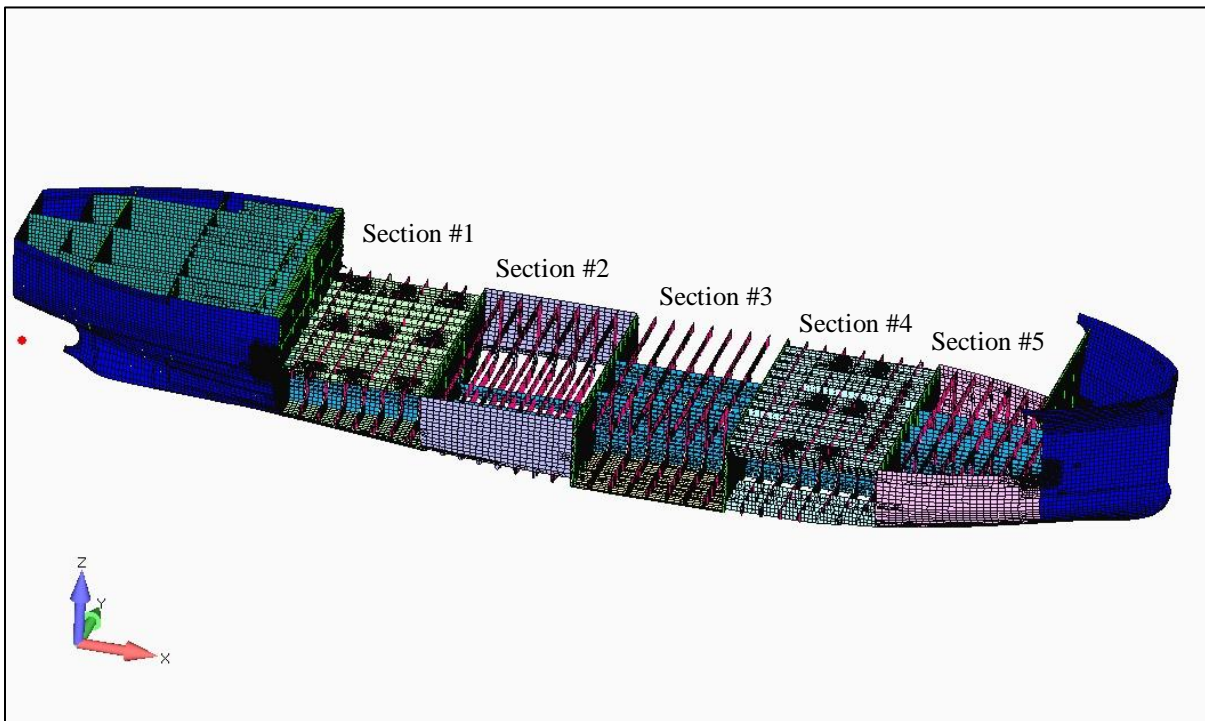


Figure 3-6: ESB Midbody Sections
(Each with different groupings displayed)

In addition, as FEMAP allows for the grouping of groups, the five midbody sections are each composed of the different groups of structural elements. Furthermore, the five sections of the midbody can be combined into a single group containing all of the elements within the midbody.

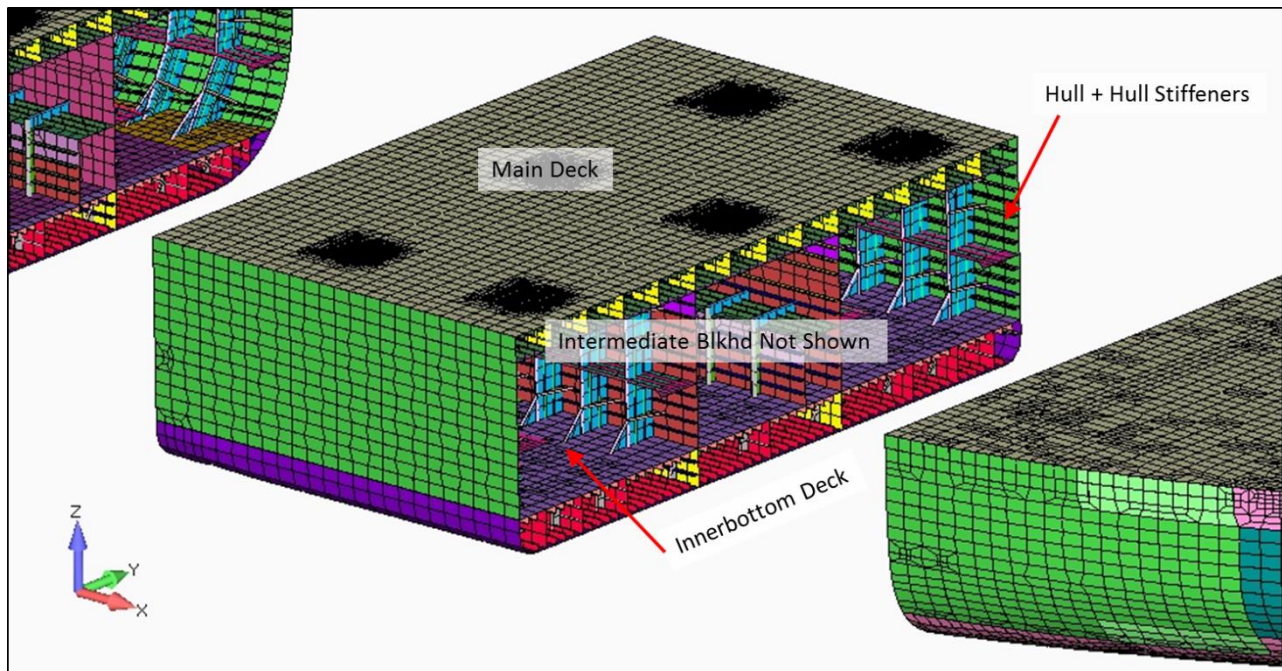


Figure 3-7: ESB Midbody Section Cutaway
(Flight Deck not shown for clarity)

3.2.2 Units

The structural analysis of the ESB was performed using the metric system units shown in the table below:

Table 3–3: System of Units used for the Structural Analysis of the ESB

Length	mm
Force	N
Mass	mT
Acceleration	mm/s ²
Pressure	MPa
Stress	MPa

3.2.3 Material Properties

The ESB is constructed of A-36 (Mild Steel) and AH-36 (High Strength Steel), with the higher strength AH-36 specified in the midbody. Material properties used in the FEA model for the ESB are specified in Table 3–4 below. Figure 3-8 shows where each is used.

Table 3-4: Structural Material Specifications

A-36 Steel	
Modulus of Elasticity	206000 MPa
Poisson's Ratio	0.3
Yield Stress	235 MPa
AH-36 Steel	
Modulus of Elasticity	206000 MPa
Poisson's Ratio	0.3
Yield Stress	355 MPa

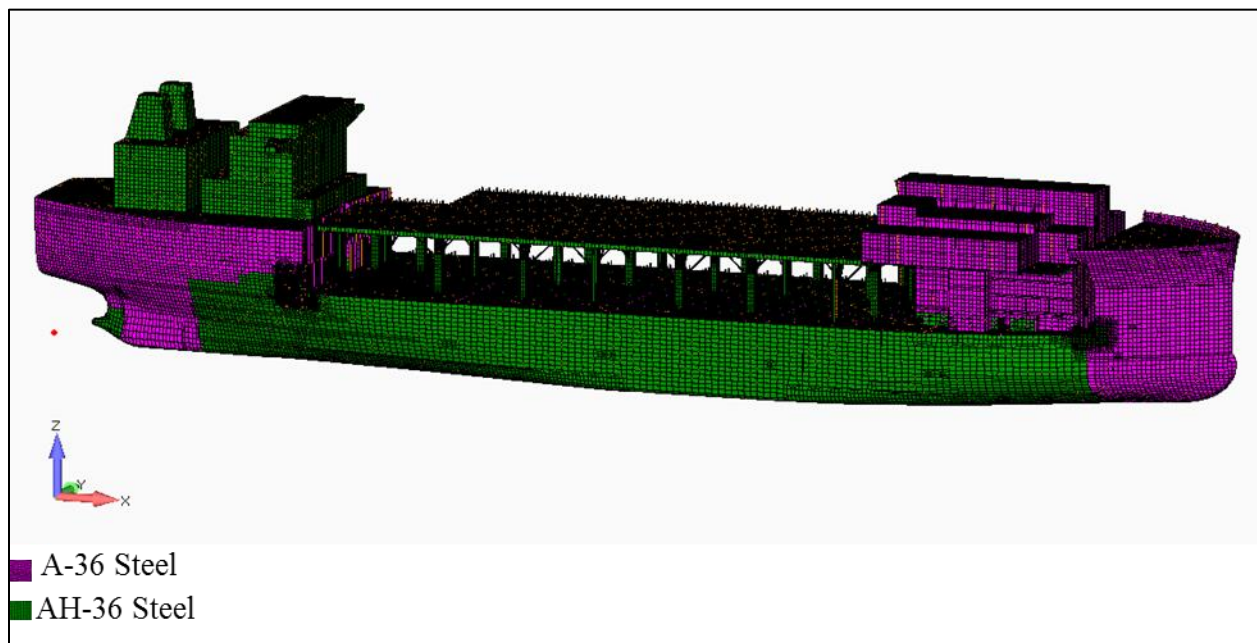


Figure 3-8: ESB Material Specification Key

3.2.4 Mass Modeling

To model the weight distribution of the AMCM Mission Loaded – Departure condition (9.5m draft) chosen for the study, the ship was divided into the 18 zones defined in the ESB Longitudinal Strength Assessment, Reference 3. The density of the steel in each zone was adjusted upward to match this loading condition's associated station weight, which includes not just steel but possibly ballast, fuel, machinery, outfitting, etc. To enable this process, structural groups were generated for each zone.

When the ship corrodes, the plating and stiffeners thin and therefore become lighter. To maintain a constant ship weight, the density in each zone is again adjusted to maintain the same weight in the zone, simulating the additional ballast that would be carried to achieve the desired draft. This process is repeated for each corrosion level analyzed.

The mass of the mission loaded ship at departure is 82,112mT. Table 3–5 shows the weight in each zone, which is plotted in Figure 3-9.

Table 3–5: ESB Longitudinal Weight Distribution Numbers

LOCATION	20.585	17	16	FR57	15	14	13	12	11
Approx FRAME	AP	46	56	57	59	62	65	67.5	71.5
Dist from AP	0	36.23	47.82	52.22	59.41	70.99	82.58	94.17	105.76
FEM WEIGHT	0	8676	4502	1814	2207	3147	3369	3702	3727

10	9	8	7	6	5	4	3	2	0	TOTAL
73	76	79	82	85	88	91	94	97	FP	
117.35	128.94	140.52	152.11	163.7	175.29	186.88	198.47	210.06	239.325	
4153	5337	5383	5545	5504	5625	6424	5671	4668	2658	82112

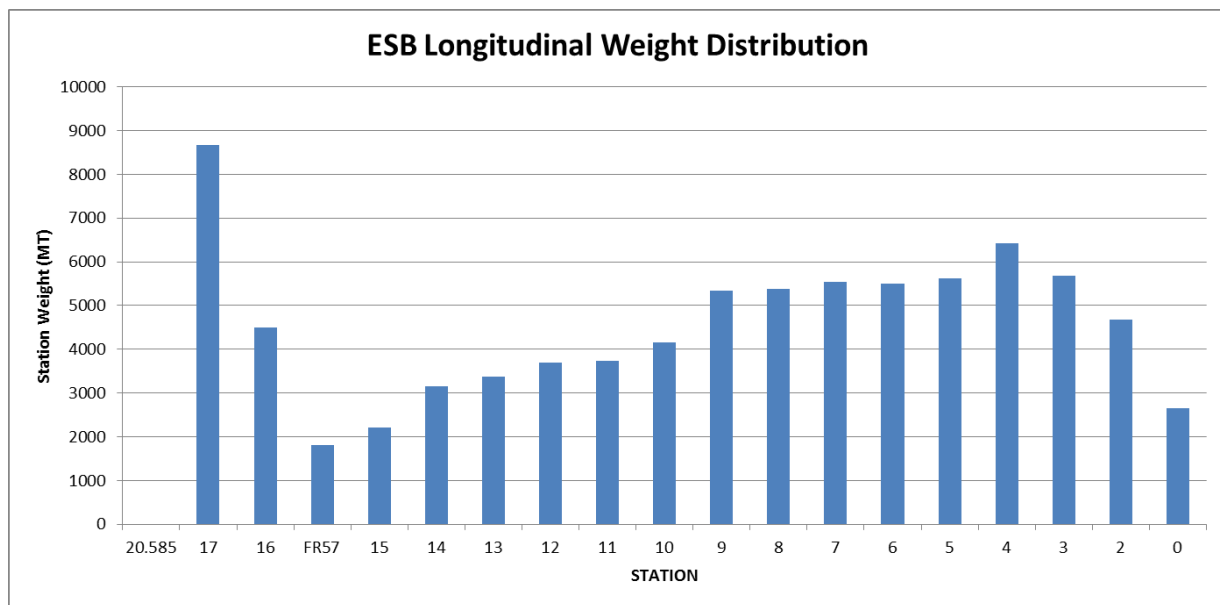


Figure 3-9: ESB Longitudinal Weight Distribution Graph

3.2.5 Corrosion Modeling

Corrosion is modeled at 0%, 25% (maximum allowable limit for renewal under Navy and ABS/IACS), 40%, 55%, and 70% as uniformly reduced plate & stiffener thicknesses across the whole ship (plating and both web and flange of stiffeners). This method of applying and modelling corrosion is conservative as it reduces the overall hull girder strength rather than reducing strength locally, increasing the ship’s overall deflection and stress for a given load case. The higher percent wastages were included in this study in order to incorporate realistic situations where corrosion wastages may be in excess of 25% and the ship is required to be operating at sea.

The procedures and files used to parse the geometrical properties from the property card listings, and the steps required to corrode and then update the structure's inertial values and re-establish the proper mass are outlined in Appendix C.

3.2.6 Load Application

The wave pressure and body CG acceleration data from the WASIM seakeeping model must be translated into the FEMAP model and combined to produce the loadsets required for analysis. The process for importing the wave pressure and body CG acceleration data is outlined below:

- Mirror pressure inputs from port to starboard (for head seas only)
- Convert pressure and location units
- Import pressures at pseudo-node locations into FEMAP
- Expand pressure application to all submerged plating panels using FEMAP interpolation controls
- Generate display of wave pressure from loading input and inspect.
- Generate loadsets by combining body CG accelerations and wave pressure loads.

Figure 3-10 illustrates the location of the 300 pseudo-nodes representing the center of port-side pressure panels from WASIM (yellow marks). These pressure values are mirrored to the corresponding starboard side locations to represent the head seas conditions modeled and the units adjusted in an EXCEL file. Using the Data Surface Tool within FEMAP the discrete pressure locations are interpolated across the entire surface of the submerged hull. Proper selection of the built-in interpolation controls allows for the smooth pressure distribution shown in Figure 3-10. Details of this process and the remaining nine (9) hull pressure distributions examined as part of this analysis are included in Appendix C.

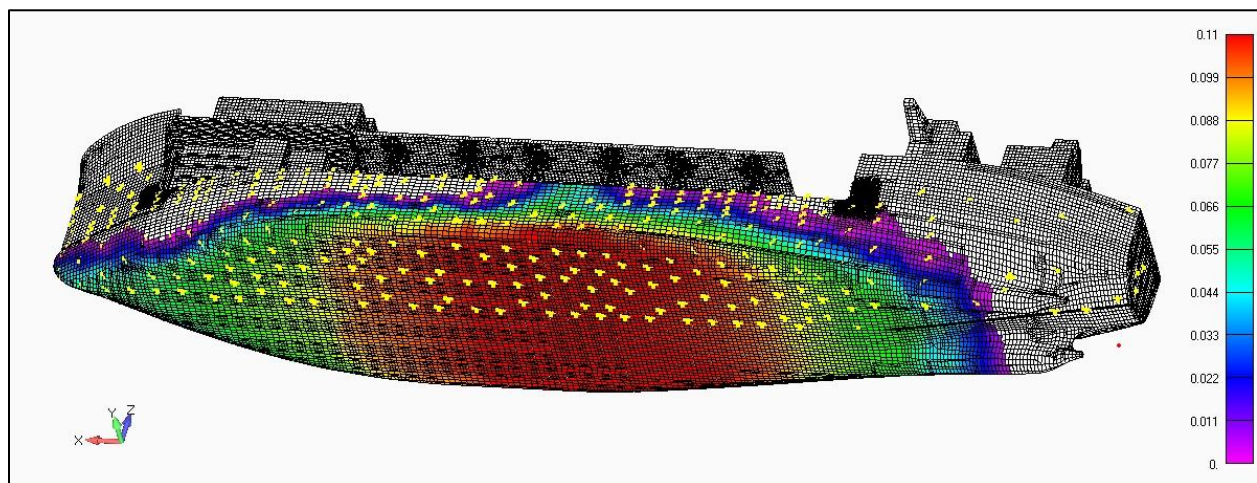


Figure 3-10: Pressure Point Locations and 14m Hog Wave Pressure Distribution

Table 3-6 contains the acceleration data of the ship's CG from the WASIM output. It is noted that these acceleration values are from the time step that produced the largest bending moment at the midship location for the given significant wave height and are not necessarily the highest acceleration during the 20 minute run.

The wave-induced pressure load is then combined with the 3 translational and 1 rotational body acceleration to form the ten (10) loadsets initially used in the analysis. A_z is a combination of gravity (-1g) and the vertical acceleration. The acceleration values are low compared to typical structural design accelerations associated with long-term exposure.

Table 3–6: Acceleration Data

WAVE		A_x	A_y	A_z	R_y
(m)	Type	(G's)			(rad/s ²)
14	HOG	-0.122	-0.119	-1.108	0.025
	SAG	0.180	0.067	-1.039	-0.004
11.5	HOG	-0.067	-0.077	-1.187	0.024
	SAG	0.139	0.063	-1.005	-0.005
9	HOG	-0.096	-0.107	-1.084	0.023
	SAG	0.135	0.074	-1.050	-0.005
6	HOG	-0.054	-0.061	-1.023	0.011
	SAG	0.088	0.068	-1.008	-0.010
4	HOG	-0.006	-0.015	-1.044	-0.001
	SAG	0.021	0.028	-0.983	-0.006

3.2.7 Load Cases

Initially, both hog and sag cases were run at both the baseline (0% corroded) and 25% corroded for all wave cases. After analyzing the response it was determined that in the maximum sag case the midbody sees much lower stresses than in the maximum hog condition. The reason for this is the ship selected for this project has a natural hog in still water. The low stresses in the main deck are unlikely to produce a buckling response. The higher wastage percentage runs were therefore limited to the maximum hog cases for the final runs, and no structural analysis was undertaken on the maximum sag cases. The final load cases analyzed are numbered and listed below in Table 3–7.

Table 3-7: Final Load Cases (All Hogging)

LOAD CASE	H _{1/3} (m)	Ship Speed (knots)	Percent Corroded
1	4	16	0
2	6	9	0
3	9	5	0
4	11.5	5	0
5	14	5	0
6	4	16	25
7	6	9	25
8	9	5	25
9	11.5	5	25
10	14	5	25
11	4	16	40
12	6	9	40
13	9	5	40
14	11.5	5	40
15	14	5	40
16	4	16	55
17	6	9	55
18	9	5	55
19	11.5	5	55
20	14	5	55
21	4	16	70
22	6	9	70
23	9	5	70
24	11.5	5	70
25	14	5	70

3.3 Yielding Criteria

An assessment against yielding criteria defined in the IACS Common Structural Rules was performed. The midbody sections are constructed of AH-36 Steel, therefore the mild steel base yield strength of 235 MPa is divided by the AH-36 material factor of .72 for an allowable stress of 326.4 MPa as described in Part 1, Chapter 3, Section 1, 2.2.1. This allowable stress criteria is compared against the Von Mises stress results from the FEA model to calculate a yielding evaluation ratio (FEA model stress/allowable stress).

3.4 Buckling Criteria

Buckling assessment is performed in accordance with the IACS Common Structural Rules.

3.4.1 Plate Buckling

The limit stress in the plating must satisfy four (4) separate interaction formulas. The equations in section 2.2.1 of Reference 4 are simplified and rewritten as 4 separate Buckling Coefficients (BC), the largest of which is the limiting case and which must remain less than unity to indicate a no-buckling response:

$$\left(\frac{\sigma_x}{\sigma_{cx}} \right)^{e_0} - B * \left(\frac{\sigma_x}{\sigma_{cx}} \right)^{e_0/2} * \left(\frac{\sigma_y}{\sigma_{cy}} \right)^{e_0/2} + \left(\frac{\sigma_y}{\sigma_{cy}} \right)^{e_0} + \left(\frac{|\tau|}{\tau_c} \right)^{e_0} = BC_1$$

$$\left(\frac{\sigma_x}{\sigma_{cx}} \right)^{2/Bp0.25} + \left(\frac{|\tau|}{\tau_c} \right)^{2/Bp0.25} = BC_2$$

$$\left(\frac{\sigma_y}{\sigma_{cy}} \right)^{2/Bp0.25} + \left(\frac{|\tau|}{\tau_c} \right)^{2/Bp0.25} = BC_3$$

$$\frac{|\tau|}{\tau_c} = BC_4$$

The variables e_0 and B , and Bp are geometry and material dependent factors as defined in Section 2.2.1 of Reference 4. The ultimate buckling stress terms (σ_{cx} , σ_{cy} , τ_c) are dependent on the stiffened panel edge conditions and the stiffener type (Tee, Bulb, Flat bar, etc) and are defined in Sect. 2.2.3 of the same reference.

3.4.2 Stiffener Buckling

The single buckling coefficient (BC) that determines the initiation of stiffener buckling is composed of three (3) stress components that are combined and compared to the material yield stress. These stress components are the effective axial stress (σ_a) acting at the midspan of the stiffener, the bending stress (σ_b) due to lateral pressure loading, and the stress due to torsional deformation (σ_w).

$$\left(\sigma_a + \sigma_b + \sigma_w \right) / F_{TY} = BC$$

The derivation of each stress term is described in detail in Appendix D. The computation of these variables was easily accomplished in an EXCEL spreadsheet.

4 STRUCTURAL ANALYSIS

Analysis of the FEMAP model is carried out with the NeiNastran solver (v10.1.0.410). As previously noted, the still water bending moment of ESB class vessel produces a hog response. This is mainly due to the ships unequal weight distribution with more weight concentrated in the ends. Therefore in small waves (whether analyzing the maximum hog or maximum sag case) the ship bridges over multiple waves and there is little difference in the plate or stiffener stress (or buckling) response from the still water condition. In fact, the 14m maximum sag wave is the only condition that produced a sag response in the ship. As this sag response is working against the still water hog condition it generates minimal stress in the hull and main deck as shown in Figure 4-1. Conversely, a hog wave reinforces the natural hog response of the ship, resulting in significant stresses as seen in Figure 4-2.

For the buckling analyses, the normal stress in the X (longitudinal) and Y (transverse) directions are utilized. From the 14m maximum hog von mises stress plot shown in Figure 4-3 it is clear that the main deck is in tension while the lower hull experiences compressive stress.

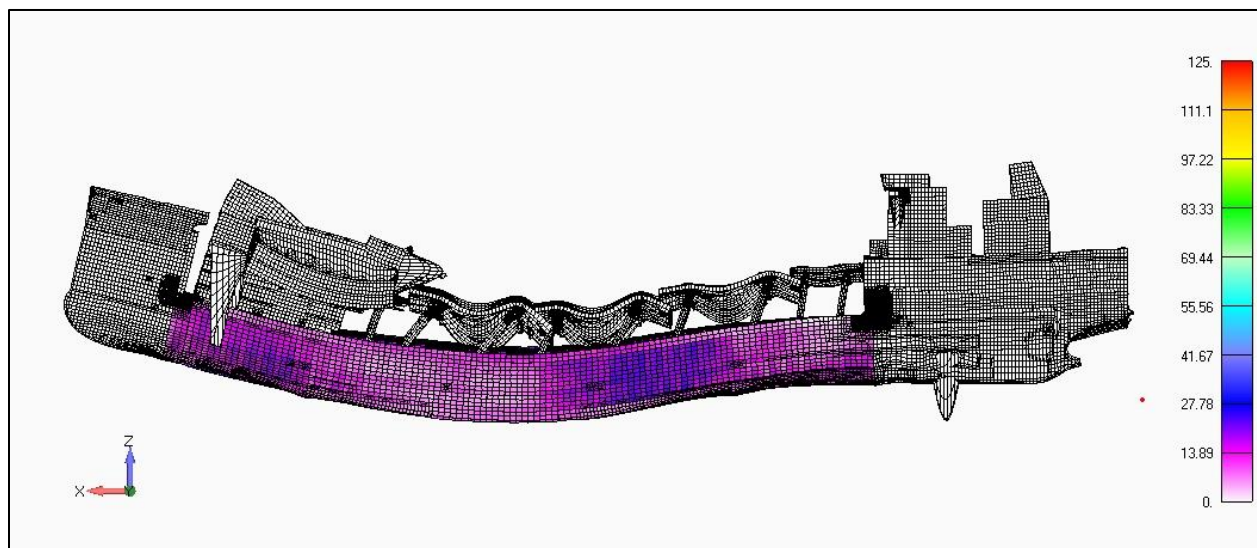


Figure 4-1: 0% Corroded (14m) Maximum Sag - Von Mises Stress Plot

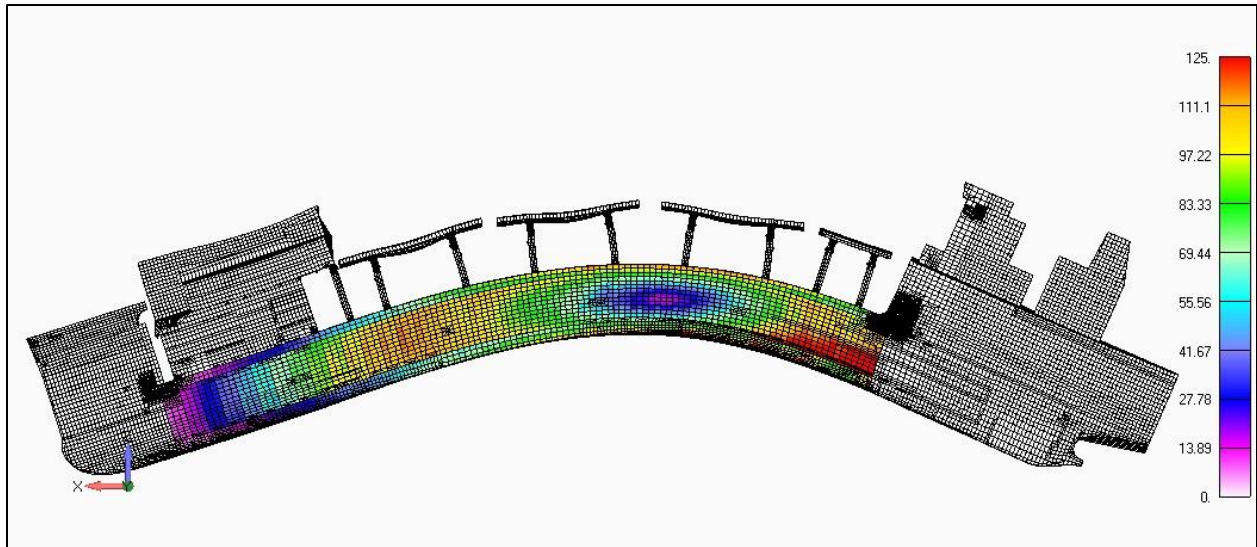


Figure 4-2: 0% Corroded (14m) Maximum Hog - Von Mises Stress Plot

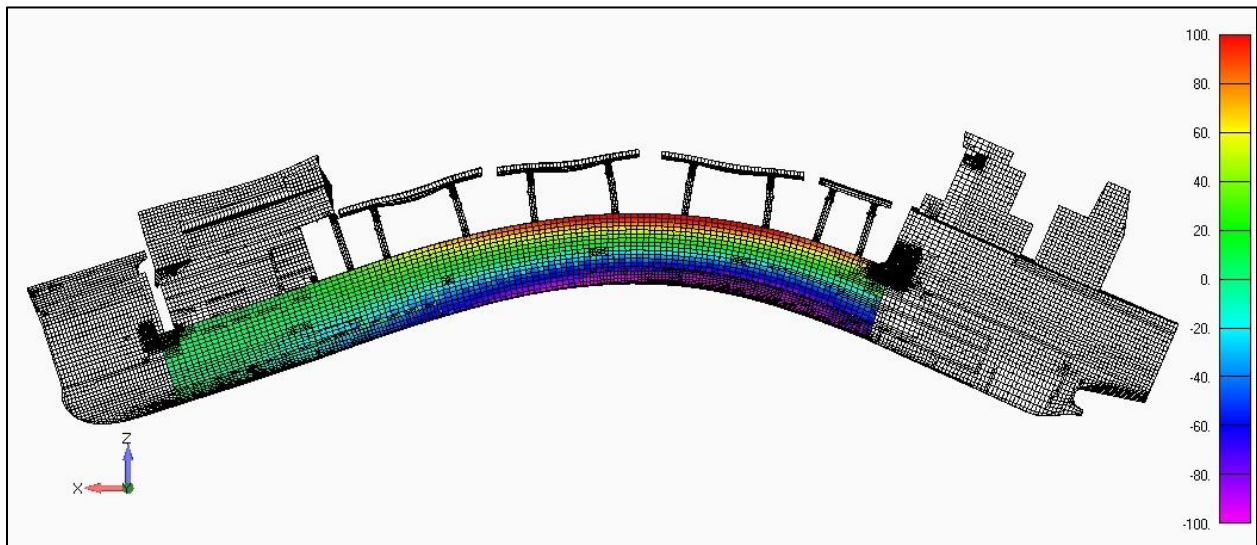


Figure 4-3: 0% Corroded (14m) Maximum Hog - Normal X Stress Plot

4.1 Model Plots and Stress Results

A maximum yielding assessment of the various groups in each midbody section are presented in

Table 4–1 below including the maximum ratio of calculated stress to allowable stress. Purple shading indicates where stresses exceed allowable and yellow shading indicates where they are close to exceeding allowable. Plots showing the 0% corrosion stress distribution in each of these structural groups are seen in Figure 4-4 through Figure 4-12. The 14m maximum hog load case typically produced the maximum von mises stresses at the various corrosion levels. The maximum stresses for the 70% corroded case far exceeded the material yield strength and therefore were not included in the results.

Table 4-1: Maximum Yielding Assessment Results

Group	Midbody Section	0% Corroded		25% Corroded			40% Corroded			55% Corroded			
		VM Stress	Ratio	VM Stress	Ratio	% Increase	VM Stress	Ratio	% Increase	VM Stress	Ratio	% Increase	
Hull Plating	1	161	0.49	216	0.66	34%	271	0.83	68%	355	1.09	120%	
	2	165	0.51	211	0.65	28%	257	0.79	56%	336	1.03	104%	
	3	125	0.38	161	0.49	29%	203	0.62	62%	278	0.85	122%	
	4	148	0.45	198	0.61	34%	251	0.77	70%	332	1.02	124%	
	5	95	0.29	164	0.50	73%	254	0.78	167%	446	1.37	369%	
Main Deck Upper Plating	1	190	0.58	250	0.77	32%	308	0.94	62%	400	1.23	111%	
	2	165	0.51	208	0.64	26%	255	0.78	55%	324	0.99	96%	
	3	143	0.44	184	0.56	29%	226	0.69	58%	291	0.89	103%	
	4	108	0.33	131	0.40	21%	159	0.49	47%	205	0.63	90%	
	5	40	0.12	50	0.15	25%	60	0.18	50%	78	0.24	95%	
Main Deck Lower Plating	1	140	0.43	188	0.58	34%	234	0.72	67%	304	0.93	117%	
	2	103	0.32	133	0.41	29%	165	0.51	60%	217	0.66	111%	
	3	105	0.32	133	0.41	27%	165	0.51	57%	216	0.66	106%	
	4	84	0.26	111	0.34	32%	139	0.43	65%	183	0.56	118%	
	5	49	0.15	64	0.20	31%	80	0.25	63%	104	0.32	112%	
Main Deck Framing	1	265	0.81	343	1.05	29%	425	1.30	60%	551	1.69	108%	
	2	277	0.85	358	1.10	29%	443	1.36	60%	579	1.77	109%	
	3	236	0.72	305	0.93	29%	379	1.16	61%	503	1.54	113%	
	4	205	0.63	278	0.85	36%	346	1.06	69%	465	1.42	127%	
	5	103	0.32	131	0.40	27%	162	0.50	57%	215	0.66	109%	
Inner Bottom Plating	1	152	0.47	195	0.60	28%	235	0.72	55%	292	0.89	92%	
	2	117	0.36	154	0.47	32%	192	0.59	64%	250	0.77	114%	
	3	87	0.27	113	0.35	30%	140	0.43	61%	183	0.56	110%	
	4	71	0.22	94	0.29	32%	117	0.36	65%	154	0.47	117%	
	5	53	0.16	69	0.21	30%	85	0.26	60%	112	0.34	111%	
Inner Bottom Framing	1	163	0.50	208	0.64	28%	258	0.79	58%	337	1.03	107%	
	2	206	0.63	271	0.83	32%	341	1.04	66%	451	1.38	119%	
	3	137	0.42	184	0.56	34%	229	0.70	67%	301	0.92	120%	
	4	105	0.32	136	0.42	30%	171	0.52	63%	224	0.69	113%	
	5	66	0.20	87	0.27	32%	109	0.33	65%	143	0.44	117%	
Longitudinal Bulkheads	1	222	0.68	290	0.89	31%	365	1.12	64%	483	1.48	118%	
	2	103	0.32	134	0.41	30%	168	0.51	63%	220	0.67	114%	
	3	143	0.44	187	0.57	31%	233	0.71	63%	307	0.94	115%	
	4	200	0.61	259	0.79	30%	326	1.00	63%	429	1.31	115%	
	5	110	0.34	143	0.44	30%	180	0.55	64%	235	0.72	114%	
Transverse Frames & Blkhds	Blkhd 64	86	0.26	112	0.34	30%	139	0.43	62%	181	0.55	110%	
	FR 65 -> 71	1	174	0.53	243	0.74	303	0.93	74%	405	1.24	133%	
	Blkhd 72	73	0.22	100	0.31	37%	125	0.38	71%	166	0.51	127%	
	FR 73 -> 79	2	182	0.56	257	0.79	318	0.97	75%	421	1.29	131%	
	Blkhd 80	81	0.25	109	0.33	35%	137	0.42	69%	183	0.56	126%	
	FR 81 -> 87	3	213	0.65	300	0.92	41%	375	1.15	76%	503	1.54	136%
	Blkhd 88	75	0.23	101	0.31	35%	126	0.39	68%	168	0.51	124%	
	FR 89 -> 95	4	205	0.63	278	0.85	36%	346	1.06	69%	465	1.42	127%
	Blkhd 96	157	0.48	200	0.61	27%	246	0.75	57%	319	0.98	103%	
	FR 97 -> 103	5	99	0.30	129	0.40	30%	162	0.50	64%	215	0.66	117%
Blkhd 104	19	0.06	25	0.08	32%	31	0.09	63%	42	0.13	121%		

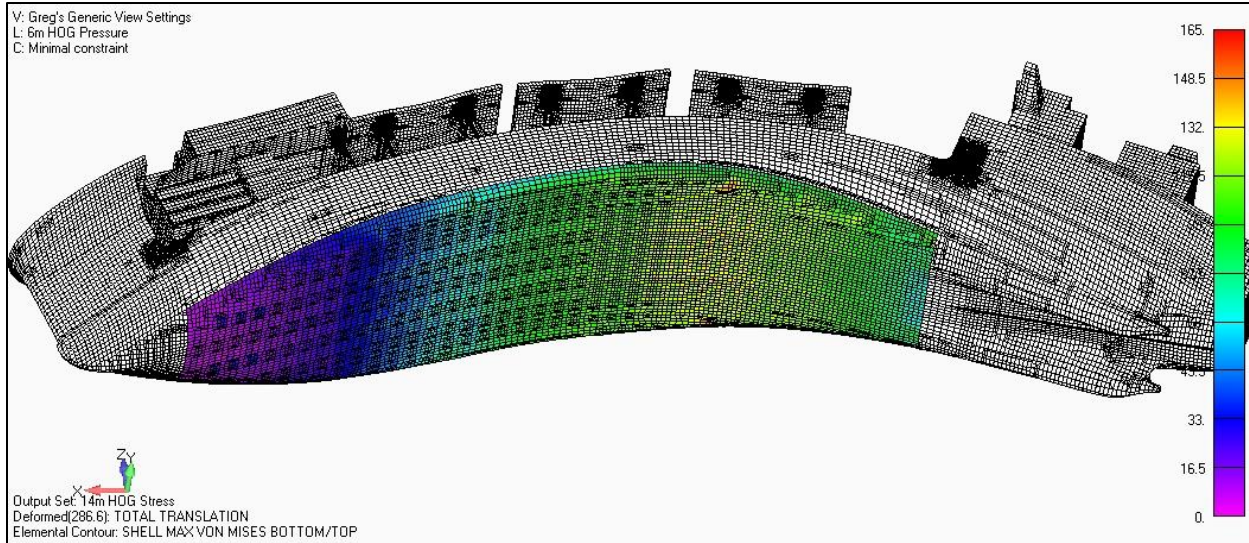


Figure 4-4: Hull Bottom Plating - 0% Corrosion – 14m Hog – Von Mises Stress

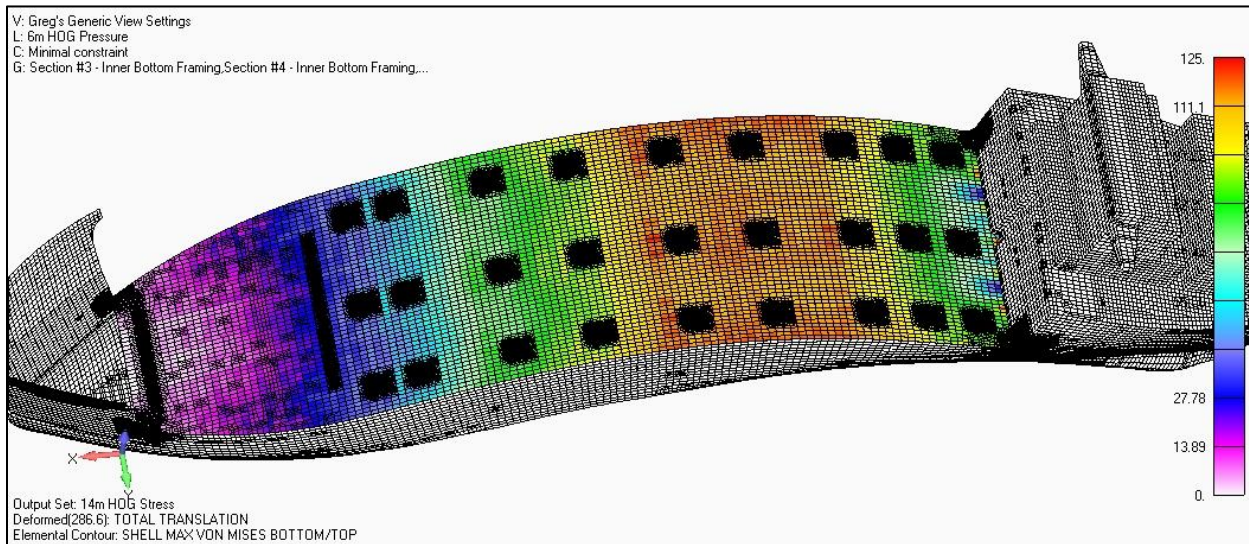


Figure 4-5: Main Deck Plating – 0% Corrosion – 14m Hog – Von Mises Stress

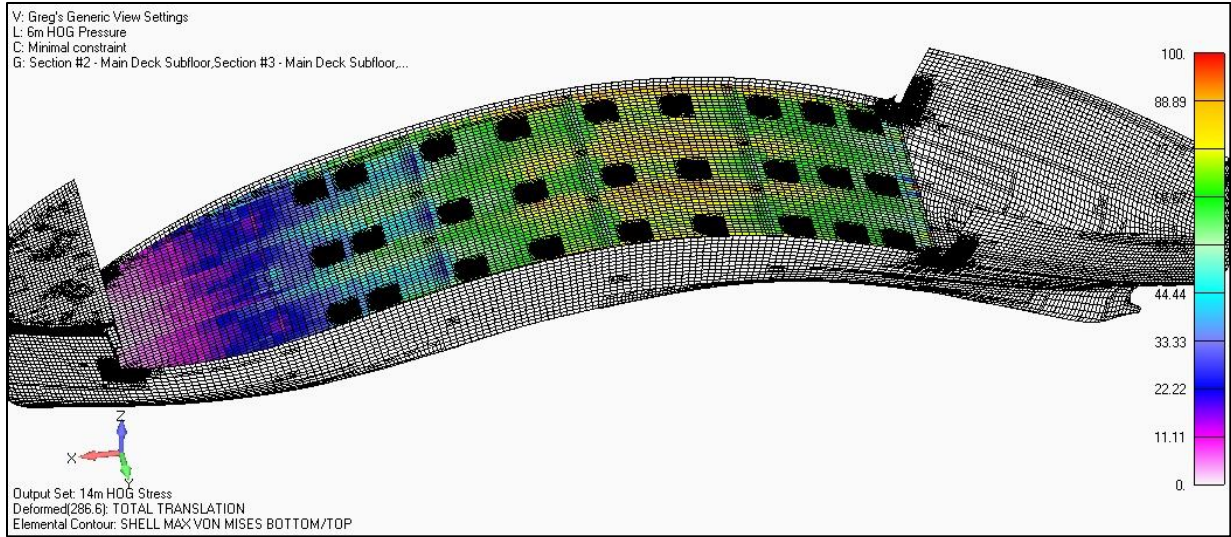


Figure 4-6: Main Deck Inner Top Plating - 0% Corrosion – 14m Hog – Von Mises Stress

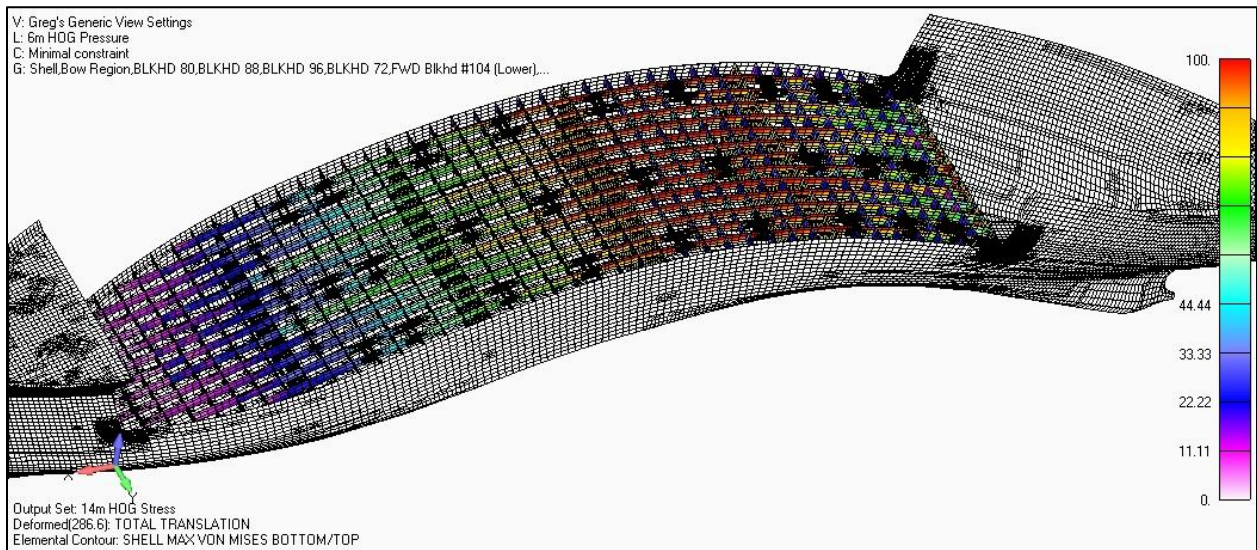


Figure 4-7: Main Deck Framing - 0% Corrosion – 14m Hog – Von Mises Stress

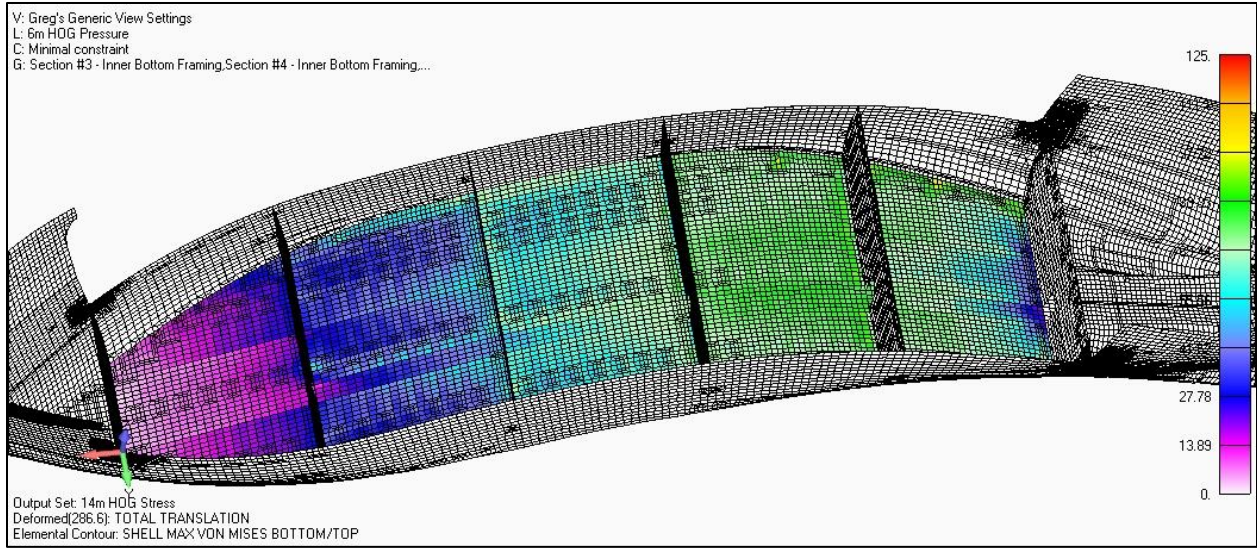


Figure 4-8: Inner Bottom Plating – 0% Corrosion – 14m Hog – Von Mises Stress

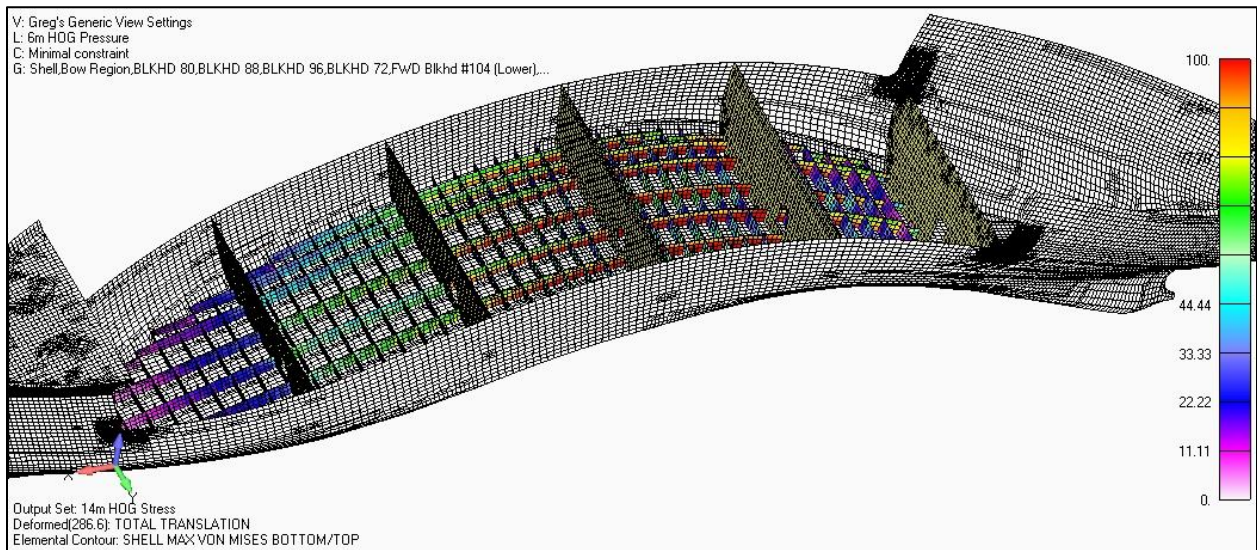


Figure 4-9: Inner Bottom Framing – 0% Corrosion – 14m Hog – Von Mises Stress

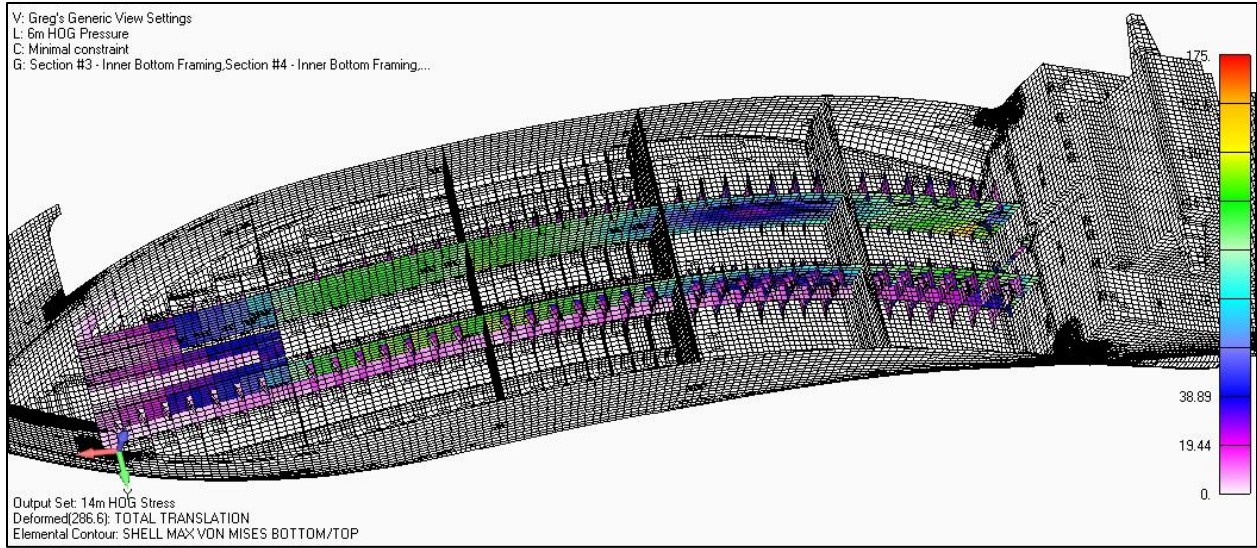


Figure 4-10: Long'l Blkhd's – 0% Corrosion – 14m Hog – Von Mises Stress

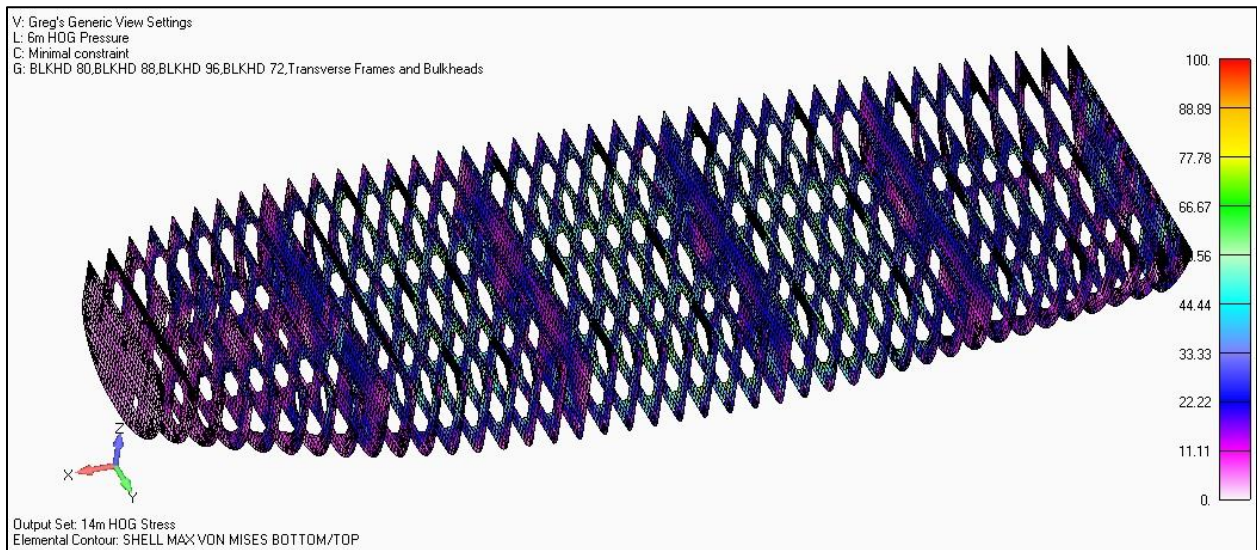


Figure 4-11: Transverse Frames and Bulkheads – 0% Corrosion – 14m Hog – Von Mises Stress

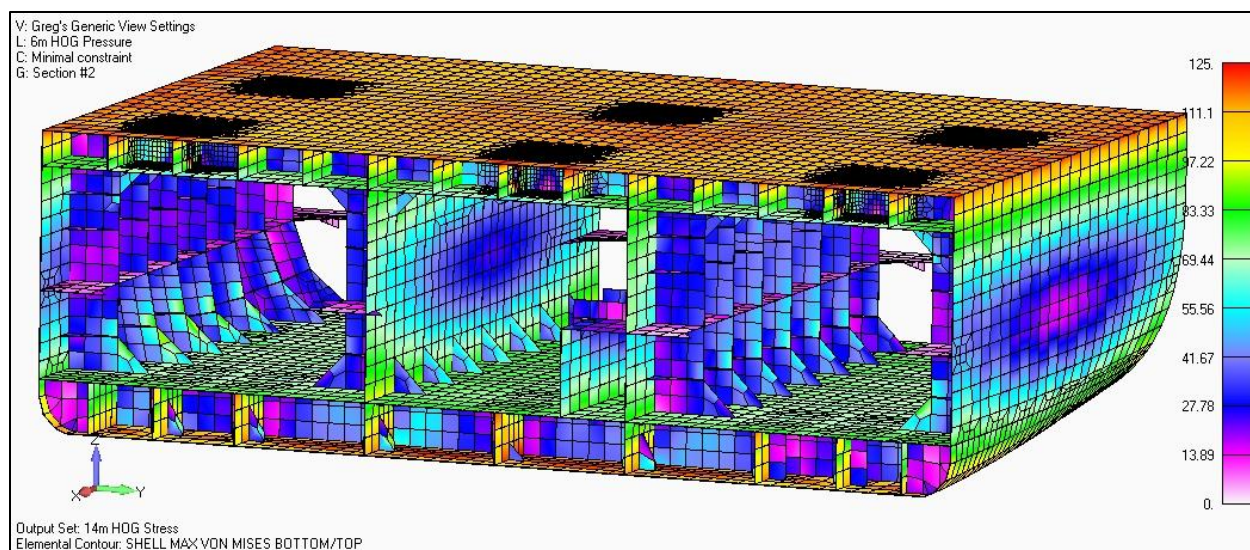


Figure 4-12: Section 2 – 0% Corrosion – 14m Hog – Von Mises Stress

4.2 Determining Buckling Capacities

Buckling capacities were determined using the IACS Common Structural Rules. The buckling coefficients (BC) were determined at each wave state and corrosion level for the maximum hog condition. A detailed explanation of the procedure employed to determine buckling coefficients is included in Appendix D.

4.2.1 Buckling Strength – Hull Bottom Longitudinal Stiffeners

The buckling coefficients calculated for the hull bottom longitudinal stiffeners in the various significant wave heights for corrosion levels of 0%, 25% and 40% are shown in Table 4–2. All are below 1.0 so are acceptable.

Table 4–2: ESB Hull Bottom Longitudinal Stiffener Buckling Response for 0%, 25% & 40% Corrosion

Long'l	CORROSION = 0%					CORROSION = 25%					CORROSION = 40%				
	14m	11.5m	9m	6m	4m	14m	11.5m	9m	6m	4m	14m	11.5m	9m	6m	4m
-27															
-26	0.496	0.404	0.354	0.235	0.233	0.627	0.508	0.443	0.290	0.287	0.801	0.650	0.567	0.372	0.372
-25															
-24	0.598	0.495	0.464	0.355	0.347	0.763	0.629	0.590	0.448	0.437	0.978	0.807	0.757	0.577	0.577
-23	0.508	0.424	0.412	0.326	0.322	0.654	0.543	0.528	0.414	0.409	0.836	0.695	0.676	0.532	0.532
-22	0.522	0.435	0.424	0.335	0.331	0.667	0.554	0.539	0.424	0.418	0.853	0.709	0.691	0.544	0.544
-21															
-20	0.454	0.380	0.349	0.279	0.276	0.597	0.497	0.462	0.370	0.366	0.750	0.627	0.584	0.471	0.471
-19	0.461	0.368	0.354	0.287	0.289	0.604	0.487	0.466	0.372	0.371	0.758	0.614	0.589	0.472	0.472
-18	0.461	0.372	0.352	0.281	0.279	0.604	0.493	0.468	0.376	0.374	0.759	0.622	0.590	0.478	0.478
-17	0.463	0.387	0.357	0.276	0.276	0.608	0.492	0.472	0.355	0.350	0.763	0.621	0.597	0.453	0.453
-16															
-15	0.461	0.385	0.358	0.283	0.280	0.605	0.504	0.474	0.354	0.350	0.759	0.635	0.599	0.479	0.479
-14	0.461	0.385	0.354	0.280	0.277	0.605	0.504	0.469	0.372	0.368	0.759	0.635	0.593	0.473	0.473
-13	0.456	0.380	0.354	0.279	0.276	0.598	0.497	0.469	0.370	0.367	0.751	0.626	0.593	0.471	0.471
-12	0.457	0.380	0.350	0.274	0.271	0.598	0.498	0.463	0.364	0.361	0.752	0.627	0.586	0.463	0.463
-11	0.453	0.377	0.351	0.275	0.272	0.594	0.493	0.464	0.364	0.360	0.746	0.621	0.586	0.463	0.463
-10	0.455	0.378	0.348	0.272	0.268	0.597	0.495	0.460	0.360	0.355	0.749	0.624	0.582	0.458	0.458
-9	0.453	0.376	0.347	0.271	0.266	0.595	0.492	0.459	0.358	0.353	0.747	0.620	0.580	0.456	0.456
-8															
-7	0.449	0.372	0.347	0.271	0.267	0.589	0.489	0.460	0.359	0.353	0.740	0.615	0.581	0.458	0.458
-6	0.454	0.377	0.349	0.273	0.269	0.595	0.494	0.462	0.361	0.356	0.747	0.622	0.584	0.461	0.461
-5	0.456	0.379	0.353	0.277	0.272	0.598	0.497	0.466	0.366	0.360	0.751	0.626	0.589	0.466	0.466
-4	0.462	0.385	0.354	0.276	0.272	0.605	0.503	0.466	0.366	0.360	0.759	0.634	0.590	0.466	0.466
-3	0.462	0.385	0.357	0.280	0.276	0.605	0.504	0.473	0.371	0.366	0.760	0.634	0.597	0.473	0.473
-2	0.467	0.390	0.359	0.281	0.277	0.612	0.510	0.474	0.372	0.367	0.768	0.643	0.599	0.474	0.474
-1	0.468	0.390	0.363	0.285	0.281	0.614	0.512	0.480	0.378	0.372	0.771	0.644	0.607	0.481	0.481
0															
1	0.470	0.392	0.362	0.285	0.281	0.616	0.514	0.480	0.377	0.372	0.774	0.648	0.607	0.480	0.480
2	0.467	0.390	0.362	0.272	0.281	0.613	0.511	0.480	0.358	0.353	0.770	0.644	0.606	0.456	0.456
3	0.469	0.391	0.361	0.282	0.278	0.614	0.512	0.474	0.373	0.368	0.771	0.645	0.599	0.476	0.476
4	0.463	0.386	0.359	0.282	0.278	0.607	0.505	0.474	0.374	0.368	0.762	0.636	0.599	0.476	0.476
5	0.463	0.386	0.355	0.278	0.274	0.607	0.505	0.469	0.368	0.363	0.762	0.636	0.593	0.469	0.469
6	0.456	0.379	0.354	0.277	0.273	0.598	0.497	0.468	0.367	0.362	0.752	0.626	0.592	0.468	0.468
7	0.452	0.375	0.350	0.274	0.270	0.594	0.492	0.464	0.363	0.357	0.746	0.620	0.586	0.463	0.463
8															
9	0.456	0.378	0.349	0.273	0.269	0.598	0.496	0.462	0.361	0.356	0.752	0.625	0.584	0.460	0.460
10	0.456	0.379	0.351	0.275	0.270	0.599	0.497	0.464	0.363	0.358	0.752	0.626	0.587	0.463	0.463
11	0.459	0.382	0.351	0.274	0.270	0.601	0.499	0.464	0.363	0.359	0.754	0.629	0.586	0.463	0.463
12	0.456	0.380	0.354	0.278	0.274	0.598	0.497	0.468	0.368	0.364	0.751	0.626	0.592	0.468	0.468
13	0.462	0.385	0.354	0.277	0.274	0.604	0.504	0.468	0.368	0.365	0.759	0.634	0.592	0.469	0.469
14	0.461	0.384	0.358	0.272	0.269	0.604	0.504	0.474	0.359	0.354	0.759	0.634	0.599	0.458	0.458
15	0.465	0.388	0.359	0.269	0.265	0.610	0.509	0.475	0.356	0.351	0.765	0.641	0.601	0.453	0.453
16															
17	0.463	0.374	0.359	0.272	0.274	0.608	0.496	0.475	0.353	0.348	0.764	0.626	0.600	0.450	0.450
18	0.465	0.371	0.352	0.278	0.277	0.610	0.491	0.467	0.372	0.370	0.765	0.620	0.590	0.472	0.472
19	0.460	0.371	0.355	0.285	0.287	0.603	0.491	0.464	0.372	0.369	0.757	0.619	0.586	0.472	0.472
20	0.457	0.382	0.351	0.264	0.262	0.599	0.500	0.465	0.351	0.348	0.752	0.630	0.587	0.447	0.447
21															
22	0.522	0.435	0.424	0.335	0.330	0.667	0.554	0.539	0.423	0.417	0.853	0.709	0.690	0.543	0.543
23	0.508	0.424	0.412	0.325	0.321	0.653	0.542	0.527	0.413	0.408	0.835	0.694	0.675	0.531	0.531
24	0.599	0.496	0.465	0.356	0.348	0.764	0.630	0.591	0.449	0.439	0.979	0.809	0.759	0.578	0.578
25															
26	0.496	0.405	0.355	0.236	0.234	0.628	0.510	0.445	0.292	0.289	0.803	0.652	0.569	0.375	0.375
27															
MAX	0.599	0.496	0.465	0.356	0.348	0.764	0.630	0.591	0.449	0.439	0.979	0.809	0.759	0.578	0.578

Figure 4-13 and Figure 4-14 show how these bottom stiffener buckling coefficients vary along the length and width of the midbody for the 14m hog wave with no corrosion.

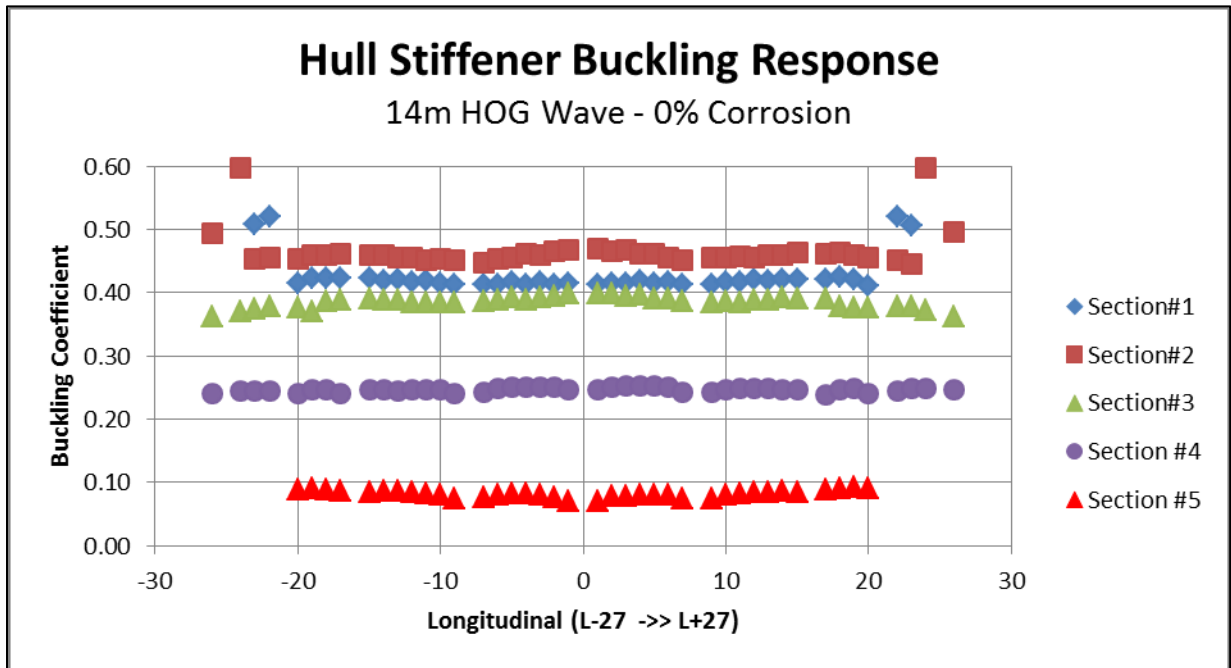


Figure 4-13: Hull Bottom Stiffener Buckling Response – 14m – 0% Corrosion

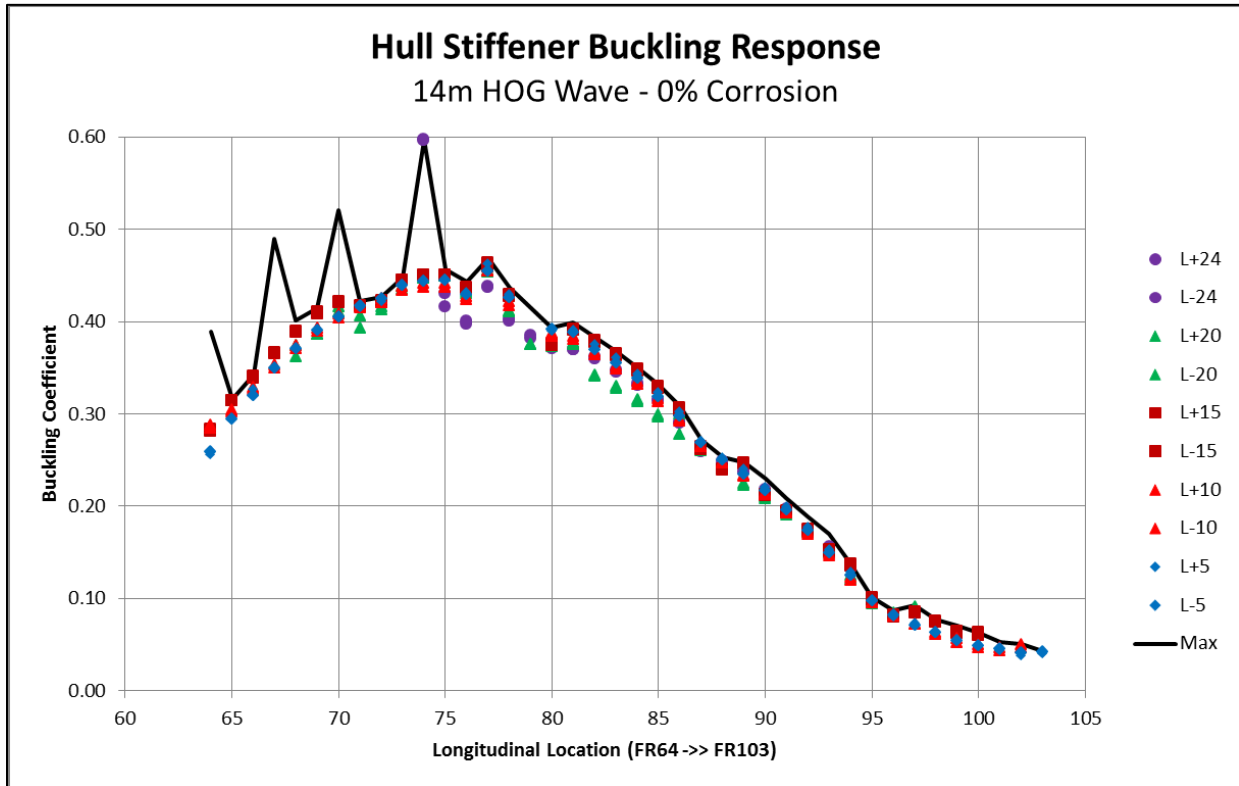


Figure 4-14: Hull Bottom Stiffener Buckling Response – 14m – 0% Corrosion

Figure 4-15 shows how the peak buckling coefficient in these stiffeners varies along the midbody length and for the different corrosion levels up to 55%. For the 55% corrosion case, some stiffeners are likely to buckle in the 14m hog wave condition because their buckling coefficient exceeds 1.0.

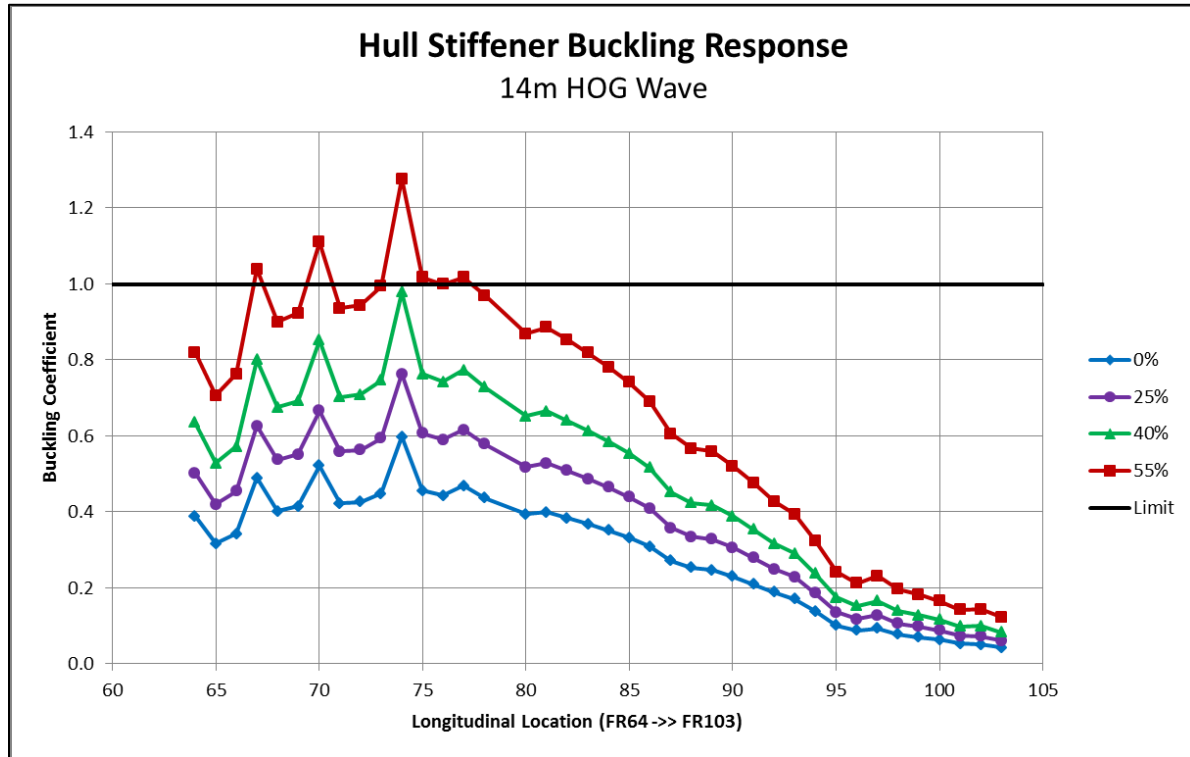


Figure 4-15: Hull Bottom Stiffener Buckling Response – 14m – 0% Corrosion

Figure 4-13 through Figure 4-20 graphically show various aspects of bottom plate buckling response.

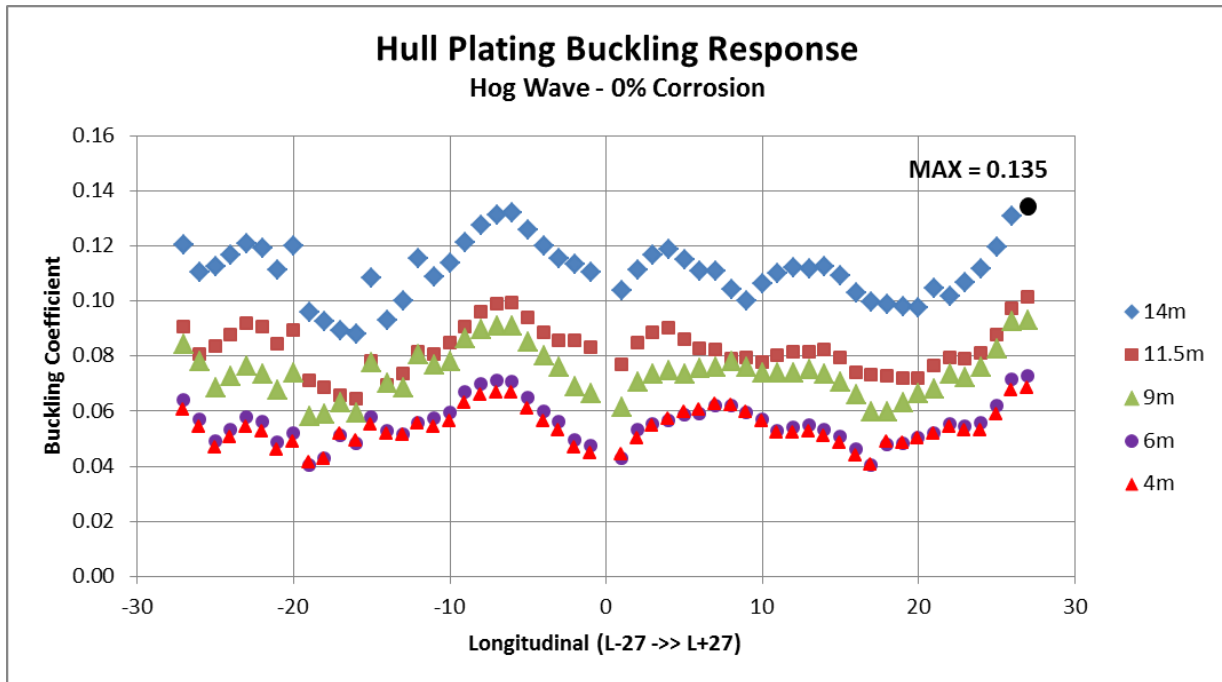


Figure 4-16: Hull Bottom Plating Buckling Response vs Transverse Location – 0% Corrosion

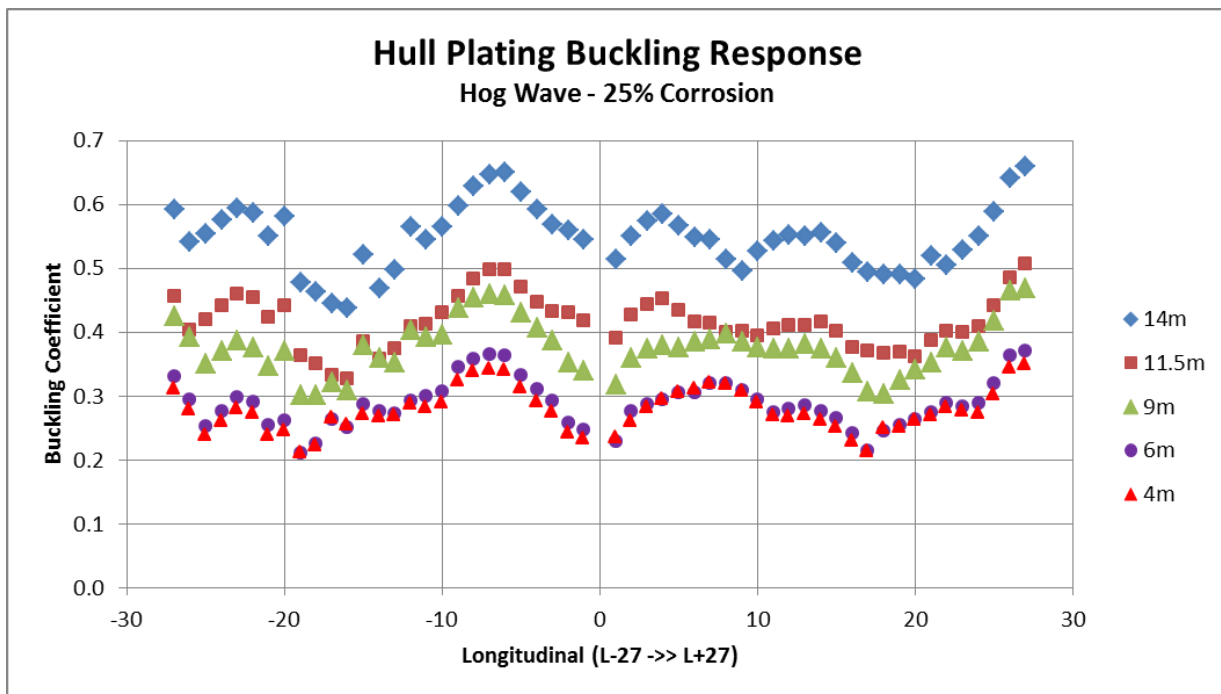


Figure 4-17: Hull Bottom Plating Buckling Response vs Transverse Location – 25% Corrosion

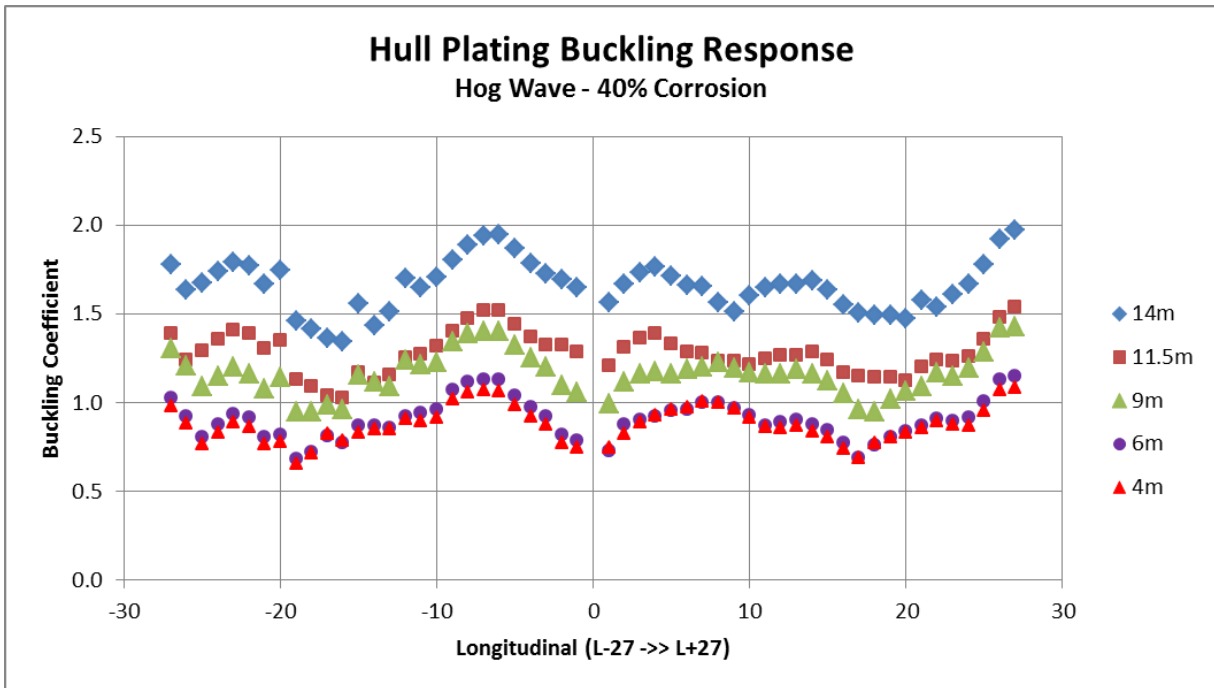


Figure 4-18: Hull Bottom Plating Buckling Response vs Transverse Location – 40% Corrosion

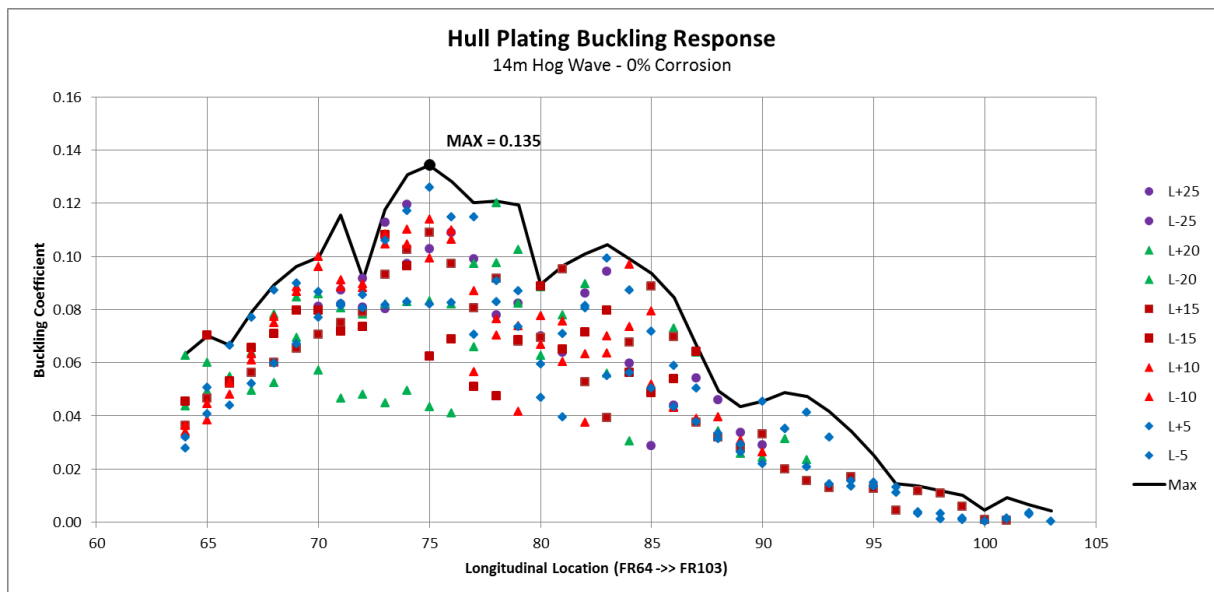


Figure 4-19: Hull Bottom Plating Buckling Response vs Longitudinal Location – 0% Corrosion

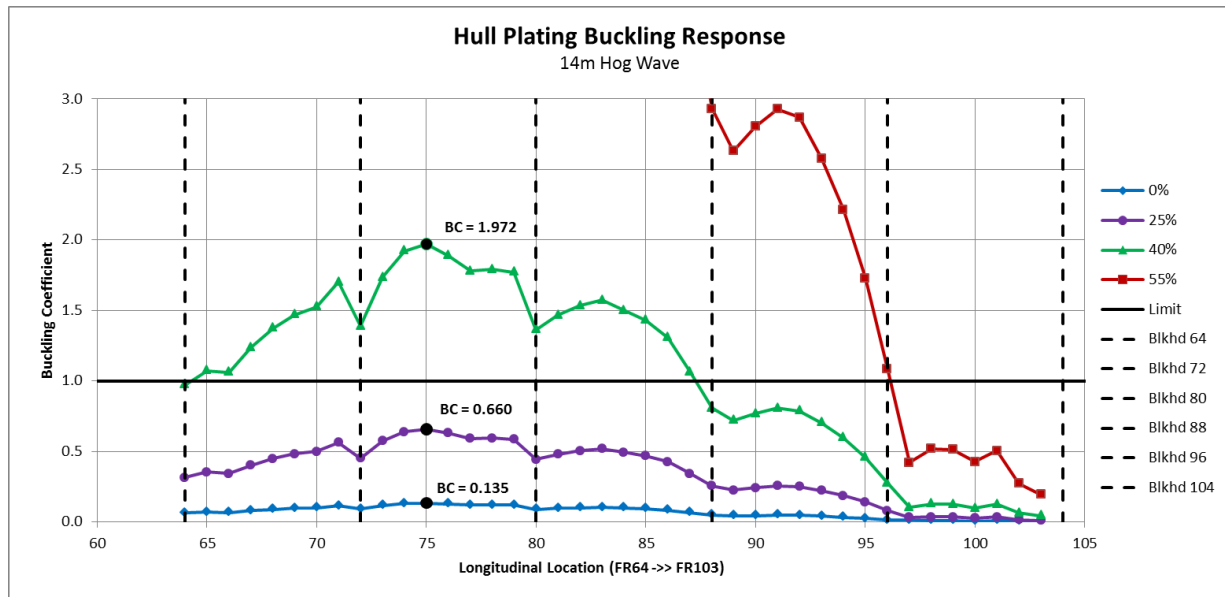


Figure 4-20: Hull Bottom Plating Buckling Response – 14m Hog

5 STRENGTH ASSESSMENT

An assessment of the analyzed failure modes for the example ESB ship indicates that corrosion levels above 25% (maximum allowable limit for renewal under Navy and ABS/IACS) may compromise the seaworthiness of the ship in the modeled conditions and duration. At these higher corrosion levels the buckling capacity of the hull bottom plating decreases significantly, and was the driving failure mode in our limited analysis. As seen in Figure 4-18, at 40% corrosion, calculated buckling coefficients for the hull plating exceed 1.0 for all wave conditions analyzed. At the 25% corrosion level (Figure 4-17) calculated hull plating and stiffener buckling coefficients remain under 1.0 in all wave conditions.

As seen in Table 4-1, at a 25% corrosion level, the maximum stress ratios (calculated stress/allowable) are below 1.0 in all but the main deck framing group. These higher stress values are not global, but located around unreinforced openings in the longitudinal main deck framing. Calculated stress is above the allowable in the unreinforced openings for the 14m hog wave condition, but under the allowable limit for the 11.5m hog wave condition. See Figure 5-1 and Figure 5-2 below.

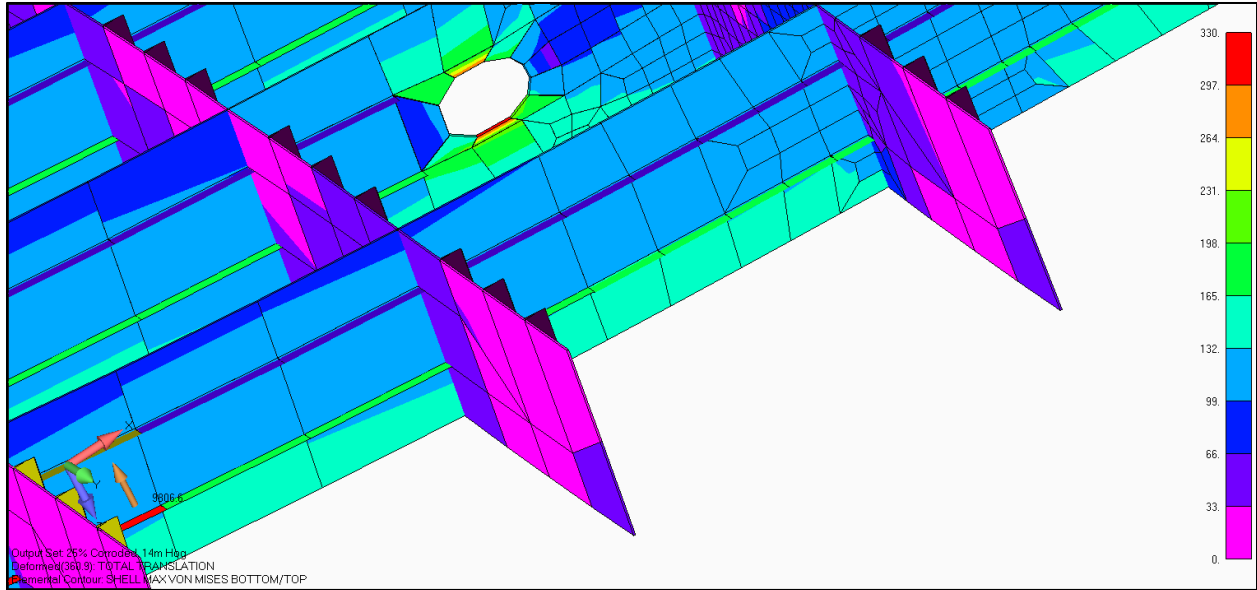


Figure 5-1: Unreinforced Opening in Longitudinal Deck Framing - 25% Corrosion - 14m Hog

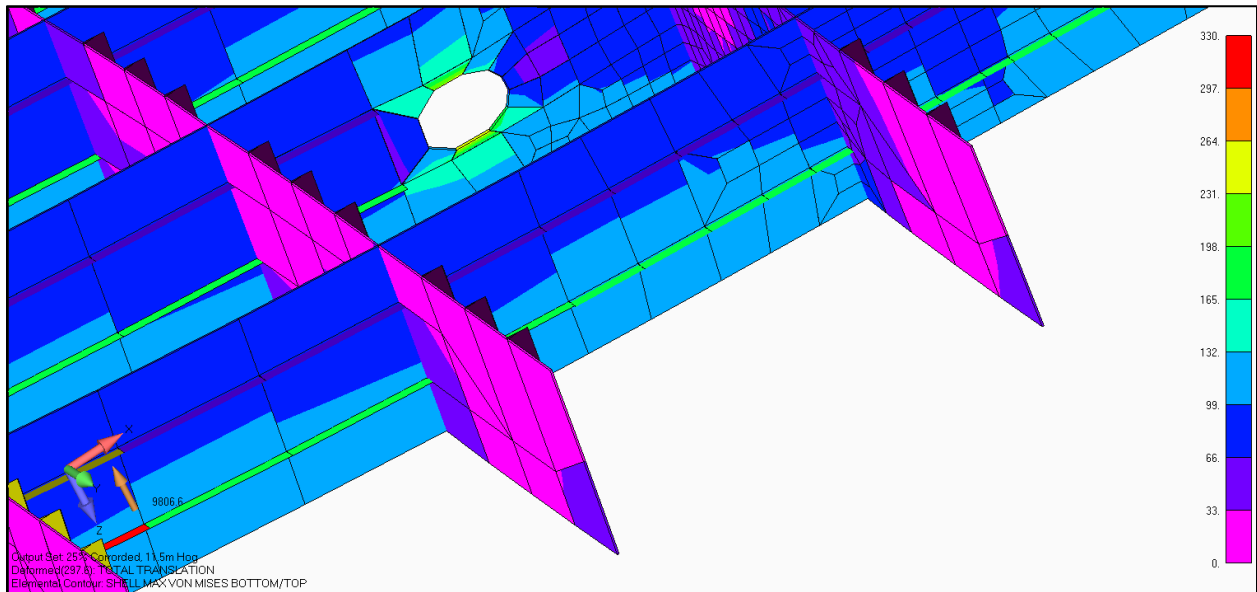


Figure 5-2: Unreinforced Opening in Longitudinal Deck Framing - 25% Corrosion - 11.5m Hog

6 CONCLUSIONS

In our limited study of the ESB ship, with uniform corrosion beyond the typical 25% limit, hull bottom plate buckling coefficients rise dramatically, so that even in the lower sea states buckling of the hull plating is possible. A more thorough investigation may reveal other failure locations with less than 25% wastage. Future research on this topic could consider and evaluate the residual strength of a ship structure with localized corrosion damage. Localized and non-uniform structural corrosion and pitting are probably more common than uniform corrosion across the entire hull structure, but is very case-specific.

The approach developed herein to assess a degraded ship structure can be expanded and then used to develop a safe operating envelope for a ship's hull structure with various degrees of corrosion. While many simplifications of scope and assumptions were made for this project, a more thorough assessment of a degraded ship structure can be accomplished, but would require modeling the ship's actual corrosion levels, more seaway conditions, more headings and more ship loading conditions, amplifying loadings to account for expected exposure times, and investigating more structural components such as internal tank bulkheads and their internal fluid loadings. In addition, green seas, whipping, and slamming effects may need to be addressed. This more rigorous assessment, while possible, would be a costly and time consuming effort.

Appendix A

Range of Seakeeping Analysis Conditions Recommended for a Full Analysis

The runs matrix required for a specific ship assessment will vary significantly depending on the vessel size and type. For example, a large ship like the ESB will have minimal susceptibility in low sea state conditions that might be fatal to a 90 foot long fishing vessel.

There are a number of parameters that should be included in the assessment matrix.

- Drafts: Loading conditions normally encountered by the vessel in question including at least a typical maximum draft and a typical minimum draft condition.
- Headings: All vessel headings from head sea to following seas in at least 30 degree increments. If the program used provides artificial nulls for roll, sway and yaw in head and following seas, then there are two choices to mitigate that concern.
 - Angles of 15 degrees and 165 degrees can be substituted for 0 and 180 for head and following seas such that some small amount of roll, sway and yaw are excited
 - If the software supports it, run the head and following seas in short crested seas where the wave components are coming from a spread of directions, typically using cosine squared spreading. This will produce reasonable motions in head and following seas but in general the maximum pitch motions will be reduced by about 20% from the long crested case.
- Speeds: The normal navigation speed of the ship should be modeled as well as the speed the Captain usually selects for rough weather. It may come out of the analysis that a slower or faster speed in rough weather will reduce the hull girder stresses by a significant amount. On ships with active ride control fins, speeding up a few knots may actually reduce the stresses and the added lift of the ride control fins can reduce the motions and slamming.
- Water depth considerations:
 - If a ship is in liner service in waters shallow enough for 10 to 12 second waves to feel the bottom, then a depth sensitive seakeeping model should be used.
 - If the ship is in liner service on a western shore or where there is not much continental shelf, it may be necessary to model both a wind sea and swell component to the wave field using the Ochi-Hubble 6 parameter spectrum or similar.
- Wave conditions:
 - Most naval architecture methods in use today utilize mathematical wave spectra to model the wave field. There are many different types, most were developed in the 1950's through 1980's based on very limited data sets from a single location on the planet. The advantage of the Bretschneider, Pierson-Moskowitz, Ochi-Hubble, ITTC, ISSC, or JONSWOP spectra is that everyone setting up an analysis with the same spectral form and same input parameters should get similar results.

- It must also be decided what significant wave heights to model. Figure A-1 shows wave energy divided up into sea state bins on the left hand panel and by 1m intervals on the right hand panel.

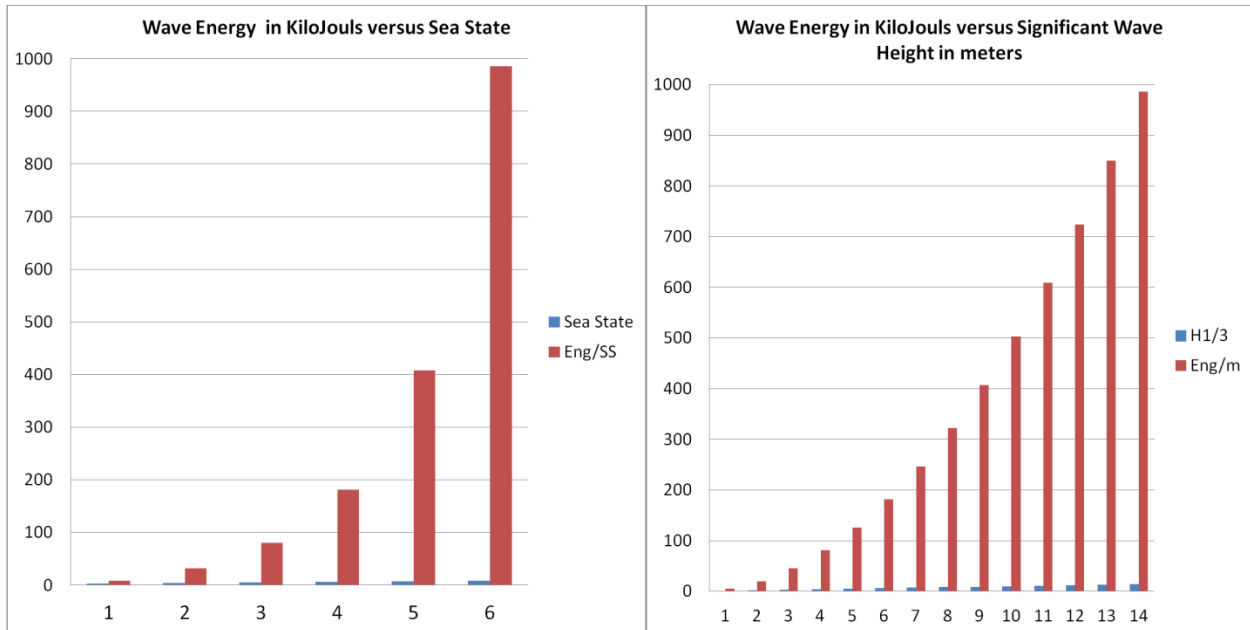


Figure A-1: Wave Energy Vs Sea State and 1m Significant Wave Height Bins

The left hand view shows that sea state is too coarse a measure to allow a meaningful search for a threshold for safe operations. The 1m steps in the right hand panel show much better granularity for finding a realistic limiting case.

While this suggests that a lot of modeling is necessary, that is not necessarily the case. For a ship the size of the ESB, anything below about the top of sea state 5 at 4m significant wave height is irrelevant. If the study starts there and works up a few sets at a time, the limit can be reached before one gets up to 14 m wave or higher.

Appendix B Hydrodynamic Pressure Distributions

Plots of nine of the ten WASIM-derived hull pressure data sets acting on the FEM are shown in Figure B-1 through Figure B-9. (The tenth is included as Figure 3-10 in the report body.)

From the pressure distribution, it is readily evident that a hog wave shows maximum pressure acting near the hull center, whereas a Sag wave shows the pressure peaking near the fore and aft ends of the ship. In addition, the wave shape can also be identified by the height reached by the wave near the bow and transom areas. The magnitude of the pressure (0.1 MPa) acting on hull bottom is approximately the same for the smaller wave sizes.

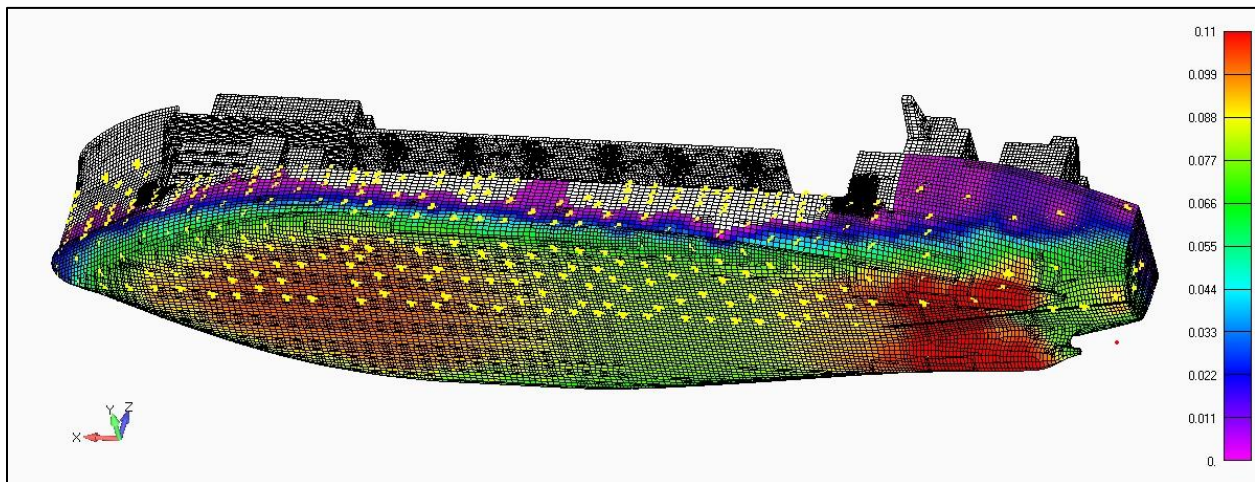


Figure B-1: 14m Sag Wave

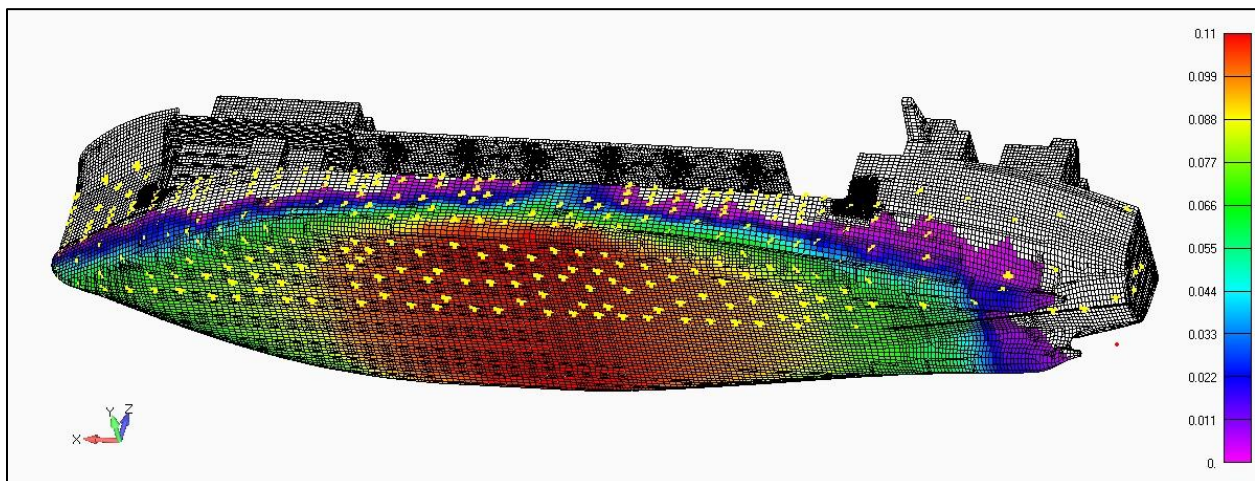


Figure B-2: 11.5m Hog Wave

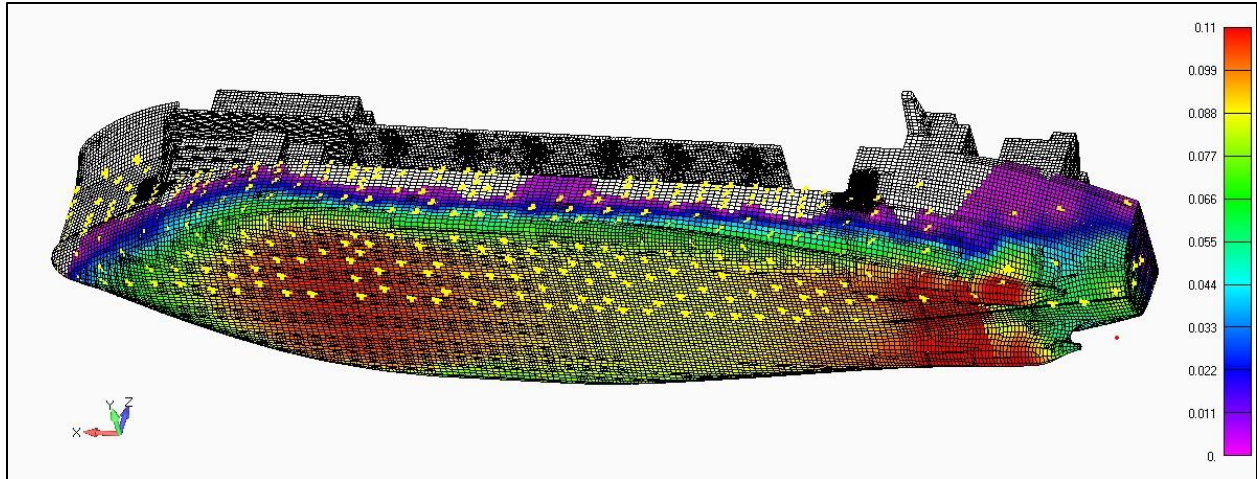


Figure B-3: 11.5m Sag Wave

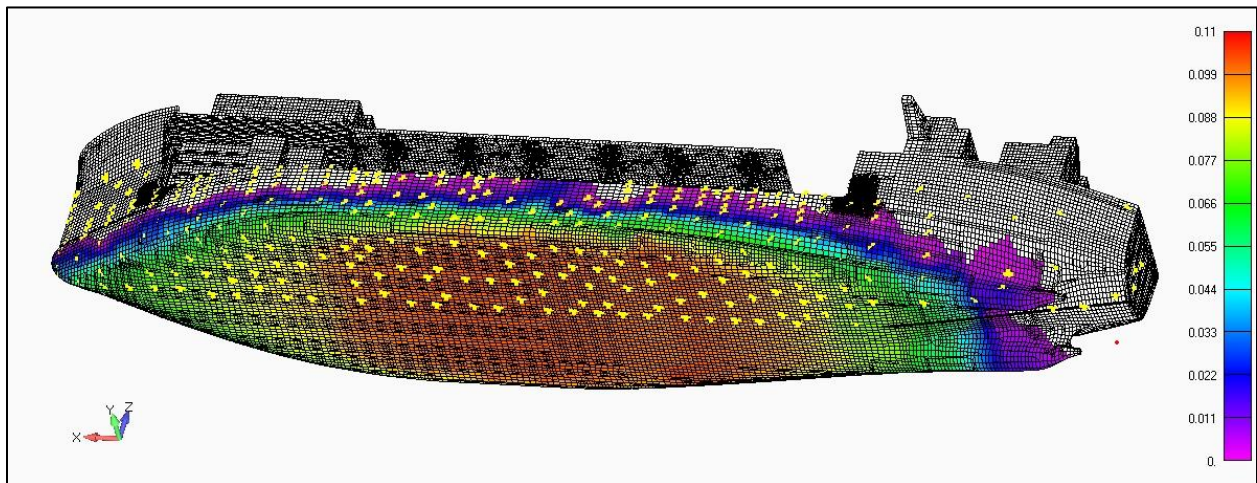


Figure B-4: 9m Hog Wave

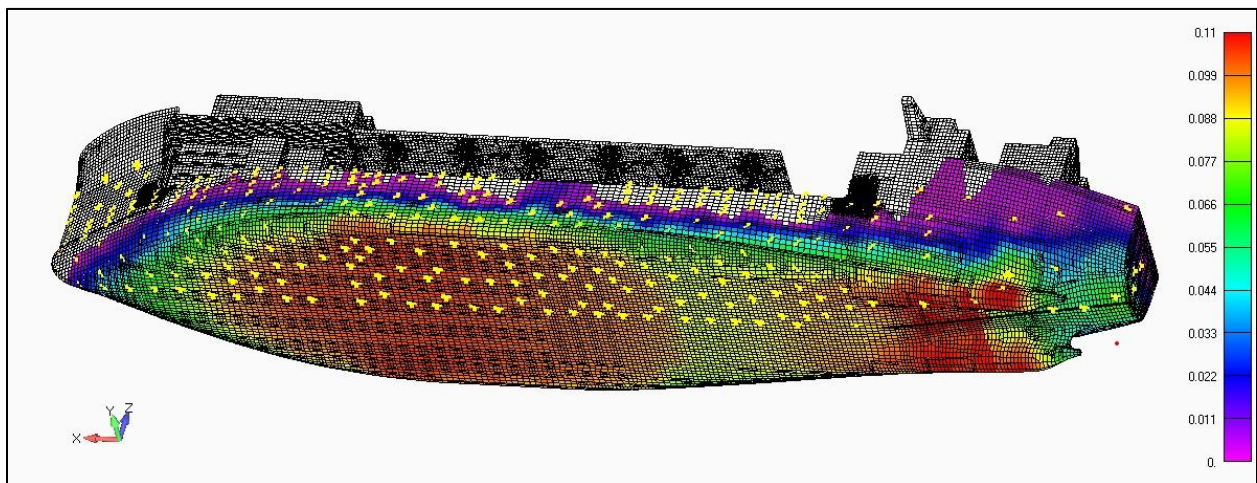


Figure B-5: 9m Sag Wave

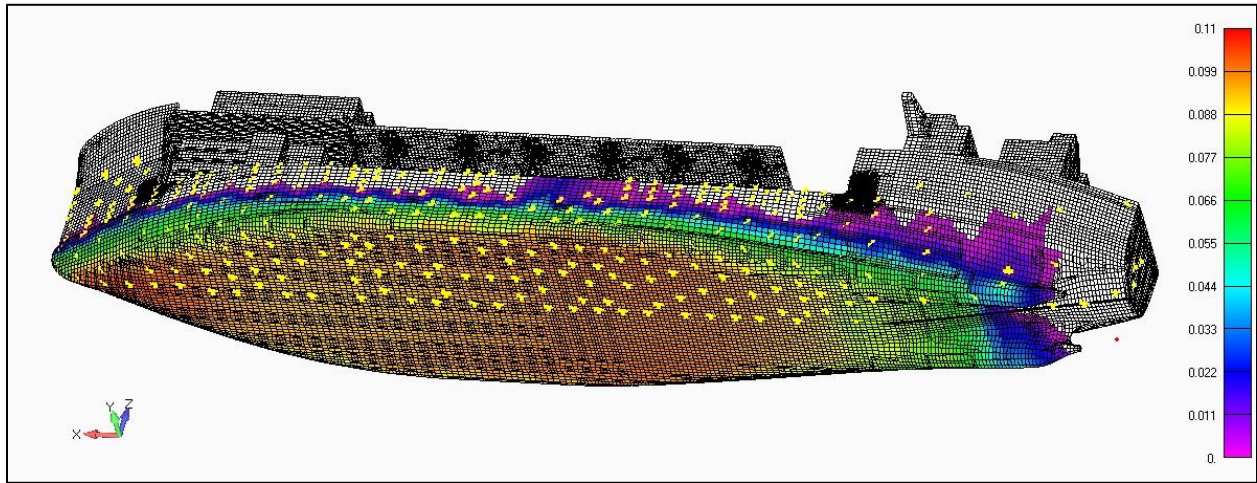


Figure B-6: 6m Hog Wave

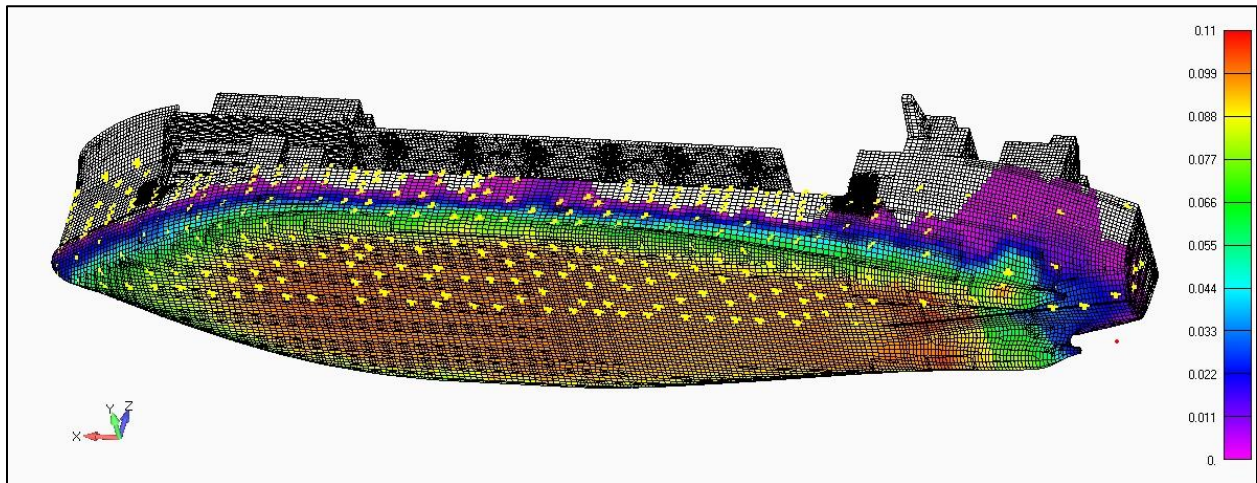


Figure B-7: 6m Sag Wave

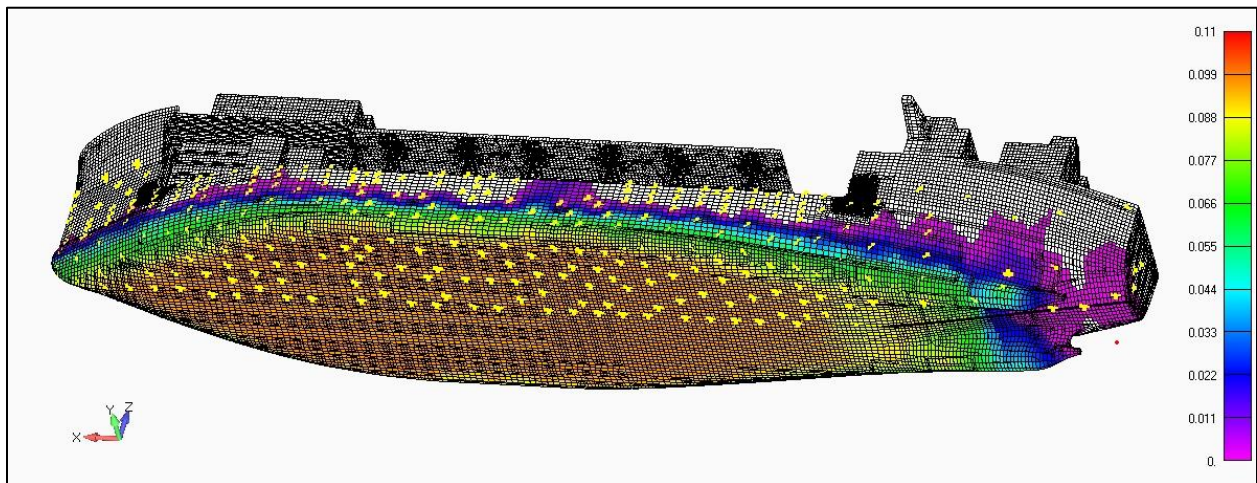


Figure B-8: 4m Hog Wave

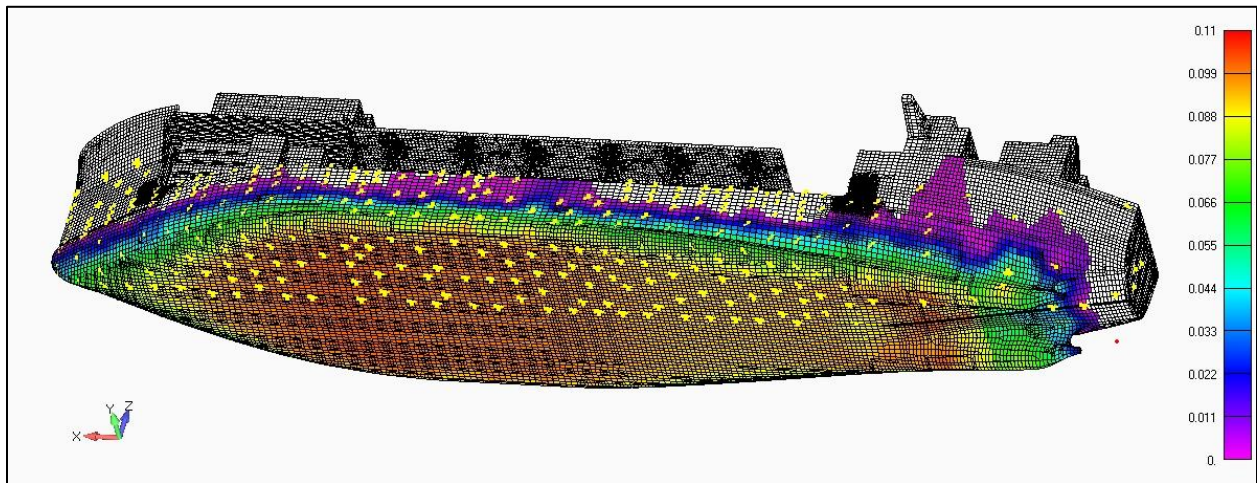


Figure B-9: 4m Sag Wave

Appendix C Structural Model Preparation Procedures

C.1 Procedure for Mapping WASIM Pressure into FEMAP Model

C.1.1 Input Data

The 300 data points received from WASIM are in column format containing the X, Y, and Z position of the panel center, and the corresponding pressure value. See Table C-1. They represent a random distribution of points along the hull, port side only.

Table C-1: Raw WASIM Position and Pressure Data

Label	xpress m	ypress m	zpress m	4m wave case		6m wave case		9m wave case		11.5m wave case		14m wave case	
				Hogging	Sagging	Hogging	Sagging	Hogging	Sagging	Hogging	Sagging	Hogging	Sagging
Panel_Cnt_1	230.420	1.994	14.963	0	0	0	0	0	0	0	0	0	0
Panel_Cnt_2	225.333	5.707	13.956	0	0	0	0	0	0	0	0	0	0
Panel_Cnt_3	214.434	12.285	13.957	0	0	0	0	0	0	0	0	0	0
Panel_Cnt_4	230.420	1.994	12.944	0	0	0	0	0	0	0	0	0	0
Panel_Cnt_5	219.936	9.087	12.949	0	0	0	0	0	0	0	0	0	0
Panel_Cnt_80	168.707	23.103	1.320	92178.55	91690.41	80999.23	86998.02	86233.95	83991.38	90412.12	77098.93	83157.82	79695.84
Panel_Cnt_81	196.027	16.105	2.071	72650.27	81944.36	65892.51	84192.74	66411.35	61777.77	65683.63	50640.09	74689.91	44561.47
Panel_Cnt_82	185.191	18.610	1.007	87584.11	92288.78	82113.01	88824.71	82489.71	77771.78	86587.93	66281.7	83640.06	62053.08
Panel_Cnt_83	174.154	20.130	0.447	97662.18	96662.4	89373.3	91095.81	92816.84	85562.66	98509.64	78898.04	88711.6	75675.49
Panel_Cnt_84	190.539	15.201	0.741	87779.11	92813.32	82247.21	91467.96	82191.13	76602.77	83628.66	66543.53	86197.71	59985.57
Panel_Cnt_85	179.569	16.987	0.143	98192.14	97657.78	92774.13	92925.68	94453.08	85644.2	98919.23	78575.85	91938.3	72739.88
Panel_Cnt_86	198.717	11.635	0.649	86609.19	92718.91	80751.64	94448.46	77922.09	73310.95	78699.61	65925.84	88337.84	56044.6
Panel_Cnt_87	184.983	13.792	0.100	96165.8	97046.84	92311.84	93965.52	92919.45	84820.79	95991.75	77419.62	93943.51	70996.17
Panel_Cnt_88	168.358	15.267	0.003	101451.8	96858.9	96403.9	93216.1	100245.9	92508.93	105122	91170.41	97053.15	90078.74
Panel_Cnt_89	190.436	10.606	0.111	94624.93	96299.53	90557.11	94392.45	90935.88	82758.79	92322.29	75454.08	94979.41	68140.02
Panel_Cnt_90	170.282	11.770	0.000	90366.58	96593.07	86391.61	92809.17	88873.3	88293.93	103670.0	82040.14	93589.34	78586.07
Panel_Cnt_91	173.833	12.137	0.000	0	0	0	0	0	0	0	0	1381.183	0
Panel_Cnt_92	195.542	5.728	0.393	93080.57	90889.58	86518.84	90255.48	88845.44	88702.85	88059.88	74542.55	95419.98	82206.55
Panel_Cnt_93	184.880	8.793	0.006	97627.59	96354.83	95425.64	93282.2	96860.56	86751.71	99513.77	81278.15	98776.76	75037.44
Panel_Cnt_94	190.393	5.899	0.000	96235.58	96266.76	93350.35	94125.08	94400.05	84920.66	95700.85	78856.78	99079.45	71880.03
Panel_Cnt_95	179.305	6.547	0.000	99459.26	95757.91	97842.69	92411.7	100765.7	89095.26	104282.6	86088.31	100179.4	80877.73
Panel_Cnt_96	184.834	3.770	0.000	97901.85	95757.65	96585.05	92721.84	98428.3	87558.97	100912.2	82914.12	100875.5	76828.66
Panel_Cnt_97	195.927	1.103	0.000	94312.98	96304.54	90512.85	95822.16	90295.33	82607.45	91240.85	77019.93	98224.16	68610.7
Panel_Cnt_98	190.375	1.180	0.000	96425.51	95908.2	94049.68	93710.6	95401.87	85518.36	96669.55	79883.84	100422.9	73103.55
Panel_Cnt_99	179.273	1.310	0.000	99488.18	95393.45	98404.3	92140.85	101484.2	89424.6	104907.6	86879.27	101185.3	81696.67
Panel_Cnt_100	173.721	1.349	0.000	100985.5	95216.66	99164.11	92070.61	103174.8	91313.78	107604.9	90648.22	101497.5	87409.98

The WASIM data should be reviewed for accuracy by inspecting both the EXCEL pressure listing (Table C-1) as well as the graphical hull pressure distribution. In our analysis, it was determined that rows 91, 191, and 291 were erroneous. So they were removed from the data set by hiding the rows. In addition, the WASIM pressure was divided by 1e6 to obtain MPa, and the position converted to mm – the unit of FEMAP.

C.1.2 Data Surface Production

This EXCEL-formatted WASIM wave pressure data is simply copied to the starboard side (now creating 600 data points) and pasted into the FEMAP’s Data Surface Tool (Arbitrary 3-D Coordinate Data Surface). All ten wave forms are loaded and made available for subsequent use. An example is seen in Figure C-1.

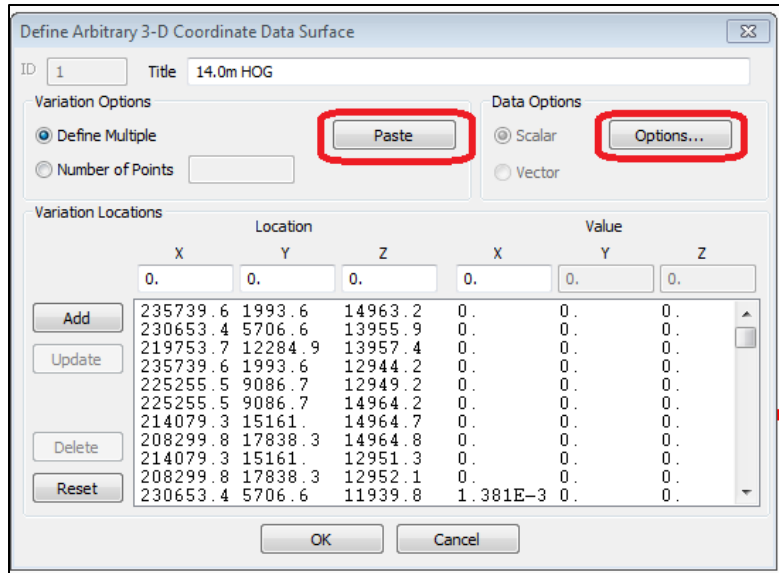


Figure C-1: FEMAP’s “Data Surface Editor” Menu

Options regarding the percentage and minimum number of locations to include are available. Based primarily on visual inspection, these values were set to 0 and 4 – respectively as seen in Figure C-2.

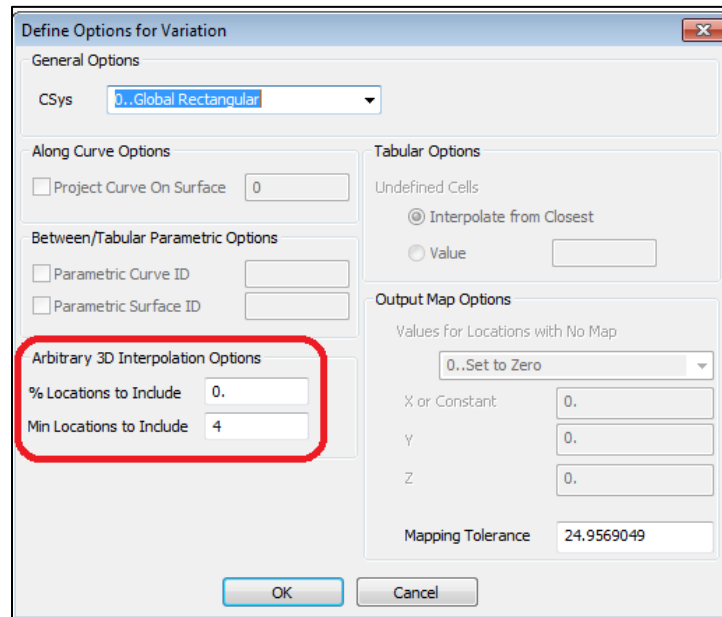


Figure C-2: FEMAP’s “Define Options for Variation” Menu

C.1.3 Loadset Generation

To transform the wave pressure data into a loadset, the user must first generate a new loadset name via “Model – Load – Create/Manage Set...” from the FEMAP menu bar.

To apply the pressure load, the user next chooses “Model – Load – Elemental...” from the FEMAP menu bar. The grouping of plate elements upon which the wave pressure acts, namely the outer hull, is then selected from the “Entity Selection” menu as seen in Figure C-3. Note in Figure C-3 that the hull elements can be also be visualized by selecting the paintbrush icon.

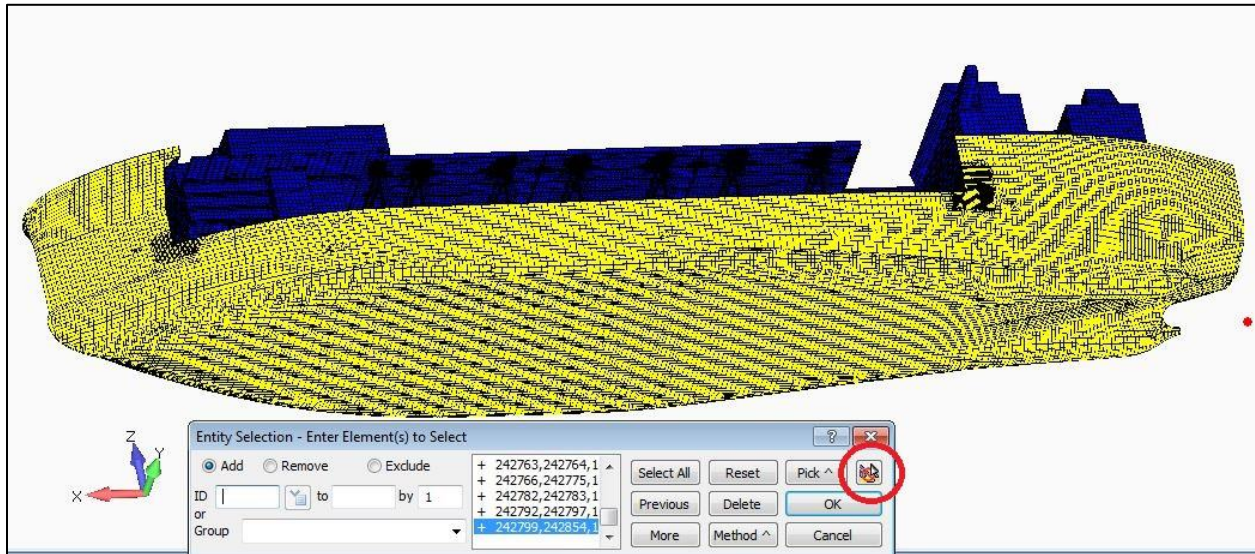


Figure C-3: FEMAP's Entity Selection Menu

Upon approval of the “Entity Selection” menu, a “Create Loads on Elements” menu similar to that shown in Figure C-4 will next appear. The pressure must be set to unity, and the Method radio button set to Data Surface. From the Data Surface drop-down the data surface desired chosen.

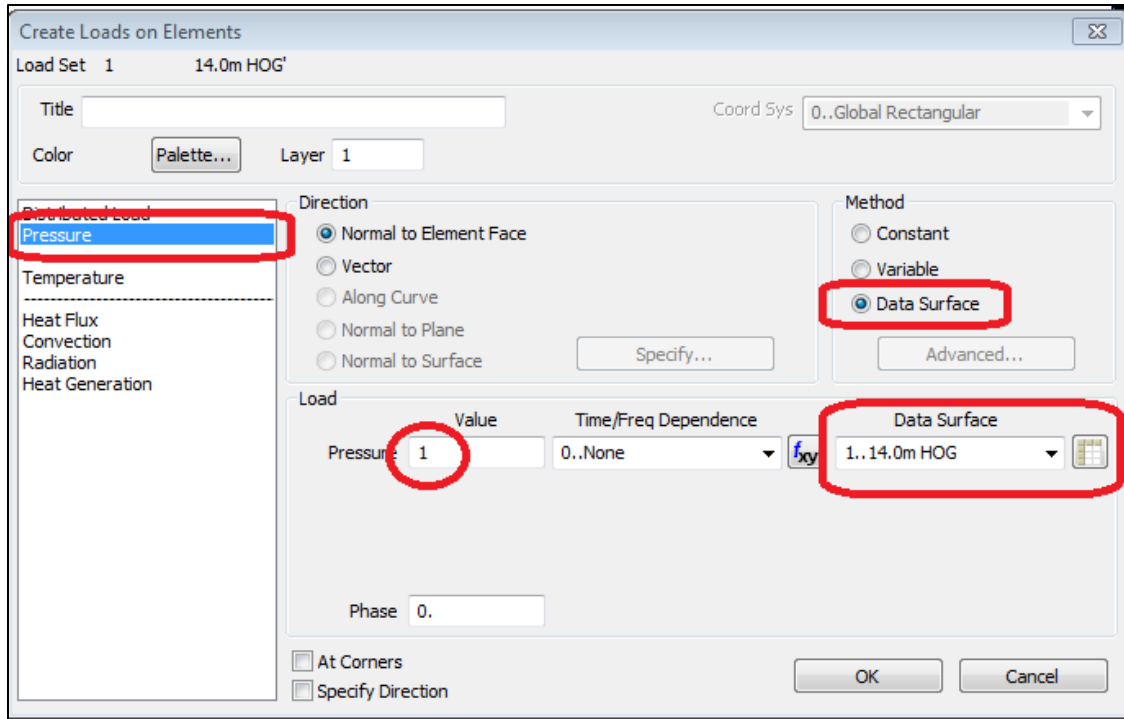


Figure C-4: FEMAP's Load Generation Menu

Next the face and side upon which the pressure acts is selected from the "Face Selection" menu as being the face 1, the front face. See Figure C-5. This face corresponds to the outer surface of the hull.

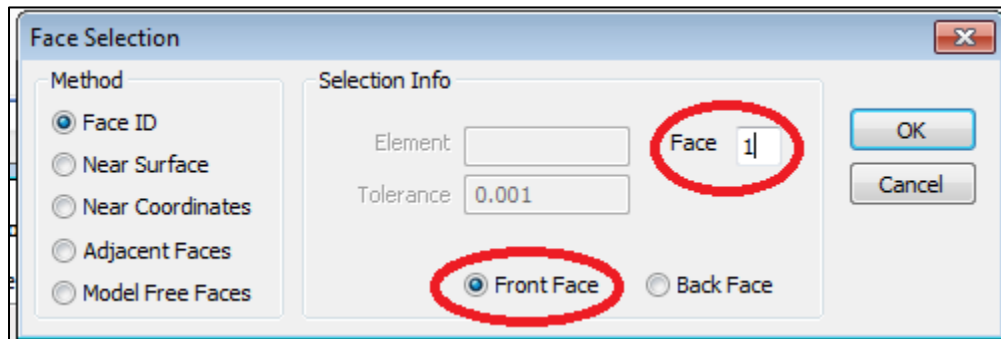


Figure C-5: FEMAP's Face Selection Menu

Asside from pressure loads, body loads (from ship motion accelerations) are also simultaneously applied to the model. The X, Y and Z accelerations that occur in the hydrodynamic model at the same time that the peak hog condition occurs for each sea state are used in the structural model. These accelerations act on the modeled mass of the elements to produce inertial forces. The applied accelerations associated with each wave condition are shown

Table C-2: Accelerations at time of MAX HOG Wave

Sea State	Wave Ht (m)	Linear Acceleration					Rotational Accel	
		X (Long)	Y (Trnsv)	Z (Down)	Resultant	Units	RY (Pitch)	Units
8	14	0.122	0.119	0.108	0.202	G's	1.412	Deg/s ²
		1196.4	1167.0	1059.1	1978.6	mm/s ²	0.025	Rad/s ²
8	11.5	0.067	0.077	0.187	0.213	G's	1.392	Deg/s ²
		657.0	755.1	1833.8	2089.2	mm/s ²	0.024	Rad/s ²
7	9	0.096	0.107	0.084	0.166	G's	1.322	Deg/s ²
		941.4	1049.3	823.7	1632.7	mm/s ²	0.023	Rad/s ²
6	6	0.054	0.061	0.023	0.085	G's	0.646	Deg/s ²
		529.6	598.2	225.5	830.1	mm/s ²	0.011	Rad/s ²
5	4	0.006	0.015	0.044	0.047	G's	0.061	Deg/s ²
		58.8	147.1	431.5	459.7	mm/s ²	0.001	Rad/s ²

C.1.4 Additional Checks

From the X,Y, and Z WASIM position data, geometry points were generated and imported into the FEMAP model. This was done to ensure that the 300 data points describing the hull pressure panels from WASIM matched the hull profile within FEMAP. In our case, it was immediately obvious that a translation in the longitudinal direction was required to match at the vertical transom. The reasons for this fixed offset remain unclear – thus pointing to the benefit of this check.

Through the actions described above, the WASIM derived pressure acting on the elements of the hull outer surface becomes an input loadset within FEMAP. To visualize and examine the pressure distribution as seen in Figure 3-10, an output set of each input pressure load set was developed. This is accomplished by first activating the desired loadset, then generating the output set by selecting from the FEMAP menu bar “Model” – “Output” – “From Load...”. This brings up the “Select Type of Load” menu seen in Figure C-6. Selecting the Pressures radio button will then populate the output with the active input loadset.

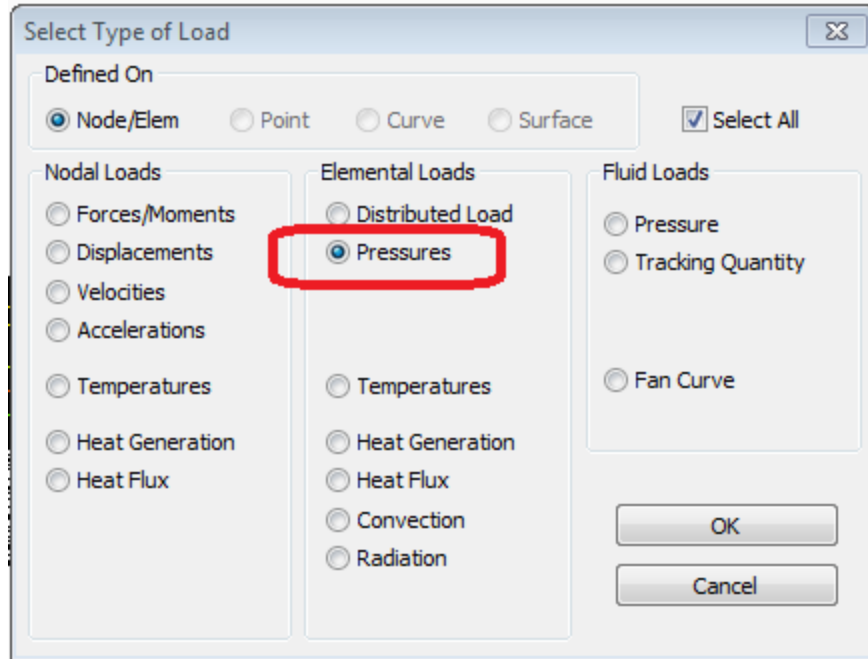
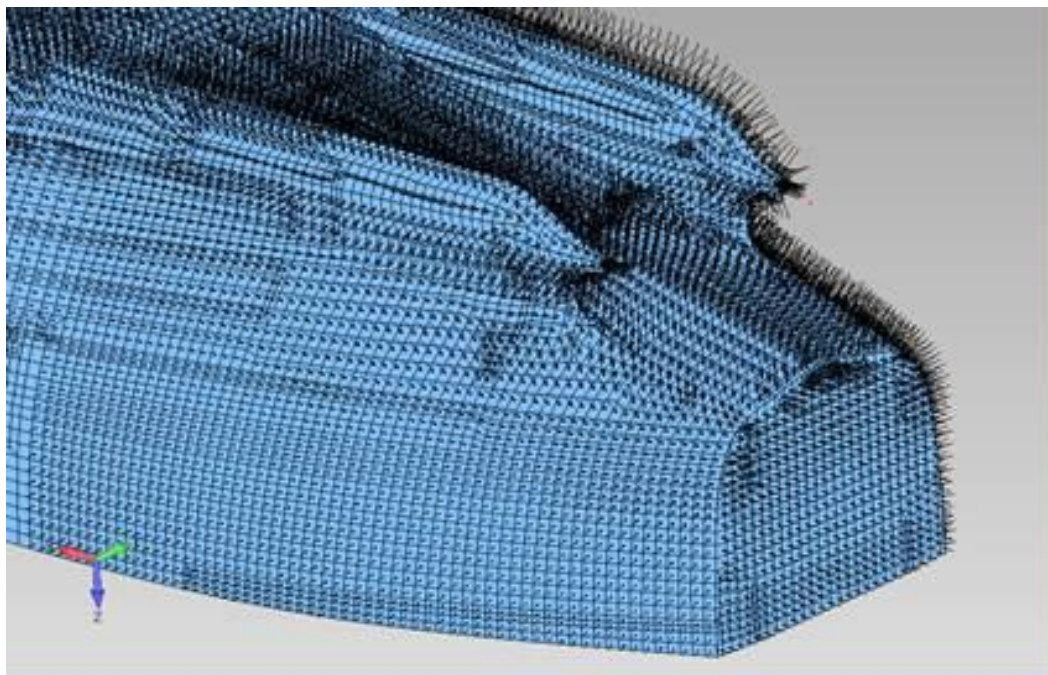


Figure C-6: FEMAP's "Select Type of Load" Menu

Finally, one should also inspect the NASTRAN generated Solve file to ensure that the pressure acts in the positive (inward) sense, in order to prevent applying suction to hull. This can be verified by displaying the pressure vectors (see picture below). The analyst should also confirm that the loads act on the outer rather than the inner surface. This can be accomplished by examining the file listing to ensure the pressure is applied to surface 1, and confirm that surface 1 is the exterior.



C.2 Procedure for Updating Corrosion Level

To update the plate and stiffener property id (PID) cards for each corrosion level, one could manually adjust the appropriate thickness to the desired value. However, to ease this effort, an EXCEL spreadsheet (PID_CONVERTOR.XLSX) and a FEMAP based macro are employed.

For shell properties the process is simpler. A listing of all PIDs is read into EXCEL from the NASTRAN *.NAS input file for an un-corroded vessel, searched and sorted for PSHELLs, and then scaled by the desired corrosion factor. The resulting data is transferred from EXCEL to a *.NAS file and then imported into FEMAP, thus replacing the existing PSHELL PIDS.

FEMAP’s property and cross section menus for a typical PBEAM (with 0% corrosion) is shown in Figure C-7 with the corresponding NASTRAN PID card shown in Table C-2. From the information contained on the commented “Property Shape” and “Property Orientation” lines the pertinent element type and dimensions can be extracted. These values are scaled to the corrosion level desired and output as commented “Property Shape” and “Property Orientation” lines. The remaining fields in the PBEAM card are set to zero.

These updated property cards are then copied from EXCEL into a *.NAS input file and then imported into FEMAP. When the PIDs are imported, and because the id was not changed, they will replace the existing area, inertia, and other properties for the PIDs as seen in Figure C-7 with zeros. A macro is then executed that opens each property card in turn, and from the “Define Property” menu seen in Figure C-7 the macro selects the “Shape” button. From the “Cross Section Definition” menu the “Change Shape” button is enabled by the macro, resulting in the repopulation of the zeros on the PID card with the pertinent corroded area, inertia, and other quantities. See Table C-4.

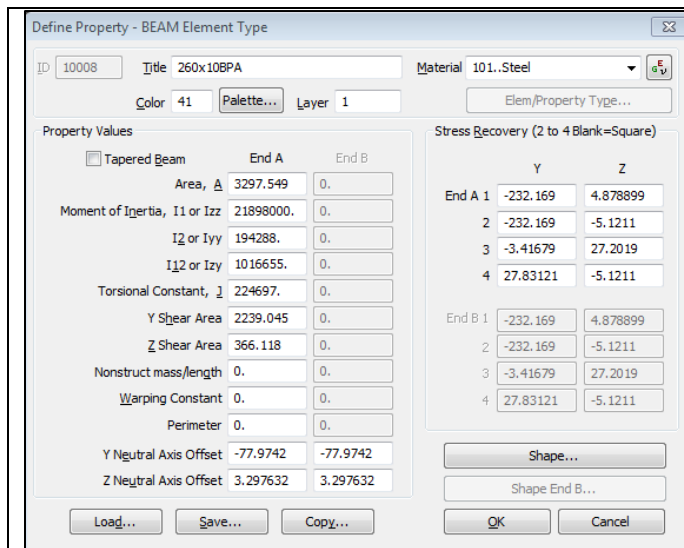


Figure C-7: Typical FEMAP Beam Property Card

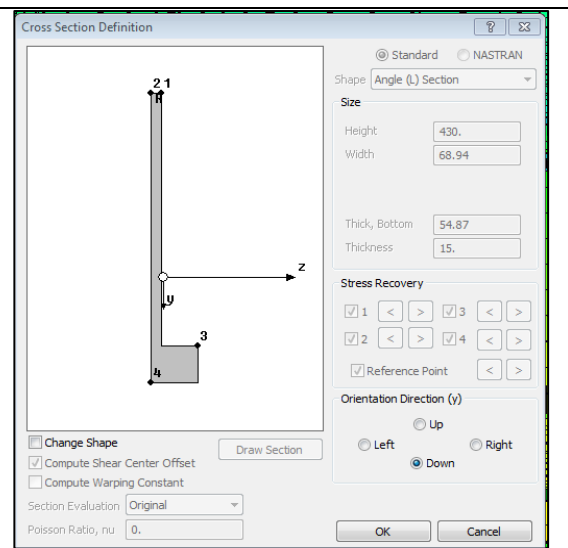


Figure C-8: FEMAP’s “Cross Section Definition” Menu

Table C-3: PID10008, 0% Corroded

\$ Femap Property 10008	:	260x10BPA						
\$ Femap PropShape 10008	:	11,0,260.,32.323,0.,0.,31.248,10.						
\$ Femap PropOrient 10008	:	11,0,3.,5.,6.,3.,1.,5.,-232.1688,4.878899						
PBEAM	10008	1013297.5492.1898+7	194288.1016655.	224697.				0.+
+		-232.1694.878899-232.169	-5.1211-3.41679	27.201927.83121				-5.1211+
+	YESA	1.						+
+		.6790028.1110273						+
+								-77.97423.297632-77.97423.297632

Table C-4: PID10008 - 25% Corrosion – Zero'd Shape

\$ Femap Property 10008	:	260x10BPA						
\$ Femap PropShape 10008	:	11,0,260,32.323,0,0,23.436,7.5						
\$ Femap PropOrient 10008	:	11,0,3,5,6,3,1,5,-232.1688,4.878899						
PBEAM	10008	101	0.	0.	0.	0.	0.	0.+
+		0.	0.	0.	0.	0.	0.	0.+
+	YESA	1.						+
+								

Table C-5: PID 10008 – 25% Corrosion – Updated Shape

\$ Femap Property 10008	:	260x10BPA						
\$ Femap PropShape 10008	:	11,0,260.,32.323,0.,0.,23.436,7.5						
\$ Femap PropOrient 10008	:	11,0,3.,5.,6.,3.,1.,5.,-157.1791,0.0363729						
PBEAM	10008	1012531.752	1.728+7	156047.	856548.	112501.		0.+
+		-157.179.0363729-157.179	-7.4636379.	3848924.	85937102.	8209-7.46363+		
+	YESA	1.						+
+		.6609545.0897133						

C.3 Procedure for Output Results File Preparation

From each analysis run the forces, moment or stress response of the desired beam and shell elements can be recovered from the FEMAP output. Although many methods can be employed, the use of FEMAP's data table has been used.

A listing of the desired output data is produced by first enabling the separate Data Table display window. From FEMAP's menu bar the user selects "List – Output – Results to Data Table" and selects the defaults from the "Send Results to Data Table" as shown in Figure C-9.

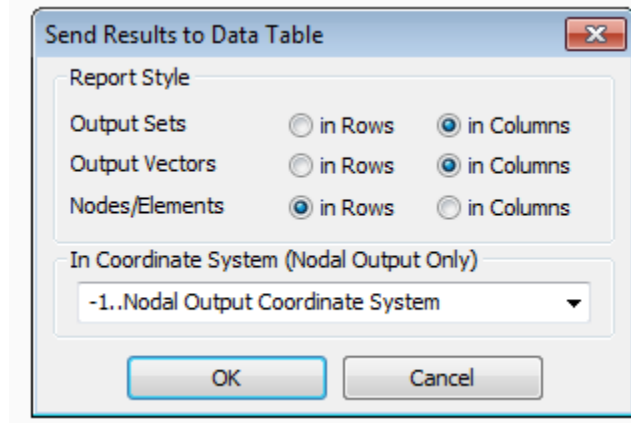


Figure C-9: FEMAP's "Send Results to Data Table" menu

From the "Results to Add to Data Table" menu that appears next select the desired output set from the available listing contained in the left hand side drop down menu. Using the Quick Filter the check boxes for the desired output stress vectors from the available listing are selected. For shells, the Normal-X, Normal-Y, and Shear-XY stresses are desired. As both the top and the bottom face of the shell are required, the output vector identifiers are 7020, 7021, and 7023 for the top, and 7420, 7421, and 7423 for the bottom face. An example is shown in Figure C-10.

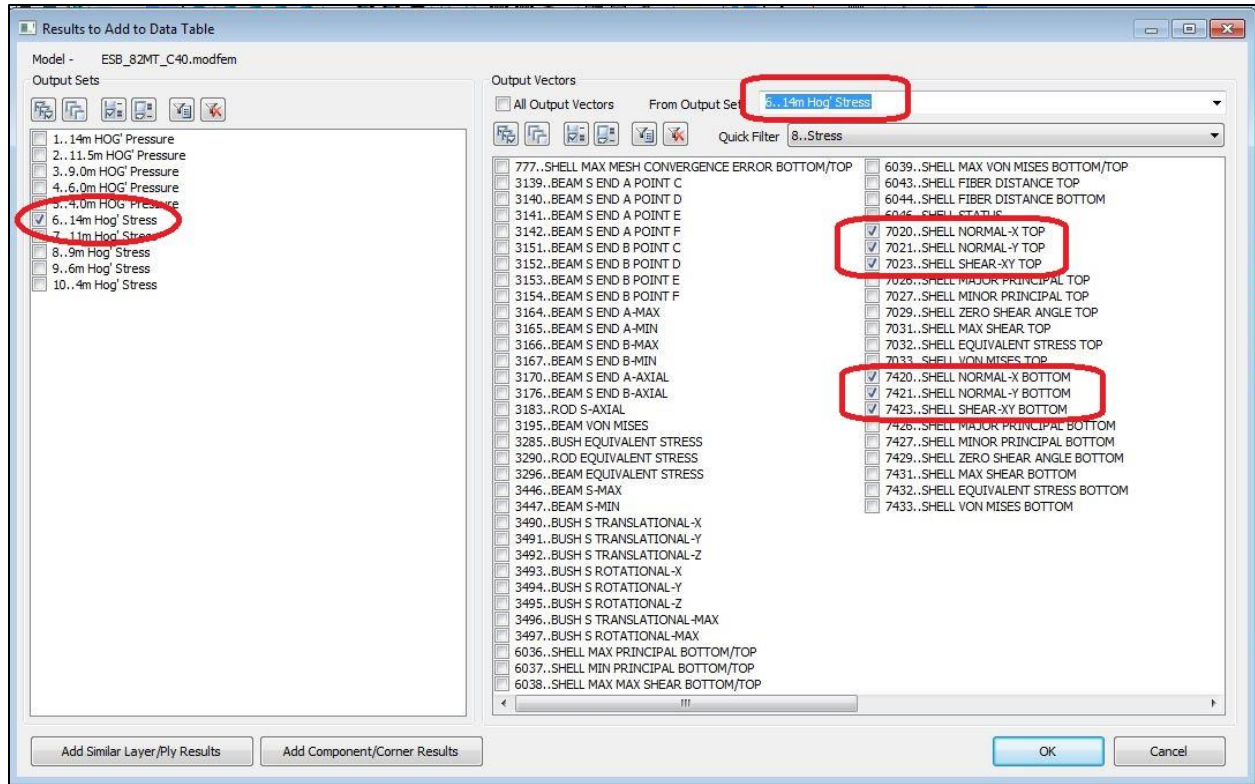


Figure C-10: FEMAP’s “Results to Add to Data Table” menu

The next step is to identify which elements to recover from the “Entity Selection” menu. The grouping RECOVERED is used in Figure C-11 – which is all of the plate and shell elements within the 5 major midbody sections and contains 211,128 elements.

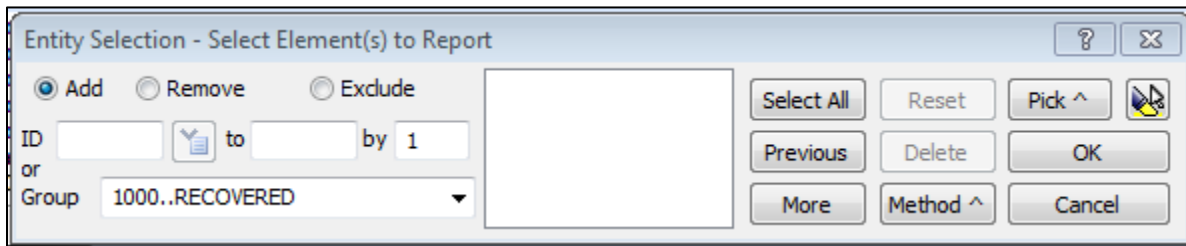
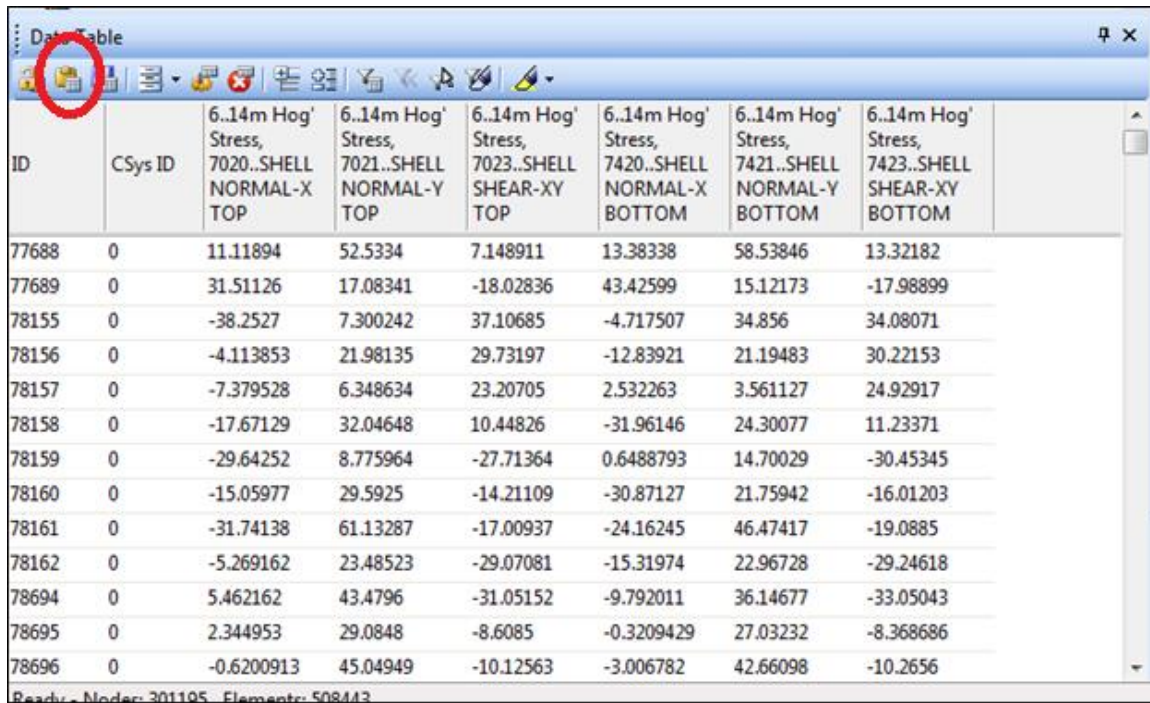


Figure C-11: FEMAP’s “Entity Selection...” menu

The stress results are automatically deposited into the data table, an example of which is seen in Figure C-12.



ID	Csys ID	6..14m Hog' Stress, 7020..SHELL NORMAL-X TOP	6..14m Hog' Stress, 7021..SHELL NORMAL-Y TOP	6..14m Hog' Stress, 7023..SHELL SHEAR-XY TOP	6..14m Hog' Stress, 7420..SHELL NORMAL-X BOTTOM	6..14m Hog' Stress, 7421..SHELL NORMAL-Y BOTTOM	6..14m Hog' Stress, 7423..SHELL SHEAR-XY BOTTOM
77688	0	11.11894	52.5334	7.148911	13.38338	58.53846	13.32182
77689	0	31.51126	17.08341	-18.02836	43.42599	15.12173	-17.98899
78155	0	-38.2527	7.300242	37.10685	-4.717507	34.856	34.08071
78156	0	-4.113853	21.98135	29.73197	-12.83921	21.19483	30.22153
78157	0	-7.379528	6.348634	23.20705	2.532263	3.561127	24.92917
78158	0	-17.67129	32.04648	10.44826	-31.96146	24.30077	11.23371
78159	0	-29.64252	8.775964	-27.71364	0.6488793	14.70029	-30.45345
78160	0	-15.05977	29.5925	-14.21109	-30.87127	21.75942	-16.01203
78161	0	-31.74138	61.13287	-17.00937	-24.16245	46.47417	-19.0885
78162	0	-5.269162	23.48523	-29.07081	-15.31974	22.96728	-29.24618
78694	0	5.462162	43.4796	-31.05152	-9.792011	36.14677	-33.05043
78695	0	2.344953	29.0848	-8.6085	-0.3209429	27.03232	-8.368686
78696	0	-0.6200913	45.04949	-10.12563	-3.006782	42.66098	-10.2656

Figure C-12: FEMAP's "Data Table" Stress Output Listing Example

Selecting the highlighted Copy to Clipboard button allows for the pasting of the data into an EXCEL file.

To enable use by subsequent spreadsheet via the VLOOKUP command., these EXCEL stress output files are given a unique identifying name. The scheme used is as follows:

LCxxHyy.XLSX where

LC simply designates loadcase

xx=Wave size (ie: 14, 11, 09, 06, or 04)

yy=Corrosion level (ie: 0%, 25%, 40%, 55%, or 70%)

For example:

LC14H00 means 14m hog wave, corrosion level 0%

LC11S55 means 11.5m sag wave, corrosion level 55%

LC09H70 means 9m hog wave, corrosion level 70%

In addition, the tab is labeled "Shells", as it contains the stress results for the shell elements and is required in subsequent lookup calls.

C.4 Procedure for Establishing Stiffener Layout

To determine the buckling response of a given stiffener, its relative position within the ship, its length, its geometric and material properties, and the stress in the shell elements that adjoin said stiffener must first be developed. To this end, an EXCEL spreadsheet has been developed that determines the stiffener's layout beginning with a listing of the element ID, along with its associated material ID and the two endpoints (node IDs) for every stiffener element in the region of interest. Note that this listing is by definition element ID-ordered.

Similar files were developed for each of the major structural components (ie: hull, main deck, longitudinal and transverse bulkheads, etc). These files are labeled as MD_Layout, or Hull_Layout, etc. Since as indicated, hull buckling is the predominate response for this ship (due to its natural hog), only this spreadsheet has been employed at this time.

From the two node IDs of the stiffener, a lookup table (NODE_LISTING.XLSX) is called to determine the X, Y, and Z position of the two nodes. Based on the node's position the stiffener elements are grouped into the proper vertical region (Main deck, hull, etc), the proper transverse location (L-27 thru L+27) and the proper longitudinal location (based on its location relative to the transverse frames FR64 thru FR103). Because of the variable mesh size, a counter is also employed to determine the number of stiffener/beam elements within each longitudinal zone. (ie: between any two transverse frames).

In addition to locating/grouping the stiffener elements, the two nodes of each stiffener element are also used to determine the element ID (EID) of those shell elements that adjoin said node. Additional checks using the four (4) nodes of the shell element are required to ensure that the shell element is within the zone of interest. From the shell EID, a lookup is used to recover the shell property ID (PID), while another lookup is employed to recover the stress in the plating for any given load set.

The normal X, normal Y and shear XY stress values for the shell elements that adjoin each side of the stiffener element(s) are then averaged based on the number recorded by the counter. Thus a single representative stiffener and associated shell stress is developed and which forms the input to the stiffener buckling response calculations.

The results are copy paste/values into a separate results file. This file is named ESB_STRESS.XLSX. and is used in subsequent stiffener buckling calculations.

The four files necessary to perform the stiffener preparation and parsing operation are:

1. NODE_LISTING.XLSX

This file is a listing of all nodes in the ship. It was found advantageous to round the Y values. The format is NODE ID, X, Y, Z. A sample listing is seen in Table C-5.

Table C-6: EXCEL File “NODE_LISTING.XLSX” – Node Positions

GID	X	Y	Z
1	0	-3568	22654
2	0	-8028	22654
3	0	0	22654
4	0	-2676	19094
5	0	-5352	19094
6	0	-6244	19094
7	0	-8931	19094
8	0	-1784	19094
9	0	-9812	19094
10	0	-7582	16380

2. BREAKOUT.XLSX

This file is a listing of the SHELL or BEAM elements in each structure. The EID, PID and associated node ID’s are then parsed from the listing. A sample listing of the PLATE data is seen in Table C-6.

Table C-7: EXCEL File: “BREAKOUT.XLSX” – Element Data

HULL								N1	N2	N3	N4	EID	PID	Index
Element	81232	-	PLATE	(Quad	4-noded)	65879	66803	66809	66436	81232	40099	1
Formulation	None							63595	66810	66804	66351	81233	40099	2
Property	40099	Color	124	Layer	1	AttachTo	0	66436	66809	66881	63609	81234	40099	3
Nodes	65879	66803	66809	66436				66006	66882	66810	63595	81235	40099	4
Element	81233	-	PLATE	(Quad	4-noded)	65878	67525	65693	0	81238	40098	5
Formulation	None							65705	67547	63626	0	81239	40098	6
Property	40099	Color	124	Layer	1	AttachTo	0	63626	67547	67499	66006	81754	40098	7
Nodes	63595	66810	66804	66351				63609	67509	67525	65878	81755	40098	8
Element	81234	-	PLATE	(Quad	4-noded)	66314	67527	67539	65879	81768	40099	9
Formulation	None							66351	67561	67549	65938	81781	40099	10
Property	40099	Color	124	Layer	1	AttachTo	0	65693	67643	67664	66445	81888	40098	11
Nodes	66436	66809	66881	63609				63580	67665	67644	65705	81889	40098	12

3. LC14H70.XLSX

4. The stress output for the loadcase in question is contained in the EXCEL file that was previously generated, a sample of which is shown in Table C-7.

Table C-8: EXCEL File “LC04H25.XLSX” – Stress Output

ID	CSys ID	19..4m HOG Stress, 7020..SHELL NORMAL-X TOP	19..4m HOG Stress, 7021..SHELL NORMAL-Y TOP	19..4m HOG Stress, 7023..SHELL SHEAR- XY TOP	19..4m HOG Stress, 7420..SHELL NORMAL-X BOTTOM	19..4m HOG Stress, 7421..SHELL NORMAL-Y BOTTOM	19..4m HOG Stress, 7423..SHELL SHEAR- XY BOTTOM
77688	0	1.881182	22.53294	2.812437	3.227229	25.61096	5.628337
77689	0	11.85451	5.868919	-9.064221	17.50307	5.323185	-8.970127
78155	0	-19.74559	0.5559489	20.05169	-0.5277855	17.01995	18.34676
78156	0	-0.5639009	9.160798	14.57978	-5.400321	8.5143	14.99051
78157	0	-3.028555	-0.6664723	12.0074	2.206941	-2.374883	13.02245
78158	0	-8.402686	13.21946	6.518071	-16.02189	9.200357	7.18394
78159	0	-14.52372	2.437006	-14.70547	1.304045	5.010872	-16.44111
78160	0	-6.876542	11.74947	-7.513249	-15.26734	7.712004	-8.776855
78161	0	-15.35836	30.73282	-8.911184	-10.81825	21.87727	-10.01136
78162	0	-1.408593	10.18745	-13.82635	-7.009713	9.701918	-14.06519
78694	0	2.156883	18.62933	-14.39856	-4.121954	15.89563	-15.16602
78695	0	1.345544	9.774034	-2.458685	-0.03283681	8.636638	-2.346073
78696	0	1.39056	19.40382	-3.090589	0.06864493	17.93862	-3.168826
78697	0	-0.1580466	8.706961	0.391422	-0.8928239	7.810345	0.3647613
78698	0	-1.884951	20.08133	-2.687165	-3.582863	18.41158	-2.552238
78699	0	-10.47664	13.50282	-2.218727	-5.13237	14.49423	-2.609998
78700	0	-12.03758	7.169945	-2.840601	2.215847	14.80852	-2.579219
78701	0	-5.456103	17.79278	1.792179	-2.314472	18.29318	1.303926
78702	0	-5.248883	12.09352	-2.736423	-4.656025	10.82621	-2.493225
78703	0	-5.443654	11.959	1.059864	-9.188404	8.621764	0.831319
78704	0	-3.218144	4.922673	-0.7277763	-5.384417	3.23007	-0.9007836

5. ESB_PRESSURE.XLSX

For hull buckling, the average value of the external wave pressure acting on every hull shell element is required. This pressure is recovered from each of the input pressure load sets and is loaded into a separate tab within the EXCEL file. As sample from the tab labeled as “14mHOG” is seen in Table C-8. It is noted that the external pressure is not required for panel buckling as its effects are included in the stress resultants.

Table C-9: EXCEL File “ESB_PRESSURE.XLSX” – Hull Pressure

ID	COLOR	LAYER	FACE ID	PRESSURE	PHASE
27416	10	1	1	0.003396	0
27417	10	1	1	0.002683	0
27418	10	1	1	0.001177	0
27422	10	1	1	0.00096	0
27750	10	1	1	0.003396	0
27751	10	1	1	0.002683	0
27752	10	1	1	0.001177	0
27756	10	1	1	0.00096	0
28529	10	1	1	0.004939	0
28530	10	1	1	0.005011	0
28537	10	1	1	0.004387	0
28538	10	1	1	0.003673	0
28539	10	1	1	0.001748	0
28540	10	1	1	0.00149	0
28541	10	1	1	0.001353	0

C.5 Procedure for Establishing Plate Layout

The procedure for defining the layout and stress within each equivalent plate panel (EPP) is performed similar to the procedure used for the stiffeners. A listing of the shell elements is first obtained from file BREAKOUT.XLSX. From the shell EID, the location of each of the four (4) nodes is recovered (again from NODE_LISTING.XLSX), from which the region or location of the individual element may be established.

The regions (EPPs) are classified using a multi-digit guide signifying the frame location plus the longitudinal location of the panel. The frames range from 64 to 103 while the longitudinals range from +27 to -27. Thus -6414 would indicate the EPP forward of frame 64, and to the port side of longitudinal L-27.

Also from the EID, the top and bottom stress for each element is parsed from the desired output file. Using the element counter for each region the top and bottom stress for all elements within a given equivalent panel region are averaged, resulting in a single stress representation for the EPP.

The resulting stress in the EPP for each loadset can be copied to file ESB_STRESS.XLSX for future use in the buckling calculations.

C.6 Procedure For Calculation Of Panel And Stiffener Buckling

The buckling calculations are contained in the files PLATE_BUCKLING.XLSX and STIFFENER_BUCKLING.XLSX and follow the rules as established in IACS Common Structural Rules. The generation of the plate or stiffener buckling coefficient (BC) requires the use of two files:

1. For stiffeners: ESB_STRESS.XLSX
For plates: PLATE_LAYOUT.XLSX
This file contains the averaged stress (and pressure) in the equivalent panel or stiffener.
2. PID_PROPS.XLSX
This file contains the stiffener properties (ie: T_{WEB} , T_{FLANGE} , H_{WEB} , H_{FLANGE}) or the plate properties (Thickness). As these properties are affected by the corrosion level, a separate tab is used for each corrosion condition. An example of the stiffener and plate property listing for the first ten (10) properties is shown in Table C-9 and Table C-10 for a corrosion level of 0%.

Table C-10: EXCEL File: "PID_PROPS.XLSX" – Stiffener Properties - Corrosion= 0%

PID	MID	AREA	I1	I2	I12	J	Description	Type	Heigh	Width	T _{Top}	T _{Flang}	T _{Web}
10008	101	3297.549	2.1898+7	194288	1016655	224697	260x10BPA	11	260	32.323	0	31.248	10
10009	101	4294.715	3.8355+7	411860	2040137	386764	300x11BPA	11	300	40.156	0	34.117	11
10010	101	10000	1.3333+8	520833	0	2010446	EngineGirderFlange	1	400	25	0	0	0
10011	101	10000	8333333	8333333	0	1.4072+7	MasslessBeam	1	100	100	0	0	0
10012	101	2153.004	8327061	62819.01	317968	89658.98	200x9BPA	11	200	24.348	0	23	9
10013	103	15625	2.0345+7	2.0345+7	0	3.4355+7	MassLess_Bar	1	125	125	0	0	0
10024	101	20280	1.457+9	7.8867+7	0	4541966	TR.FR.850X300x12/35MTA	12	850	300	35	0	12
10025	101	12575	8.2488+8	2225223	0	1052409	TR.FR.800x100x13/25MTA	12	800	100	25	0	13
10026	101	11875	5.3569+8	7145677	0	1195803	TR.FR.650x150x13/25MTA	12	650	150	25	0	13
10027	101	3729.972	2.1165+7	369055	1415228	323307	TR.FR.240x12BPA	11	240	40.95	0	29.36	12

Table C-11: EXCEL File: "PID_PROPS.XLSX" – Shell Properties – Corrosion=0%

PID	MID	T	MID2	12I/T	MID3	J	TS/T
10001	101	25	101	0	101	0	0
10002	101	56.95353	101	0	101	0	0
10003	101	63.20698	101	0	101	0	0
10004	103	50	101	0	101	0	0
10005	103	50	101	0	101	0	0
10006	101	20	101	0	101	0	0
10007	101	42.89169	101	0	101	0	0
10014	101	12	101	0	101	0	0
10015	101	14	101	0	101	0	0
10016	101	19	101	0	101	0	0

Appendix D Buckling Calculations

D.1 Plate Buckling

Three separate buckling factors (K) are determined for a plate based on the normal stress acting in the plate’s long direction (σ_x , Case #1), the plate’s short (or transverse) direction (σ_y , Case #2), or the shear stress (τ_{xy} , Case #15) in the plate. Each buckling factor is multiplied by a correction factor which is dependent on the plate’s aspect ratio (panel length / width).

For a uniform compressive stress acting in the plate’s long direction, the buckling factor is reduced to $K_x = 4.0 * F_{Long}$, where the correction factor F_{Long} is determined based on the stiffener type and end supports as detailed in Figure D-2. The critical buckling stress is equal to the plating yield strength multiplied by the reduction factor C_x as outlined in Figure D-1.

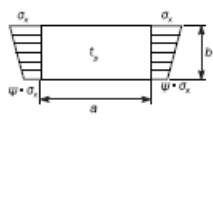
Case	Stress ratio ψ	Aspect ratio α	Buckling factor K	Reduction factor C
	$\psi \geq 0$		$K_x = F_{long} \frac{8.4}{\psi + 1.1}$	When $\sigma_x \leq 0$: $C_x = 1$
	$1 \leq \psi < 0$		$K_x = F_{long} [7.63 - \psi (6.26 - 10\psi)]$	When $\sigma_x > 0$: $C_x = 1$ for $\lambda \leq \lambda_c$ $C_x = c \left(\frac{1}{\lambda} - \frac{0.22}{\lambda^2} \right)$ for $\lambda > \lambda_c$
	$\psi \leq -1$		$K_x = F_{long} [5.975(1 - \psi)^2]$	where: $c = (1.25 - 0.12\psi) \leq 1.25$ $\lambda_c = \frac{c}{2} \left(1 + \sqrt{1 - \frac{0.88}{c}} \right)$

Figure D-1: Plate Buckling Factor (K_x)

Structural element types		F_{long}	c	
Unstiffened Panel		1.0	N/A	
Stiffened Panel	Stiffener not fixed at both ends	1.0	N/A	
	Stiffener fixed at both ends	Flat bar ⁽⁴⁾	$F_{long} = c + 1$ for $\frac{t_w}{t_p} > 1$	0.10
		Bulb profile		0.30
		Angle profile		0.40
T profile	$F_{long} = c \left(\frac{t_w}{t_p} \right)^3 + 1$ for $\frac{t_w}{t_p} \leq 1$	0.30		

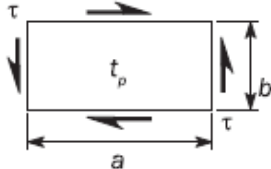
Figure D-2: Plate Buckling Correction Factor (F_{Long})

If the uniform compressive stress acts in the plate's short direction, the buckling factor K_Y reduces to $K_Y = F_{TRAN} \cdot (1 + 1/\alpha^2)^2$. While the correction factor F_{TRAN} is equal to unity, the reduction factor C_Y is governed by the relationships defined below in Figure D-3.

	$1 \geq \psi \geq 0$	$K_y = F_{tran} \frac{2\left(1 + \frac{1}{\alpha^2}\right)^2}{1 + \psi + \frac{(1-\psi)(2.4}{100}\left(\frac{2.4}{\alpha^2} + 6.9f_1\right)}$		When $\sigma_y \leq 0$: $C_y = 1$ When $\sigma_y > 0$: $C_y = c \left(\frac{1}{\lambda} - \frac{R + F^2 (H - R)}{\lambda^2} \right)$
		$\alpha \leq 6$	$f_1 = (1 - \psi)(\alpha - 1)$	where: $c = (1.25 - 0.12\psi) \leq 1.25$ $R = \lambda(1 - \lambda/c)$ for $\lambda < \lambda_c$ $R = 0.22$ for $\lambda \geq \lambda_c$ $\lambda_c = 0.5c(1 + \sqrt{1 - 0.88/c})$
		$\alpha > 6$	$f_1 = 0.6\left(1 - \frac{6\psi}{\alpha}\right)\left(\alpha + \frac{14}{\alpha}\right)$ but not greater than $14.5 - \frac{0.35}{\alpha^2}$	
		$K_y = \frac{200F_{tran}(1 + \beta^2)^2}{(1 - f_3)(100 + 2.4\beta^2 + 6.9f_1 + 23f_2)}$		$F = \left[1 - \left(\frac{K}{0.91} - 1 \right) / \lambda_p^2 \right] c_1 \geq 0$ $\lambda_p^2 = \lambda^2 - 0.5$ for $1 \leq \lambda_p^2 \leq 3$ c_1 as defined in [2.2.3]
$\psi \geq 1 - \frac{4\alpha}{3}$	$\alpha > 6(1 - \psi)$	$f_1 = 0.6\left(\frac{1}{\beta} + 14\beta\right)$ but not greater than $14.5 - 0.35\beta^2$	$H = \lambda - \frac{2\lambda}{c(T + \sqrt{T^2 - 4})} \geq R$ $T = \lambda + \frac{14}{15\lambda} + \frac{1}{3}$	
$\psi < 1 - \frac{4\alpha}{3}$	$\alpha > 6(1 - \psi)$	$f_2 = f_3 = 0$		

Figure D-3: Plate Buckling Factor (K_Y)

For shear stress loading of the plate, the buckling factor K_τ is a function of the plate geometry, while the critical shear stress reduction factor $C_\tau = 1$ for $\lambda < 0.84$, and to $0.84/\lambda$ for $\lambda > 0.84$, where λ is the reference degree of slenderness.

Case	Stress ratio ψ	Aspect ratio α	Buckling factor K
15 	-		$K_{\tau} = \sqrt{3} \left[5.34 + \frac{4}{\alpha^2} \right]$

D.2 Stiffener Buckling

The ultimate buckling capacity for stiffeners is developed not from the recovered beam stresses in the stiffener itself, but rather from the stress response of the adjoining plating.

The buckling response is a function of three stress quantities according to the following interaction formula:

$$BC = (\sigma_a + \sigma_b + \sigma_w) / F_{TY}$$

1. Axial stress

Predominate response.

Function of plate and stiffener geometry.

Directly proportional to plating normal stress-X.

$$\sigma_a = \sigma_x \frac{s t_p + A_s}{b_{eff1} t_p + A_s}$$

2. Bending Stress

Function of lateral deformation (w) and lateral load (Pz)

Function of external lateral pressure (P)

Function of stiffener and plate geometry

$$\sigma_b \quad : \text{ Bending stress in the stiffener, in N/mm}^2:$$

$$\sigma_b = \frac{M_0 + M_1}{1000Z}$$

Z : Net section modulus of stiffener, in cm³, it be taken as:

$$M_1 = C_i \frac{|P|s\ell^2}{24 \times 10^3} \quad \text{for continuous stiffener}$$

$$M_1 = C_i \frac{|P|s\ell^2}{8 \times 10^3} \quad \text{for sniped stiffener}$$

$$M_0 = F_E \left(\frac{P_z w}{c_f - P_z} \right) \quad \text{with } c_f - P_z > 0$$

P_z : Nominal lateral load, in N/mm², acting on the stiffener due to stresses, σ_x , σ_y and τ , in the attached plating in way of the stiffener mid span:

$$P_z = \frac{t_p}{s} \left(\sigma_{xl} \left(\frac{\pi s}{\ell} \right)^2 + 2c \gamma \sigma_y + \sqrt{2} \tau_1 \right)$$

$$\sigma_{xl} = \gamma \sigma_x \left(1 + \frac{A_s}{st_p} \right) \text{ but not less than } 0$$

$$\tau_1 = \gamma |\tau| - t_p \sqrt{R_{eH-p} E \left(\frac{m_1}{a^2} + \frac{m_2}{b^2} \right)} \text{ but not less than } 0$$

- 3. Torsional Deformation Stress
 - Function of fixity of ends
 - Function of stiffener and plate geometry
 - Function of material properties

$y_w = \frac{t_w}{2}$ for flat bar.
 $y_w = b_r - \frac{h_w t_w^2 + t_r b_r^2}{2A_r}$ for angle and bulb profiles.
 $y_w = \frac{b_r}{2}$ for T profile.

$\sigma_w = E y_w \left(\frac{t_r + h_w}{2} \right) \Phi_0 \left(\frac{\pi}{\ell} \right)^2 \left(\frac{1}{1 - 0.4 R_{eH-p}} - 1 \right)$

$\Phi_0 = \frac{\ell}{h_w} 10^{-3}$

$\sigma_{ET} = \frac{E}{I_p} \left(\frac{\epsilon \pi^2 I_w 10^2}{\ell^2} + 0.385 I_r \right)$

	Flat bars ⁽⁴⁾	Bulb, angle and T profiles
I_p	$\frac{h_w^3 t_w}{3 \times 10^4}$	$\left(\frac{A_w (e_r - 0.5 t_r)^2}{3} + A_r e_r^2 \right) 10^{-4}$
I_r	$\frac{h_w t_w^3}{3 \times 10^4} \left(1 - 0.63 \frac{t_w}{h_w} \right)$	$\frac{(e_r - 0.5 t_r) t_w^3}{3 \times 10^4} \left(1 - 0.63 \frac{t_w}{e_r - 0.5 t_r} \right) + \frac{b_r t_r^3}{3 \cdot 10^4} \left(1 - 0.63 \frac{t_r}{b_r} \right)$
I_w	$\frac{h_w^3 t_w^3}{36 \times 10^6}$	$\frac{A_r e_r^2 b_r^2}{12 \times 10^6} \left(\frac{A_r + 2.6 A_w}{A_r + A_w} \right)$ for bulb and angle profiles. $\frac{b_r^3 t_r e_r^2}{12 \times 10^6}$ for T profiles.

(1) t_r is the net web thickness, in mm. t_{r-net} as defined in [2.3.2] is not to be used in this table.

e_r : Distance from attached plating to centre of flange, in mm.
 $e_r = h_w$ for flat bar profile.
 $e_r = h_w - 0.5 t_r$ for bulb profile.
 $e_r = h_w + 0.5 t_r$ for angle and Tee profiles.

$\epsilon = 1 + \frac{\left(\frac{\ell}{\pi} \right)^2 10^{-3}}{\sqrt{I_w \left(\frac{0.75}{t_p^3} + \frac{e_r - 0.5 t_r}{t_w^3} \right)}}$

Appendix E ESB Buckling Response

In a hogging condition, the bottom and lower sides of the ship’s hull will be in compression while the upper sides and Mission Deck experience a tensile condition. As stated previously, the natural (still-water) hog of the ship coupled with hogging from waves is the driving loading condition. The buckling coefficients seen in the following figures are therefore for the bottom and lower side plating and stiffeners of the ship in hogging conditions.

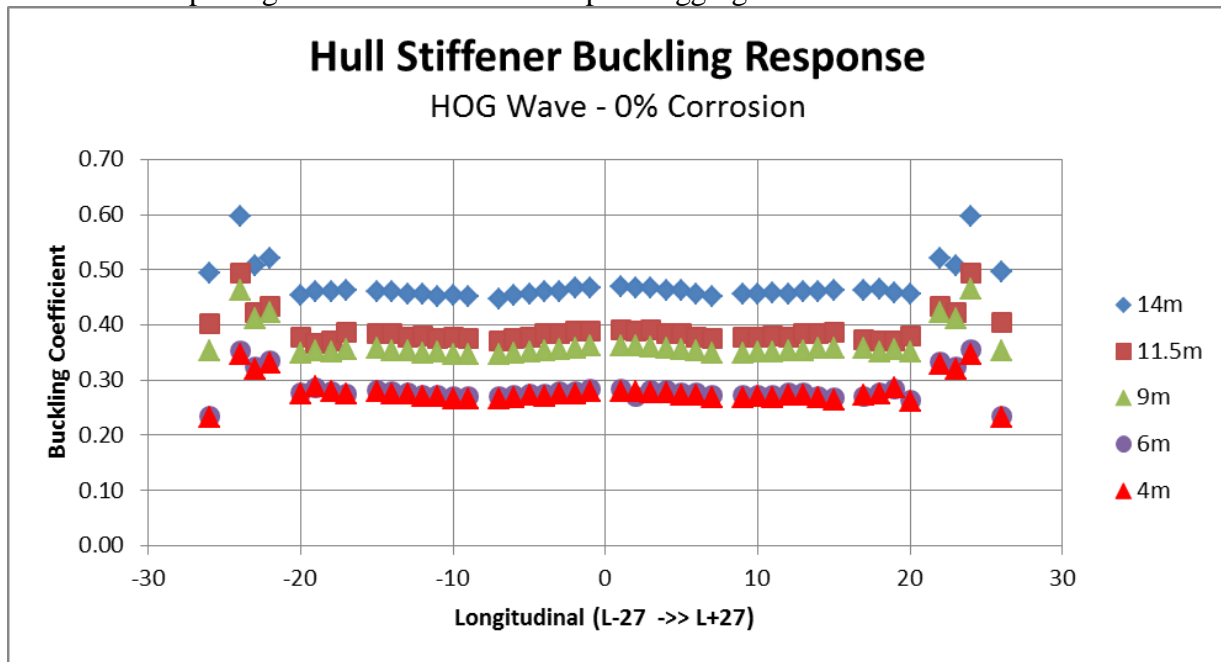


Figure E-1: Hull Stiffener Buckling Response – Hog Wave - 0% Corrosion

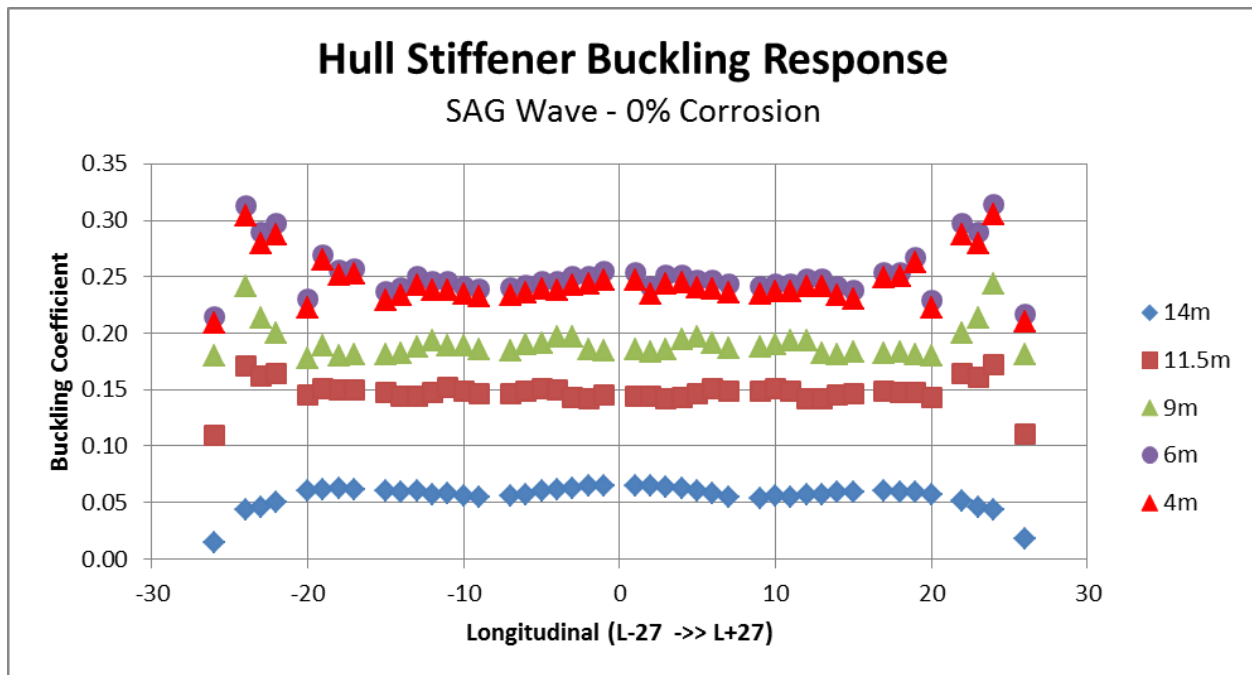


Figure E-2: Hull Stiffener Buckling Response – Sag Wave - 0% Corrosion

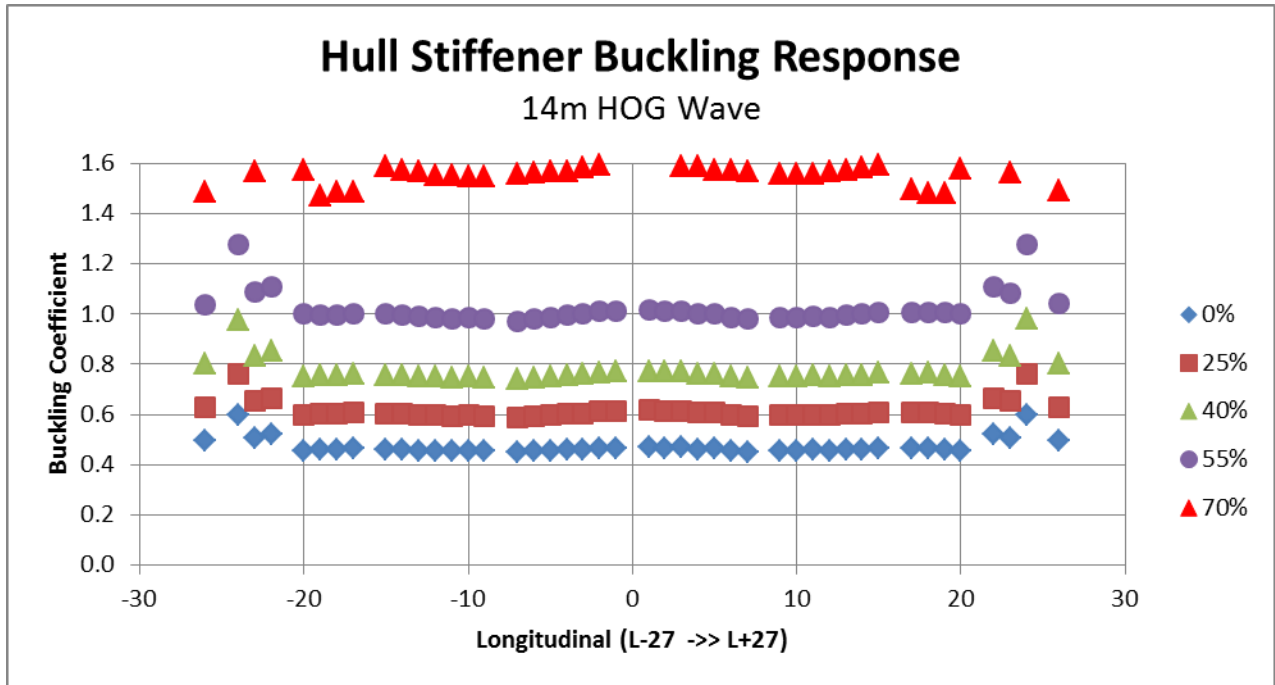


Figure E-3: Hull Stiffener Buckling Response for Various Corrosion Levels – 14m Hog Wave

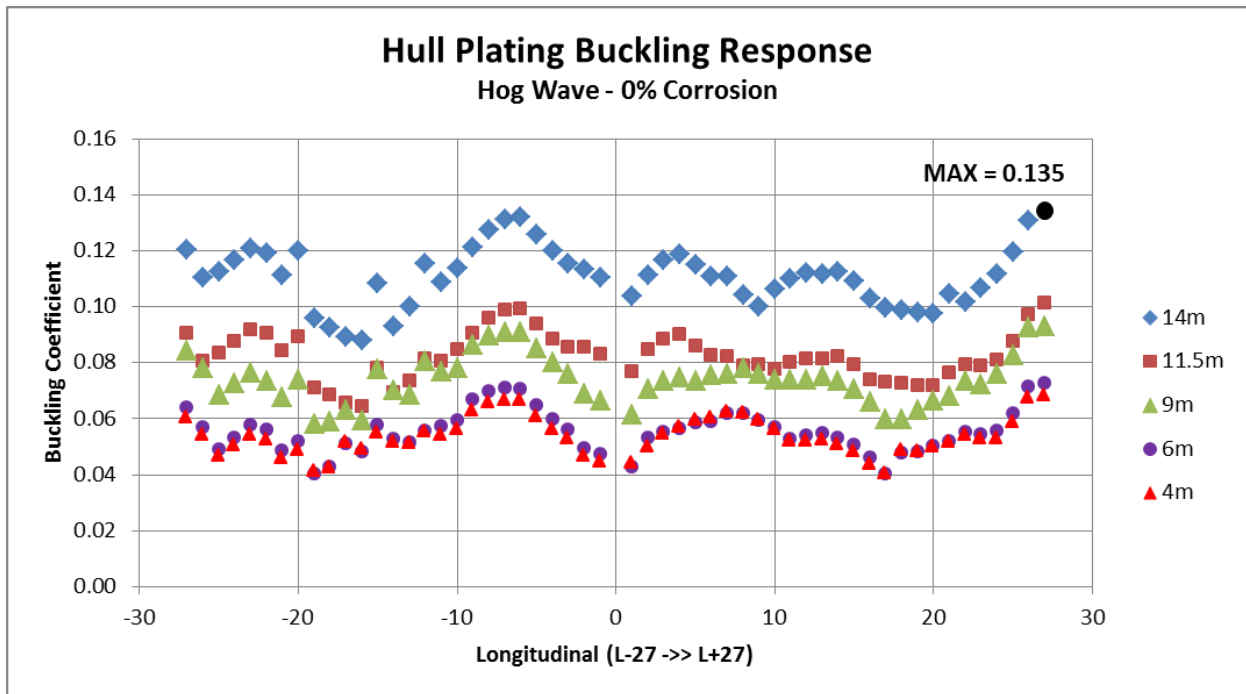


Figure E-4: Hull Plating Buckling Response - Hog Wave - 0% Corrosion

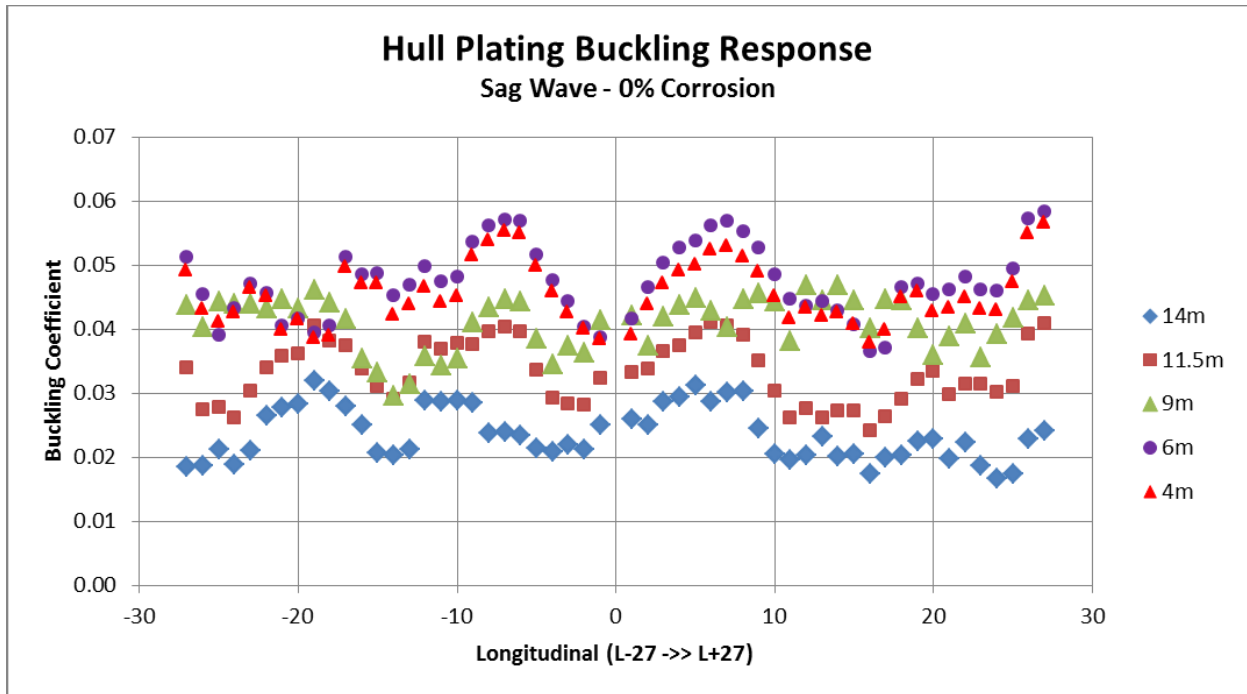


Figure E-5: Hull Plating Buckling Response – Sag Wave - 0% Corrosion

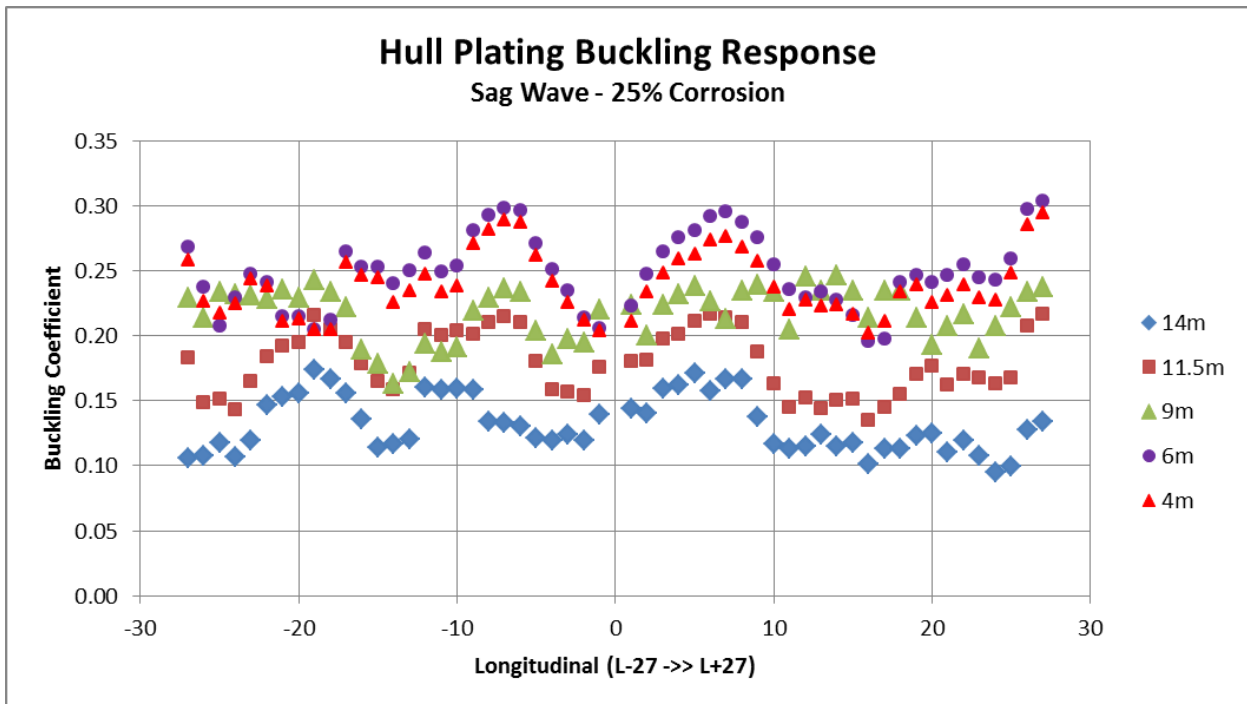


Figure E-6: Hull Plating Buckling Response – Sag Wave - 25% Corrosion